



**Pomegranate Peel as Bio-adsorbent for Nutrients Removal
and Recovery from Aqueous Solutions**

PH.D. thesis

By

Naoufal Bellahsen

Supervisor

Prof. Dr. Cecilia Hodúr

Co-supervisor

Dr. Szabolcs Kertész

Assistant Professor

Doctoral School of Environmental Sciences

Department of Biosystems Engineering

Faculty of Science and Informatics

University of Szeged

Szeged, 2021

To My Family

ACKNOWLEDGEMENTS

I would like to express my sincere thanks to my supervisor Prof. Dr. Cecilia Hodùr for giving me the chance to pursue and successfully complete my Ph.D. studies, I will be thankful for her forever in my life for her full support, constant guidance, constructive feedbacks, intellectual input, and continuous encouragement. I am truly fortunate to have had the opportunity to work under her supervision.

I would also like to thank my co-supervisor Dr. Szabolcs Kertész for his friendly guidance, helpful suggestions, and the valuable advices that he offered to me over the years. I truly appreciate that he encouraged and guided me towards my academic life.

I would also like to thank Prof. Etelka Tombácz for her help and advice during my research studies.

I extend my gratitude to all colleagues in the department of Biosystems Engineering for their valuable help in my research and for giving me the opportunity of being part of their research team. I also thank all colleagues in the Biotechnology department for their lab help and cooperation.

I would like also to express my gratitude to all colleagues in the Department of Carbohydrate and Food Technologies at the University of Novi Sad, Serbia, for their cooperation and contribution in this research.

The financial support was provided by the project Hungarian Scientific Research Fund (NKFI contract number K115691) and EFOP-3.6.2- 16-2017- 00010 – RING 2017.

Finally, I wish to acknowledge the University of Szeged and Tempus foundation for their financial support during my study.

Table of contents

| | |
|---|----|
| ACKNOWLEDGEMENTS..... | 3 |
| Table of contents | 4 |
| List of figures..... | 7 |
| List of tables | 9 |
| Nomenclature/ Abbreviations | 10 |
| 1 Introduction | 11 |
| 2 Literature review..... | 14 |
| 2.1 Nutrients removal and recovery | 14 |
| 2.1.1 Nitrogen cycle..... | 14 |
| 2.1.2 Methods of NH_4^+ removal and recovery..... | 15 |
| 2.1.3 Phosphorus cycle..... | 17 |
| 2.1.4 Methods for phosphorus removal and recovery..... | 18 |
| 2.2 Biosorption of NH_4^+ and phosphate (PO_4^{3-}) using AFW..... | 20 |
| 2.2.1 Modification of AFW for PO_4^{3-} removal..... | 21 |
| 2.2.2 Examples of AFW used as bio-adsorbents for NH_4^+ and PO_4^{3-} | 22 |
| 2.2.3 Mechanisms and properties of NH_4^+ and PO_4^{3-} biosorption using AFW | 23 |
| 2.2.4 Biosorption Modelling..... | 27 |
| 2.3 Pomegranate peel as bio-adsorbent | 31 |
| 2.4 Application of nutrient-loaded bio-adsorbents for soil fertilization: | 33 |
| 3 Aims..... | 35 |
| 4 Materials and methods | 36 |
| 4.1 Bio-adsorbents preparation | 36 |
| 4.2 Activation of PP | 36 |
| 4.3 Preparation of stock solutions | 36 |
| 4.4 Screening experiments..... | 36 |
| 4.5 Characterization of PP | 37 |
| 4.5.1 Particle size distribution and porosity | 37 |
| 4.5.2 Zeta potential | 37 |
| 4.5.3 FT-IR ATR analysis | 38 |
| 4.5.4 Scanning electron microscope SEM | 38 |
| 4.5.5 Batch adsorption studies..... | 38 |
| 4.6 Milking parlour wastewater (MPWW)..... | 39 |
| 4.7 Application of nitrogen-loaded PP and phosphorus-loaded IL-PP as fertilizer..... | 40 |

| | | |
|-------|--|----|
| 4.7.1 | Germination test..... | 41 |
| 4.7.2 | Pot experiments..... | 41 |
| 5 | Results and discussion | 43 |
| 5.1 | Screening results | 43 |
| 5.2 | Characterization of PP and IL-PP | 43 |
| 5.2.1 | Particle size distribution and porosity | 43 |
| 5.2.2 | Zeta potential | 44 |
| 5.2.3 | FTIR- ATR analysis | 47 |
| 5.2.4 | SEM results..... | 48 |
| 5.3 | Biosorption of NH_4^+ from NH_4Cl solution using PP | 49 |
| 5.3.1 | Effect of initial $\text{NH}_4\text{-N}$ concentration | 49 |
| 5.3.2 | Effect of solution pH | 50 |
| 5.3.3 | Effect of PP dose..... | 51 |
| 5.3.4 | Effect of stirring rate | 51 |
| 5.3.5 | Effect of contact time | 52 |
| 5.3.6 | Process modeling | 53 |
| 5.4 | Biosorption of NH_4^+ from MPWW using PP | 57 |
| 5.4.1 | Effect of PP dose..... | 57 |
| 5.4.2 | Effect of solution pH | 58 |
| 5.4.3 | Effect of stirring rate | 58 |
| 5.4.4 | Effect of temperature..... | 59 |
| 5.4.5 | Effect of contact time | 60 |
| 5.4.6 | Process modeling | 60 |
| 5.5 | Biosorption of PO_4^{3-} from Na_2HPO_4 solution using IL-PP..... | 64 |
| 5.5.1 | Effect of solution pH..... | 64 |
| 5.5.2 | Determination of equilibrium time..... | 65 |
| 5.5.3 | Factorial design study..... | 66 |
| 5.5.4 | Process modelling | 72 |
| 5.6 | Application of N-PP and P-IL-PP as fertilizer..... | 75 |
| 5.6.1 | Germination test..... | 76 |
| 5.6.2 | Pot experiments..... | 78 |
| 6 | Conclusion..... | 83 |
| 7 | Summary | 85 |
| 8 | Összefoglalás..... | 89 |

| | | |
|----|------------------------------------|-----|
| 9 | New scientific results | 94 |
| 10 | Publications | 95 |
| 11 | Presentations in conferences | 96 |
| | References | 97 |
| | Appendices | 112 |

List of figures

| | |
|--|----|
| Figure 1. Aim of using AFW as bio-adsorbents for nutrients removal and recovery | 13 |
| Figure 2. Criteria for selection of AFW for nutrients removal and recovery | 21 |
| Figure 3. Schematic representation of contaminants removal via different adsorption mechanisms [85]. | 24 |
| Figure 4. General aspect of adsorption isotherm [68]..... | 27 |
| Figure 5. General aspect of kinetics of adsorption process [68]..... | 28 |
| Figure 6. Steps of adsorption kinetics | 29 |
| Figure 7. Example of linear plot of $\ln(k_d)$ versus $(1/T)$ | 30 |
| Figure 8. a. Particle size distribution of PP, b. Pore size distribution of PP | 44 |
| Figure 9. a. Zeta Potential of PP as function of pH (NH_4Cl Concentration= 10 mmol.L^{-1}), b. Zeta potential of PP as function of NH_4Cl concentration (pH=4). | 45 |
| Figure 10. a. Zeta potential of PP and IL-PP in NaCl and Na_2HPO_4 solution as function of pH, b. Zeta potential of IL-PP in different Na_2HPO_4 solution concentrations..... | 46 |
| Figure 11. a. FTIR of PP before (A) and after adsorption of NH_4^+ (B), b. FTIR spectrum of PP and IL-PP before and after PO_4^{3-} adsorption | 48 |
| Figure 12. a. SEM of PP, b. SEM of IL-PP | 49 |
| Figure 13. Effect of initial $\text{NH}_4\text{-N}$ concentration (pH 4, 100 mg of PP, stirring rate of 100 rpm and contact time of 120 min). | 50 |
| Figure 14. Effect of pH (initial $\text{NH}_4\text{-N}$ concentration of 30 mg.L^{-1} , 100 mg of PP, stirring rate of 100 rpm and contact time of 120 min)..... | 50 |
| Figure 15. Effect of PP dose (pH 4, initial $\text{NH}_4\text{-N}$ concentration of 30 mg.L^{-1} , stirring rate of 100 rpm and contact time of 120 min)..... | 51 |
| Figure 16. Effect of stirring rate (pH 4, initial $\text{NH}_4\text{-N}$ concentration of 30 mg.L^{-1} , 100 mg of PP and contact time of 120 min) | 52 |
| Figure 17. Effect of contact time (initial $\text{NH}_4\text{-N}$ concentration of 30 mg.L^{-1} , pH 4, 400 mg of PP and stirring rate of 150 rpm) | 52 |
| Figure 18. Isotherm of NH_4^+ biosorption by PP | 53 |
| Figure 19. Langmuir model..... | 54 |
| Figure 20. Kinetics of NH_4^+ biosorption by PP (400 mg PP, 30 mg.L^{-1} $\text{NH}_4\text{-N}$, pH 4, stirring rate 100 rpm, contact time 120 min) | 55 |
| Figure 21. Pseudo-second order model..... | 56 |
| Figure 22. Intra-particle diffusion model | 56 |
| Figure 23. Effect of PP dose (pH 6, stirring rate of 300 rpm, 25°C temperature and contact time of 120 min) | 57 |
| Figure 24. Effect of pH (1.5g PP, stirring rate of 300 rpm, 25°C temperature and contact time of 120 min)..... | 58 |
| Figure 25. Effect of stirring rate (1.5g PP, pH 6, 25°C temperature and contact time of 120 min)..... | 59 |
| Figure 26. Effect of temperature (1.5g PP, pH 6, stirring rate of 300 rpm and a contact time of 120 min)..... | 59 |
| Figure 27. Effect of contact time (1.5g PP, pH 6, 25°C temperature and 300 rpm stirring rate). | 60 |
| Figure 28. Isotherm of NH_4^+ biosorption from MPWW by PP | 61 |
| Figure 29. Langmuir isotherm | 62 |
| Figure 30. Kinetics of NH_4^+ biosorption from MPWW by PP. (1.5g PP, 80 mg.L^{-1} $\text{NH}_4\text{-N}$, pH 6, 300 rpm stirring rate and 25°C temperature) | 62 |

| | |
|---|----|
| Figure 31. Pseudo second-order kinetic model..... | 63 |
| Figure 32. Intra-particle diffusion model | 63 |
| Figure 33. Effect of pH on PO_4^{3-} removal by IL-PP ($\text{PO}_4\text{-P}$ concentration: 40 mg.L^{-1} , adsorbent dose 100 mg, temperature: $25 \text{ }^\circ\text{C}$, stirring speed: 150 rpm)..... | 65 |
| Figure 34. Effect of contact time on PO_4^{3-} removal by IL-PP ($\text{PO}_4\text{-P}$ concentration: 40 mg.L^{-1} , temperature: $25 \text{ }^\circ\text{C}$, stirring speed: 150 rpm) | 66 |
| Figure 35. Cube plots for PO_4^{3-} removal by IL-PP | 67 |
| Figure 36. Main effects plot for PO_4^{3-} removal by IL-PP | 70 |
| Figure 37. Interaction plot for PO_4^{3-} removal by IL-PP | 70 |
| Figure 38. Pareto chart of the standardized effects for PO_4^{3-} removal by IL-PP | 71 |
| Figure 39. Normal plot of the standardized effects for PO_4^{3-} removal by IL-PP..... | 71 |
| Figure 40. Langmuir and Freundlich isotherm fitting for PO_4^{3-} biosorption by IL-PP | 73 |
| Figure 41. Experimental kinetics and Elovich model fitting for PO_4^{3-} biosorption by IL-PP | 74 |
| Figure 42. Van't Hoff plot for PO_4^{3-} biosorption by IL-PP..... | 75 |
| Figure 43. RSG of Brassica napus L. using tested treatments. | 76 |
| Figure 44. RRE of Brassica napus L. using tested treatments. | 77 |
| Figure 45. GI of Brassica napus L. using tested treatments. | 78 |
| Figure 46. Plant habits of Brassica napus L. using tested treatments | 79 |
| Figure 47. Number of produced leaves of Brassica napus L. using tested treatments | 79 |
| Figure 48. Root fresh weight of Brassica napus L. using tested treatments | 80 |
| Figure 49. Shoots fresh weight of Brassica napus L. using tested treatments | 81 |
| Figure 50. Roots dry weight of Brassica napus L. using tested treatments | 82 |
| Figure 51. Shoots dry weight of Brassica napus L. using tested treatments | 82 |

List of tables

| | |
|--|----|
| Table 1. Examples of AFW used for NH_4^+ and PO_4^{3-} removal and recovery..... | 23 |
| Table 2. Freundlich and Langmuir isotherm models | 28 |
| Table 3. Kinetic models and their equations | 29 |
| Table 4. Chemical composition of PP [121] | 32 |
| Table 5. Possible applications of PP for heavy metals and/or pollutants removal from wastewaters / process waters..... | 33 |
| Table 6. Characteristics of MPWW..... | 40 |
| Table 7. Removal rates of NH_4^+ by AFW tested | 43 |
| Table 8. FTIR analysis of PP (before and after NH_4^+ adsorption) and IL-PP (before and after PO_4^{3-} adsorption)..... | 47 |
| Table 9. Parameters and properties of Langmuir and Freundlich models | 54 |
| Table 10. Kinetic models properties and parameters of NH_4^+ adsorption by PP | 55 |
| Table 11. Parameters of Langmuir model for NH_4^+ biosorption from MPWW by PP | 61 |
| Table 12. Parameters of kinetic models for NH_4^+ biosorption from MPWW by PP | 63 |
| Table 13. Factors and levels used in the factorial design for PO_4^{3-} removal by IL-PP | 66 |
| Table 14. Design matrix and results of 2^3 full factorial design for PO_4^{3-} removal by IL-PP..... | 67 |
| Table 15. Estimated effects and coefficients for PO_4^{3-} removal by IL-PP | 68 |
| Table 16. Analysis of variance (ANOVA) for PO_4^{3-} removal by IL-PP | 69 |
| Table 17. Isotherm models and parameters of PO_4^{3-} biosorption by IL-PP | 72 |
| Table 18. Kinetic models and parameters of PO_4^{3-} biosorption by IL-PP..... | 74 |
| Table 19. Thermodynamics parameters of PO_4^{3-} adsorption by IL-PP..... | 75 |

Nomenclature/ Abbreviations

AC: Activated Carbon

AFW: Agricultural and Food Waste

Anammox: Anaerobic ammonium oxidation

ANOVA: Analysis Of Variance

BES: Bio-electrochemical System

C_e: The equilibrium concentration

EBPR: Enhanced Biological phosphorus Removal

Eq.: Equation

FAO: Food and Agriculture Organization

FT-IR: Fourier Transform Infrared spectroscopy

GI: Germination Index

IFA: International Fertilizer Association

IL-PP: Iron-Loaded Pomegranate Peel

IS: Ionic Strength

K₁: Pseudo-first kinetics model constant

K₂: Pseudo-second kinetics model constant

K₃: Intra-particle diffusion kinetics model constant

K_L: Langmuir constant

K_F: Freundlich constant

MBR_s: Membrane Bioreactors

MPWW: Milking Parlour Wastewater

N-PP: Nitrogen-loaded Pomegranate Peel

PFO: Pseudo-First order kinetics model

P-IL-PP: Phosphorus-loaded Iron-Loaded Pomegranate Peel

PP: Pomegranate Peel

PSO: Pseudo-Second order kinetics model

q_e: The amount of solute adsorbed at equilibrium

q_{max}: The maximum amount of solute adsorbed

q_t: The amount of solute adsorbed at time (t)

R_L: Separation factor

RO: Reverse osmosis

RRE: Relative Root Elongation

RSG: Relative Seed Germination

SDG 2030: Sustainable Development Goals 2030

SEM: Scanning Electron Microscopy

ΔG°: Free energy change:

ΔH°: Enthalpy change:

ΔS°: Entropy change:

1 Introduction

Environmental issues are closely intertwined to one another and among them, water pollution stand in the top, not only because of the vital role of water in all life forms and human activities but also due to other ecological, socio-economic and political issues that revolve around it in one way or another. Human activities and the lack of respect for nature have led to the deterioration of water quality by several pollution forms such as salinization, microbiological contamination, eutrophication, acidification, heavy metals and toxic wastes contamination, thermal pollution, and increases in total suspended solids. As a result, serious environmental issues are recognized while the cost-effectivity of existent water and wastewater treatment systems is in debate [1,2]. Moreover, global water resource limits will be reached in the near future, and along with the effect of climate change, the situation is expected to worsen, especially in densely populated and industrial areas [3]. Therefore, water pollution control became a major challenge and alarm bells started to ring to develop efficient technologies for water recycling that can play key role in the conservation and sustainability of water resources. Among human activities, agricultural sector is recognized as the dominant user of water accounting for around 80% of global water withdrawals, therefore, its contribution in water shortage and pollution is the highest [4]. Furthermore, continued increase in irrigation for agricultural production over many years has led to the oversaturation of soils, salt build-up, lowering of groundwater tables and land degradation [5]. Hence, it is obvious that if we want to mitigate water shortage and pollution problems we should look critically at the use and management of water by agricultural sector [6]. However, water is key driver in agricultural production, and irrigation remains one of the most critical inputs into farming to meet food demand [7]. Moreover, continued increase in demand for water by urban and industrial sectors can dramatically impact food security although the efforts expanded for rationalization of water-use efficiency in agriculture [8]. Therefore, providing sustainable and practicable approach ensuring agricultural water demand without compromising environmental protection is highly required.

Additionally, agriculture, industry, and wastewater treatment sites are recognized as the main sources of nitrogen (N) and phosphorus (P) released into water systems. The presence of these elements in freshwaters and marine ecosystems leads to several harmful impacts such as eutrophication [9,10], formation of dead zones [11], contamination of drinking water [12,13], reduction of crop yields [14], global warming [15], over-fertilization of soils [16], decrease of the recreational value of the environment, and severe economic damage [17]. On the other

hand, in addition to their principal role in many industries [18,19], nitrogen and phosphorus are indispensable components of fertilizers and their role is critical in agricultural production because they are irreplaceable and essential elements for the growth of aquatic life and plants [20,21]. Moreover, the role of these fertilizers is more than ensuring food security as they contribute in achieving several goals of the Sustainable Development Agenda 2030 (SDG 2030) including No poverty, No hunger, Gender equality, Sustainable management of water, Sustainable industrialization, Climate change, Clean oceans and life on land according to the International Fertilizer Association (IFA) [22]. Therefore, there will be a continuous need to supply phosphorus and nitrogen to agriculture and industry. However, the increase of demand for fertilizers makes stress on phosphate rock sources and it is estimated that they will be exhausted in between the second half of this century to several centuries from now [23,24]. Moreover, phosphate industry is facing serious obstacles concerning phosphate rock quality and water availability for mining process which makes phosphorus extraction increasingly expensive [25]. On the other hand, nitrogen is a renewable resource and abundantly exists in atmosphere in a highly stable and non-reactive form, dinitrogen gas (N_2). However, its content in soils is limited and the Haber–Bosch process by which ammonia (NH_3) is industrially synthesized is energetically intensive [26]. Hence, the recovery of nitrogen and phosphorus from wastewater is highly required and has recently become a matter of urgency to preserve water resources, protect the environment and mitigate the disruption in fertilizers supply. For this purpose, many physical, chemical, and biological methods have been developed, however, most of these methods showed different shortcomings such as high operational and maintenance costs, generation of toxic sludge, low-purity of recovered products and complicated procedure which limit their application [27]. Comparatively, adsorption process takes advantage from all existent methods due to several advantages such as cost-effectivity, ease of operation, simplicity of design and wide range of existing and potential adsorbents with the possibility of direct application of nutrient-loaded adsorbents for soil fertilization [28,29]. However, despite the increasing recognition of the adsorption technology benefits, the costs of nutrients recovery procedure cannot yet compete in the market against mining industry [30]. Hence, it is necessary to search for more cost-effective adsorbents and methods.

Furthermore, as a result of expanding agricultural activities and irresponsible food production and consumption, more than 1.3 billion tons of agricultural and food waste (AFW) are produced annually according to the Food and Agriculture Organization of the United Nations (FAO) [31]. Disposal of this waste into landfills has proven to be responsible for not only

social and economic damage, but for a considerable ratio in the greenhouse gas emissions in addition to odours, fires, and groundwater contamination by leachate [32]. Moreover, reduction of this waste is one of SDG 2030 "12. Responsible production and consumption", however, interventions to reduce its burden remain insufficient because they require radical changes in consumers' attitude and economic policy. Hence, several methods were followed for the development of sustainable management solutions of this biomass waste in order to turn its burden into social, economic and environmental benefits. The traditional management option was using this waste for feeding livestock in addition to modern revalorization in different fields such as energy production, bioactive compounds recovery, food industry and soil fertilization [33–35]. Nowadays, a new management way is showing up by the use of these valueless biomaterials as a renewable resource of low-cost adsorbents with the aim of the removal and recovery of valuable contaminants including nutrients [36,37]. The use of AFW as bio-adsorbents for nutrients removal and recovery from wastewater presents an eco-friendly, innovative and sustainable approach for water, nutrients and solid waste management according to the 4R principle (Reduce, Recycle, Reuse and Recover); Reduce the overuse of water and fertilizers; Recycle wastewater, Reuse AFW and Recover nutrients (Figure 1). However, in spite of the growing interest given to this approach, there are many obstacles concerning its large-scale application.

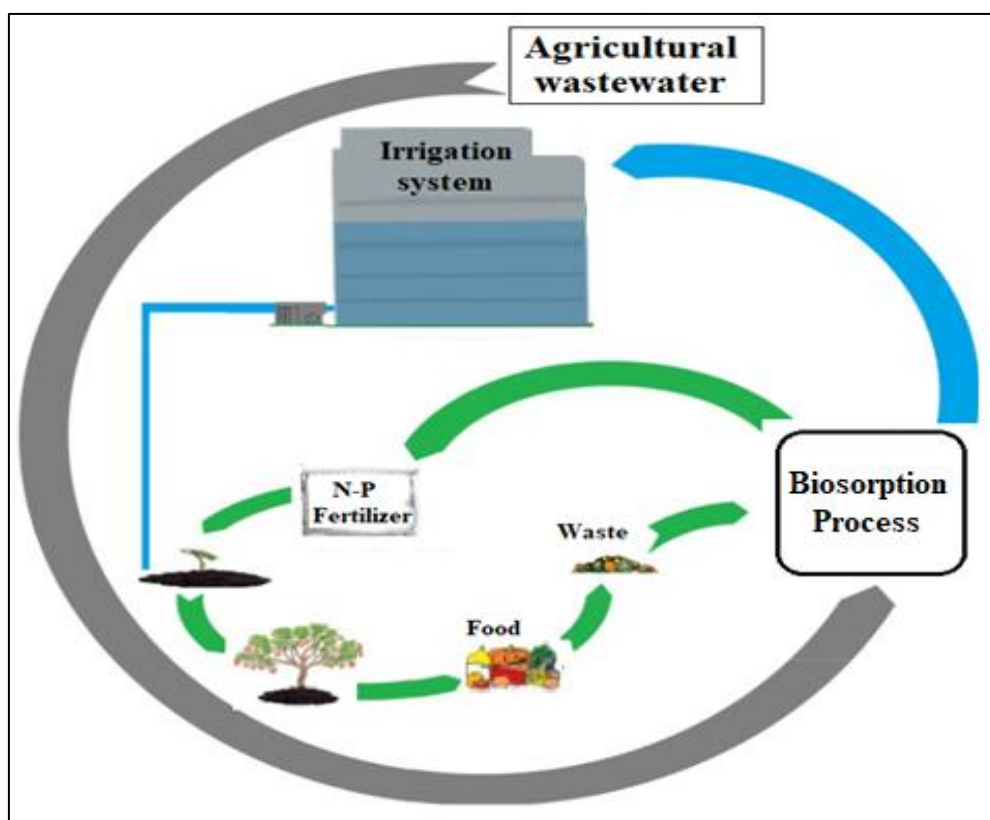


Figure 1. Aim of using AFW as bio-adsorbents for nutrients removal and recovery

2 Literature review

Nitrogen is the major nutrient that is more widespread than phosphorus in most estuaries and coastal areas thus it is more responsible for eutrophication [38]. However, phosphorus concentration as low as 1 mg.L^{-1} is sufficient to stimulate eutrophication in lakes [39]. In wastewater bodies, the predominant form of nitrogen is organic nitrogen, which may be biologically converted to NH_3 or ammonium (NH_4^+) by one of several different metabolic pathways. While, forms of phosphorus found in waters include organic phosphates, inorganic phosphate (soluble orthophosphates), and polyphosphates [40]. Nitrogen and phosphorus are released to water bodies from point and non-point sources. The amount and rate of their release depend on their concentration in the effluent, soil type, and distance from water bodies. The most common point sources of nitrogen and phosphorus are specific locations or facilities such as urban and industrial wastewater effluents, and leachate from waste disposal sites [41]. These point sources tend to be continuous with little variability over time thus they are easily identified and controlled. However, non-point sources are discrete discharges that are difficult to measure and they are linked to agricultural activities such as land fertilization, heavy precipitation, urban storm, animal farms, pastures, atmospheric deposition, drainage, seepage or erosion therefore they are difficult to control [42].

2.1 Nutrients removal and recovery

2.1.1 Nitrogen cycle

Nitrogen cycle is the biogeochemical cycle by which nitrogen is converted into multiple chemical forms as it circulates among the atmosphere, terrestrial, and marine ecosystems. This conversion can be carried out through biological processes as described below [43].

- a) Fixation: A special type of bacteria called nitrogen-fixing bacteria such as *Rhizobium*, *Azotobacter* and *Clostridium* take nitrogen present in atmosphere and combine it with hydrogen to produce NH_3 that can be dissolved in water to form NH_4^+ .
- b) Assimilation: In this process, plants and animals take up NH_4^+ and nitrate (NO_3^-) through their roots and integrate them into various proteins and nucleic acids. Animals take up this nitrogen forms by consuming the plant tissues.
- c) Ammonification (mineralization): This process takes place in soils. The death of a plant or animal or the waste excretion by an animal is the initial form of organic nitrogen. Many bacteria and fungi convert this organic nitrogen into NH_4^+ that takes part in other biological processes.

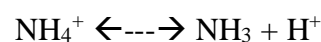
- d) Nitrification: This two-step process also occurs in soils and converts NH_3 to NO_3^- . In the first step, *Nitrosomonas* and *Nitrococcus*, soil bacteria, convert NH_3 to nitrite (NO_2^-), once this step is done, *Nitrobacter*, another soil bacteria, takes forward the second step of nitrification by oxidizing NO_2^- to NO_3^- .
- e) Denitrification: It is the reduction of NO_3^- into N_2 in anaerobic conditions by anaerobic bacteria such as *Pseudomonas* and *Clostridium*. These bacteria are facultative organisms and can survive in the presence of oxygen.

Anthropogenic impact

The production and use of nitrogen fertilizers, fossil fuels burning, power generation plants, and industries have altered dramatically the natural balance of the nitrogen cycle by increasing the rate of its fixation. The consequences of this imbalance are manifold because when present in excess, reactive nitrogen such as nitric oxide (NO) and nitrogen dioxide (NO_2), cause a range of negative environmental effects and pose risks to human health [44]. Water containing high concentrations of NO_3^- had a high risk of developing methemoglobinemia, commonly referred to as *bluebaby syndrome*. Additionally, recent research has shown that NO_3^- can be converted within the food chain to nitrosamine that is known carcinogen. Furthermore, the dissolution and enrichment of nitrogen compounds in water can cause acidification. In addition, high level of NH_4^+ promotes eutrophication in coastal ecosystems and thus ultimately reduces the biodiversity due to a lack of oxygen needed for the survival of many species of aquatic plants and animals. Moreover, nitrogen has several warming effects through the formation of N_2O and O_3 .

2.1.2 Methods of NH_4^+ removal and recovery

The most encountered nitrogen form in wastewater is NH_4^+ which exists in equilibrium with NH_3 [45]. This equilibrium shifts to NH_3 when pH is equal to 9.0 or higher and shifts to NH_4^+ when pH is neutral or lower according to the following chemical equation:



The most common technologies for NH_4^+ removal and recovery are:

- Biological nitrification: It is a simple and cost-effective process that is known as the biological conversion of NH_4^+ to NO_3^- which is less toxic [46]. This autotrophic process occurs in two steps according the following chemical equations:



In the first step, *Nitrosomonas* bacteria convert NH_4^+ into NO_2^- . While during the second step, *Nitrobacter* bacteria consume NO_2^- to produce NO_3^- , which is a form of fixed nitrogen that plants and microorganisms can absorb. The main shortcomings of this technology is the sensitivity of nitrifying bacteria to a variety of parameters such as high concentration of NH_4^+ and nitrous acid (HNO_2), pH, temperature and dissolved oxygen concentration in addition to the presence of inorganic agents that can inhibit the growth and action of these organisms.

- Anaerobic ammonium oxidation (Anammox): This relatively new biological method shows good efficiency in converting NH_4^+ and NO_3^- directly into N_2 . Contrasted with biological nitrification, which is a two-step process, Anammox bacteria convert NH_4^+ and NO_3^- directly into N_2 and H_2O by passing over the traditional denitrification process. However, Anammox shares many commonalities with traditional biological nitrification and it is compatible with much existing infrastructure [47]. This technology comes with advantages such as lower oxygen demand, less sludge production and lower carbon dioxide (CO_2) emissions, which reduce the environmental impacts and operating costs, however, slow growth rate of Anammox bacteria and high costs of aeration equipment are the main limiting factors of this technology.
- Air stripping: It is an effective technology for treatment of wastewaters with low NH_4^+ concentration. It consists of converting NH_4^+ to NH_3 and then dispersing the liquid in air over an evaporation material with cooling-tower type structure. However exhausting this air to the atmosphere may be not permissible in some locations. This technology present several advantages such as less place requirements, simple construction and ease of operation. However, cost-efficiency at high NH_4^+ concentration, the necessity of pH adjustment (pH must be greater than 11 for complete conversion of NH_4^+ to NH_3), noise, air pollution and odours are the main disadvantage of this technology [48].
- Breakpoint chlorination: in this process, chlorine (Cl_2) converts NH_4^+ into various chloramines, depending on the pH of solution. An average of 8:1 ratio of Cl_2 to NH_4^+ is required to convert all NH_4^+ into chloramines [49]. This method presents advantages such as the high efficiency and ability of destroying other pollutants present in solution, however, the high Cl_2 consumption and the necessity of dosage, pH and temperature control in addition to the large volumes of chlorines produced are the main drawbacks of this technology.

- Adsorption-based processes: Application of these methods for NH_4^+ removal has been encouraged due to a plenty of advantages such as low cost and energy requirements, high selectivity, promising efficiency in a short contact time, good response at low temperatures, ease of operation, environmental friendliness and wide range of available adsorbents and resins [50]. Moreover, the utilization of the used adsorbent loaded with nitrogenous compounds as fertilizer is another advantage associated with this technology [51]. However, chemicals required for adsorbent regeneration, amount of adsorbent required for complete removal and presence of competitive foreign ions are some of the challenges hindering this technology. In recent years, most efforts have been made to find adsorbents with higher efficiency and lower cost [52].
- Bio-electrochemical systems (BES): It is a technology where chemical energy contained in the organic matter is directly converted into electrical energy by certain microorganisms. In the case of NH_4^+ recovery, organic matter present in wastewater is oxidized at the anode by bacteria, while NH_4^+ ions are transported over a cation exchange membrane to the cathode chamber where the high pH allows its recovery as NH_3 through gas aeration [29]. This technology seems to be a sustainable way for NH_4^+ removal and recovery, however, there is a need for the optimization of various parameters such as pH and NH_4^+ concentration.
- Membrane-based processes: This technology, especially reverse osmosis (RO), offers distinct advantages for NH_4^+ removal and recovery such as independency from liquid flow rates and NH_4^+ concentration in addition to absence of secondary pollutants in permeate. However, shortcomings such as membrane fouling, chemical stability and high energy consumption remain unaddressed [53].

2.1.3 Phosphorus cycle

The most significant difference between phosphorus and nitrogen cycles is that no gaseous compounds of phosphorus exist as it is only found in soil and aquatic environments. Similar to nitrogen cycle, bacteria play a vital role in weathering, mineralization, assimilation, precipitation, and dissolution of phosphorus. When plants and animals die, the decomposition of the biomass by bacterial activities converts organic phosphorus into inorganic phosphorus that is released back to the environment [54].

- a) Weathering: Phosphorus-rich minerals present in soil are weathered over long periods and become available for plants and microorganisms.

- b) Mineralization: It is the process by which organic phosphorus compounds are converted to orthophosphate by the help of microorganisms such as bacteria (e.g., *Bacillus Subtilis*), and fungi (e.g., *Penicillium*). Phosphatases are the enzymes responsible for the degradation of phosphorus compounds.
- c) Assimilation: Microorganisms assimilate and store phosphorus in the form of polyphosphates in special granules for their own nutritional needs.
- d) Precipitation: In aquatic environment, the solubility of orthophosphate is controlled by pH and by the presence of other minerals such as Al^{3+} , Ca^{2+} , Fe^{3+} , and Mg^{2+} . Reaction of phosphorus with these minerals results in insoluble compounds such as hydroxyapatite $\text{Ca}_{10}(\text{PO}_4)_6(\text{OH})_2$, vivianite $\text{Fe}_3(\text{PO}_4)_2 \cdot 8\text{H}_2\text{O}$ and variscite $\text{AlPO}_4 \cdot 2\text{H}_2\text{O}$.
- e) Solubilisation of insoluble phosphorus: Metabolic activity of microorganisms contributes to the solubilisation of phosphorus compounds. The process involves enzymes and produces organic and inorganic acids, CO_2 , and hydrogen sulfide (H_2S).

Anthropogenic impact

The most important change to the global phosphorus cycle is related to a number of industrial and agricultural activities mainly phosphate rock extraction for crops cultivation, livestock production, and waste deposit, which results in a massive transfer from the vast and unavailable reserve pool to the wide biologically available forms on land [10]. The impact of these activities is usually accompanied with an overuse of resources such as water, energy and phosphate rock. The rapid increase in phosphate rock extraction is continuously exhausting global phosphorus reserves and as a result, global food safety is threaten. On the other hand, human-induced phosphorus losses contribute to eutrophication through rapid growth of algal blooms, which reduces dissolved oxygen and therefore reduces the aquatic biodiversity.

2.1.4 Methods for phosphorus removal and recovery

Orthophosphate is the most phosphorus form found in wastewater systems and it is presented in a variety of forms including PO_4^{3-} , HPO_4^{2-} , H_2PO_4^- depending on pH [11]. In the field of wastewater treatment technology, numerous methods have been developed for phosphorus removal and recovery and they encompass three main categories: biological, chemical, and physical and/or a combination of them. However, some of these techniques are only experimental projects [55]. The main phosphorus removal and recovery methods can be summarized as follow:

- Membrane technology: This method is of growing interest for wastewater treatment in general and for phosphorus removal in particular as it has the added benefit of collecting dissolved and solid phosphorus. Some of the more common membrane filters used for phosphorus removal and recovery are membrane bioreactors (MBRs), tertiary membrane filtration and RO. However, although the high efficiency, membrane technology is often expensive and does not provide an easily recoverable source of phosphorus [29].
- Chemical precipitation: This technology is the main commercial process for removing phosphorus from wastewater effluents [56]. Chemicals most often employed are compounds of calcium, aluminium, lime and iron. These chemicals have the ability to aggregate with phosphorus to form particles with larger sizes that they can be easily removed. In this process, effluents containing phosphate ions react with salts of ferric ions, aluminium ions, or lime to form metal-phosphate precipitates. A major concern with this method continues to be the produced sludge at the end of the reaction and the high cost of consumed chemicals. Moreover, phosphorus precipitation by metal salts makes the precipitate unrecoverable for potential use in soil fertilization [57].
- Biological assimilation and Constructed wetlands: These methods are based on the incorporation of phosphorus as an essential element in the biomass of a photosynthetic organism such as plants, algae, and some bacteria [58]. In constructed wetlands, bacteria residing in the roots of a macrophyte plant degrade phosphorus and other organic matter that are later absorbed by the plant's roots. However, susceptibility to climate, accumulation of heavy metals and hazardous pollutants in addition to the necessity to remove the used plants in order to prevent possible re-release of phosphorus in water limit the wide application of this method [57].
- Enhanced biological phosphorus removal (EBPR): This technology is based on a selective enrichment of inorganic polyphosphate by bacteria as an ingredient of their cells. In this process, phosphate accumulating organisms (PAOs) store polyphosphate as an energy reserve in intracellular granules [57]. Under anaerobic conditions and in the presence of fermentation products, PAOs release orthophosphate and use the energy to accumulate simple organics and store them as polyhydroxyalkanoates (PHAs) such as poly- β -hydroxybutyrate (PHB). Afterwards, under aerobic conditions, PAOs grow on the stored organic material and use some of the energy to take up orthophosphate and store it as polyphosphate. Finally, the biomass enriched in these

bacteria is separated from the treated water and thus phosphorus is removed. This technology can achieve low or even very low total phosphorus (TP) effluent levels ($<0.5 \text{ mg.L}^{-1}$) at modest cost and with minimal additional sludge production [59]. However, temperature control, energy consumption, space requirement and complexity of operations are the main disadvantages of this technology.

- Adsorption-based processes: As for NH_4^+ removal and recovery, adsorption technology is advantageous, cheap and simple producing less sludge and offer many benefits for phosphorus removal and recovery. Ferric and aluminium hydroxides are common adsorbents used for phosphorus removal, however, some common limitations of this technology are the high cost of adsorbents and their regeneration in addition to their safe disposal [29].

2.2 Biosorption of NH_4^+ and phosphate (PO_4^{3-}) using AFW

The biosorption process is commonly defined as the removal/binding of a sorbate from a solution by a biomass such as AFW, also called ligno-cellulosic biomass and include stalks, leaves, seeds, shell, peels, husks, and straws [60]. The basic components of AFW include hemicelluloses, lignin, lipids, proteins, simple sugars, water, hydrocarbons and starch, containing a variety of functional groups especially negatively charged groups, namely hydroxyl ($-\text{OH}$) and carboxyl ($-\text{COOH}$) groups that afford them a promising ion-exchange capacity and general adsorptive characteristics. Several AFW have been studied for NH_4^+ removal from water [61,62]. Although, the adsorption capacity vary depending on the type of AFW, most of these biomaterials can be used in natural form for NH_4^+ removal, however, their activation is highly required in order to develop desirable physicochemical properties for PO_4^{3-} removal. In natural form, AFW are washed, ground to desired particle size and subsequently used in adsorption tests. While, in modified form, AFW are pre-treated by means of well-known modification techniques [63]. These biomaterials can be used also as precursor for the production of active carbon with improved adsorptive characteristics using conventional methods such as chemical and thermal activation [64]. However, the use of AFW as bio-adsorbents for nutrients removal and recovery should take in consideration several criteria such as abundancy, cost effectiveness, high efficiency at a short time, ease of regeneration after use, and the possibility of reuse (Figure 2).

Moreover, as AFW are characterized by small surface area, chemical composition of their surfaces plays a major role in their adsorption capacity and selectivity for specific sorbates such as NH_4^+ and phosphate PO_4^{3-} . Therefore, chemical characterization of AFW is

mandatory for an accurate determination of mechanisms taking place during the biosorption process. Numerous techniques are used to characterize AFW's surface such as scanning electron microscope (SEM) that investigates the surface morphology before and after contaminants adsorption. Other techniques provide suitable information on the charge of surface groups such as point of zero charge and zeta potential measurement. On the other hand, FT-IR spectroscopy technique focuses on the bulk crystallographic structure, which helps to investigate functional groups present in surface.

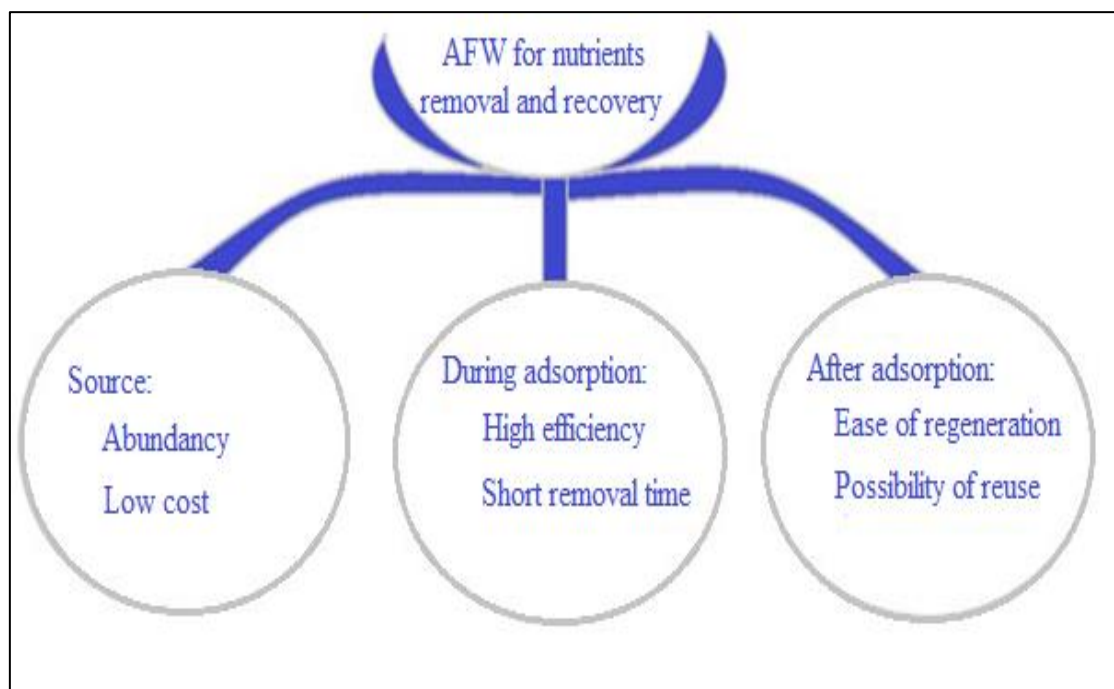


Figure 2. Criteria for selection of AFW for nutrients removal and recovery

2.2.1 Modification of AFW for PO_4^{3-} removal

AFW are characterized by the abundant availability of negatively charged functional groups (e.g., $-\text{OH}$, $-\text{COOH}$) and the lack of positively charged sites able to bind anions thus they are usually inefficient for PO_4^{3-} adsorption from aqueous solutions. Therefore, modification of AFW is highly required and plays a vital role in improving their PO_4^{3-} adsorption capacity [63]. Many modification methods of AFW exist such as thermal activation, chemical activation, steam activation, metal loading, quaternization, and protonation.

- Thermal activation: It is a process of carbonization or calcination of organic matter using high temperature (400 to 1000 °C) to produce activated carbon characterized by high surface area and porosity leading to a high adsorption capacity of many pollutants especially dissolved organic compounds [65].

- Chemical activation: It is a dehydration process at elevated temperature and under pyrolytic conditions employing inorganic chemicals such as zinc chloride ($ZnCl_2$) and phosphoric acid (H_3PO_4) to degrade the cellulose of AFW. However, the residuals of chemicals used may cause environmental contamination or equipment erosion [66].
- Steam activation: It is a selective oxidation of AFW using an activation gas (steam, CO_2 , blue gas) at high temperatures (800 °C-1000 °C) [67]. During the oxidation, the activation gas reacts with the carbon contained in AFW to form gaseous products that enhance the material porosity by opening closed pores [68].
- Quaternization (amine grafting): This method is intended to produce anion exchange resins that can be employed for PO_4^{3-} removal. Quaternization is implemented by reactions between $-OH$ groups present in AFW's surface with amines ($-NH_2$) groups in quaternary ammonium compounds [21]. This two-step process use first cross-linking agent such as epichlorohydrin to convert cellulose into epoxy cellulose ether, which is regarded to be more active and able to react with quaternary ammonium compounds. In the second step, the epoxy cellulose ether will be grafted with different amines by means of various quaternary ammonium compounds such as polyallylamine hydrochloride (PAA. HCl), dimethylamine, triethylamine and urea [69].
- Metal loading: In this method, metals ions such as zinc (Zn^{2+}), iron (Fe^{2+}) and (Fe^{3+}), lanthanum (La^{3+}), cerium (Ce^{3+}) and zirconium (Zr^{4+}) are incorporated in AFW's surface to improve their ability to bind PO_4^{3-} through electrostatic interaction. Prior to reaction with metal salts, AFW are pre-treated with bases such sodium hydroxide (NaOH) in order improve their cationic exchange capacity [70].
- Surface protonation: It is a cost-effective and attractive method for enhancing adsorption capacity of PO_4^{3-} by treating AFW with acids such as hydrochloric acid (HCl) and sulfuric acid (H_2SO_4), thereby increasing the positive surface charge density. It is expected that the elevated number of positive charges will adsorb PO_4^{3-} through electrostatic attraction. Another possible method used for AFW's surface modification is sulphate coating, however, this method has been only applied to conventional adsorbents [20].

2.2.2 Examples of AFW used as bio-adsorbents for NH_4^+ and PO_4^{3-}

A wide variety of AFW in natural and modified form or even as active carbon have been tested for their ability to adsorb NH_4^+ and PO_4^{3-} from aqueous solutions (Table 1).

Table 1. Examples of AFW used for NH_4^+ and PO_4^{3-} removal and recovery

| NH_4^+ removal | | | |
|--|---|--------------|-----------|
| Bio-adsorbents | Adsorption capacity (mg.g^{-1}) | Contact time | Reference |
| Peanut shells | 313.9 | 5h-10h | [71] |
| Corncoobs | 373.1 | | |
| Cotton stalks | 518.9 | | |
| Oak sawdust biochar | 10.1 | 24 h | [72] |
| Giant reed straw | 1.49 | 25 min | [73] |
| P. oceanica fibers | 1.80 | 30 min | [74] |
| Boston ivy leaves | 6.71 | 18 hr | [9] |
| Coconut shell-activated carbon | 2.3 | 120 min | [75] |
| PO_4^{3-} removal | | | |
| Modified Aleppo pine sawdust | 116.25 | 40 min | [76] |
| Modified Orange waste gel | 57 | 6h | [77] |
| Modified Coconut shell | 200 | 4h | [78] |
| Modified wood particles | 2.32 | 6h | [70] |
| Date palm waste | 8.5 | 2h | [79] |
| Cotton stalk | 51.54 | 15min | [80] |
| wheat straw | 60.61 | | |
| Modified Giant reed | 19.89 | 25 min | [81] |

2.2.3 Mechanisms and properties of NH_4^+ and PO_4^{3-} biosorption using AFW

Mechanisms

As in the case of adsorption by conventional adsorbents, several factors influence the biosorption of nutrients by AFW such as physical and chemical properties of adsorbate (NH_4^+ or PO_4^{3-}) and properties of the bio-adsorbent (i.e., the structure of the biomass surface). Considering the diversity of chemical functional groups present in AFW's surface, the two following mechanisms are involved in the biosorption process:

- Physisorption: It is the mechanism driven by Van Der Waals forces in the absence of electrical repulsion [82], or by coulombic attractive forces between charged functional groups present in the bio-adsorbent's surface and the solute [83].
- Chemisorption: Contrarily to physisorption, chemisorption is characterized by an exchange of electrons between active sites present in the bio-adsorbent's surface and solute molecules, thus it involves very specific interactions mainly the formation of strong chemical bonds making this adsorption mechanism irreversible and stronger than physisorption [84].

The difference between physisorption and chemisorption mechanisms can be clarified by temperature dependence and by the nature of bonds formed between adsorbent and adsorbate as illustrated in Figure 3.

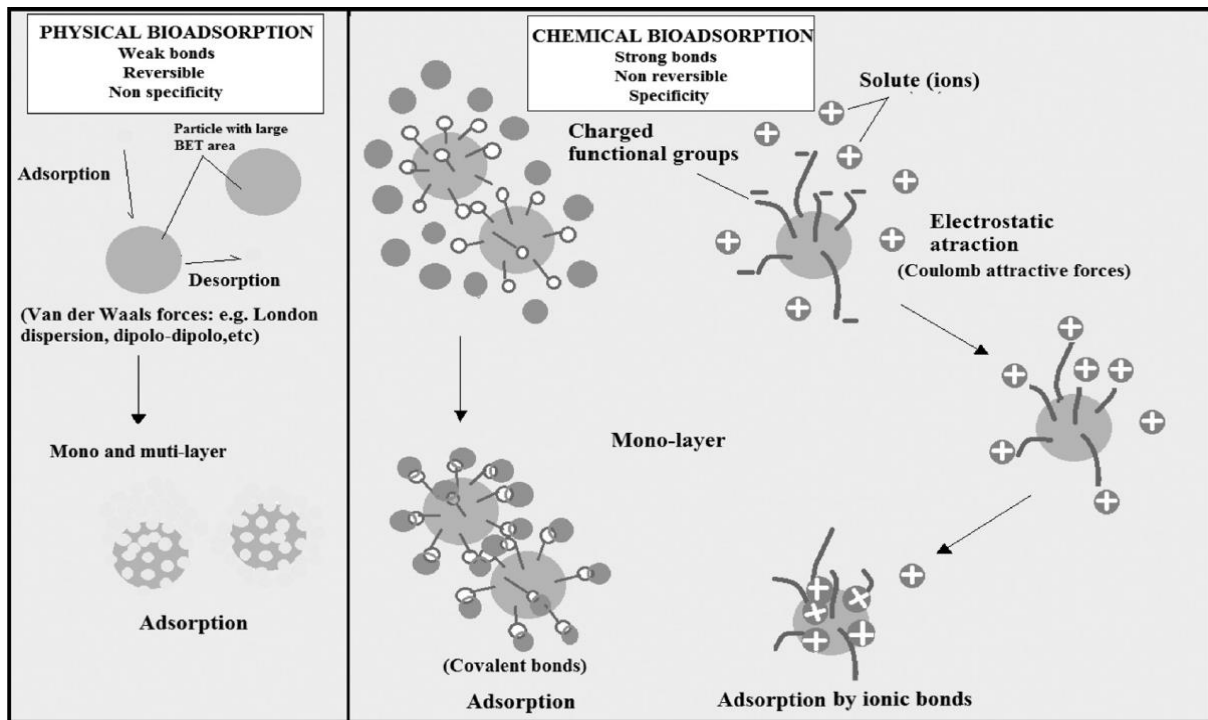


Figure 3. Schematic representation of contaminants removal via different adsorption mechanisms [85].

Influencing factors

Since biosorption is not a homogeneous process, the efficiency of NH_4^+ and PO_4^{3-} removal by AFW is affected by a variety of factors including bio-adsorbent dose, adsorbate concentration, solution pH, contact time, temperature and presence of interfering ions [36].

- **Solution pH:** Several studies on NH_4^+ and PO_4^{3-} biosorption by AFW proved that the process is highly affected by the solution pH, however detailed theoretical description of this effect is complicated because it is influenced by both adsorbent surface characteristics and adsorbate properties in a complex manner. The main pH effects are the protonation/ deprotonation of the adsorbate and the change of the surface charge of the adsorbent. Generally, the adsorption of cations increases with increasing pH, whereas the adsorption of anions increases with decreasing pH [68]. For example, Benyoucef and Amrani reported the effective pH range for PO_4^{3-} biosorption by Aleppo pine sawdust to be between 3.5 and 7.5 [76]. In another study, Xu and coworkers explored that modified cotton stalk can remove PO_4^{3-} efficiently in the pH range 4–9 [80]. On the other hand, Liu and coworkers found that the optimum pH to

remove NH_4^+ using peanut shells, corncobs and cotton stalks was neutral [71]. In another study, Ismail and Hameed found that the optimum pH for the biosorption of NH_4^+ by raw corn cob residue to be between 4.5 and 9 [86].

- **Temperature:** For adsorption of NH_4^+ and PO_4^{3-} from aqueous solution by AFW, the effect of temperature is related to the nature of AFW's surface (energetically heterogeneous or homogeneous) that governs the nature of the adsorption mechanism (exothermic physisorption or endothermic chemisorption). Moreover, it is important to note that increasing temperature can have variable effects and it is not always beneficial for the process [68]. In general, numerous studies have shown that by increasing temperature of the solution to a specific range, the removal efficiency also increases. Kumar and coworkers suggested that elevated temperature leads to an increase in the rate of diffusion of PO_4^{3-} , which in turn enhances the adsorption capacity [87]. On the other hand, Hou and coworkers found that the optimal temperature for NH_4^+ removal from aqueous solution using giant reed straw was between 10 and 40 °C [73].
- **Bio-adsorbent Dose:** All scientific studies indicated that NH_4^+ and PO_4^{3-} removal rate increased by increasing the bio-adsorbent dose but the amount of molecules adsorbed per unit mass of adsorbent (q_e) decreased [36]. One simple explanation for this effect is that by adding more bio-adsorbent to the solution, more binding sites are available for NH_4^+ and PO_4^{3-} uptake [69,86]. However, increasing the bio-adsorbent dose could not be operationally and economically beneficial.
- **Contact time:** The required contact time for the biosorption system to reach equilibrium is an indicator of the process rate and speed and it is a critical factor in evaluating the efficacy of AFW for their practical application as bio-adsorbents in wastewater treatment [24]. The equilibrium time of the biosorption process can be divided on three phases:
 - **Initial phase:** It is characterized by high removal rate because of the large amount of adsorbate attached to the large active sites present in AFW's surface.
 - **Intermediate phase:** As the contact time increases, the adsorption rate gradually becomes slower because of the decrease of available active sites able to bind the adsorbate.
 - **Saturation phase:** The lack of free active sites on the bio-adsorbent surface at this time induces the removal rate to be inconsiderable and reached a

constant value where no more adsorbate was removed from the solution (equilibrium phase).

For NH_4^+ and PO_4^{3-} biosorption by AFW, the process was found to be rapid and reaching equilibrium in less than 1h by several researchers, contrariwise, other researchers reported that longer contact time was necessary to reach equilibrium by other type of AFW as illustrated in Table 1.

- Initial adsorbate concentration: Generally, initial adsorbate concentration is one of the most influencing factors on the adsorption process [88]. The removal rate is the highest at lowest initial adsorbate concentration due to the abundance of active sites on the adsorbent's surface thus the driving force of the process is high. While, by increasing the concentration of adsorbate, the adsorption driving force decreases with time due to the saturation of free active sites [89].
- Interfering ions: Since wastewater contains various ions, investigating the effect of these interfering ions on the biosorption of NH_4^+ and PO_4^{3-} is necessary not only for possible decrease in efficiency caused by their presence, but also for toxicity that they may have and therefore regenerated bio-adsorbent cannot be used further as fertilizer. Many researchers have studied the effect of interfering ions on the biosorption of NH_4^+ and PO_4^{3-} by AFW and results showed that this parameter depends on the solid-liquid interface particularly the properties of ions present in solution and possible interactions between them and AFW's surface. Jyothi stated that the presence of anions like SO_4^{2-} , NO_3^- and CO_3^{2-} did not show any significant influence on PO_4^{3-} uptake by different AFW, while the presence of some cations such as Ca^{2+} , Mg^{2+} , Cu^{2+} , Fe^{2+} and Zn^{2+} facilitates the process [90]. Contrarily, Namasivayan and Sangeetha explored that the presence of ClO_4^- , SeO_3^{2-} and SO_4^{2-} hindered PO_4^{3-} removal by activated coir pith carbon [91]. On the other hand, Shang and coworkers reported that the presence of interfering cations such as K^+ , Na^+ , Ca^{2+} and Mg^{2+} reduced the adsorption capacity of modified biochar toward NH_4^+ [92]. In another study, yang and coworkers found that NH_4^+ biosorption by pine sawdust and wheat straw biochars were more efficient in solutions containing monovalent cations such as Na^+ and K^+ than solutions containing divalent cations such as Ca^{2+} and Mg^{2+} [93]. Contrariwise, Lee and others reported that the presence of interfering ions (i.e., Na^+ , K^+ or Ca^{2+}) has a negligible effect on the adsorption of NH_4^+ by conocut-shell activated carbon [94].

2.2.4 Biosorption Modelling

Isotherm

The usual method for evaluating the adsorption mechanisms is through adsorption isotherm which is a curve relating equilibrium concentration of a solute on the surface of an adsorbent (q_e), to the concentration of the solute in the liquid (C_e) with which it is in contact as shown in Figure 4. Determination of isotherm can be carried out using method described in (Appendix 1) which helps to understand the nature of interactions adsorbent/ adsorbate and identify the type of adsorption (i.e., monolayer or multilayer formation) [95].

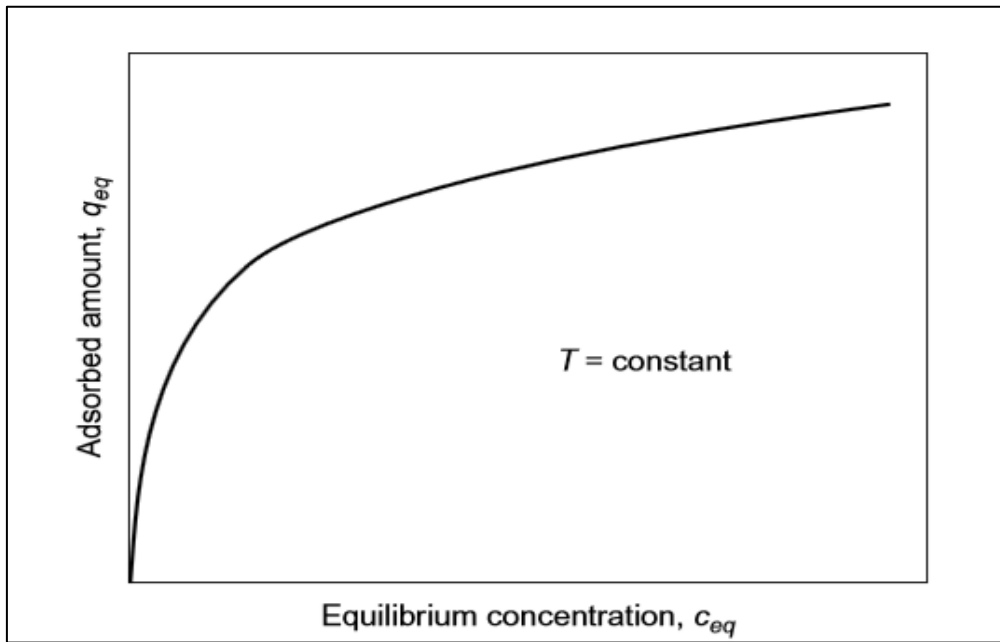


Figure 4. General aspect of adsorption isotherm [68]

The equilibrium concentration of a solute on the surface of an adsorbent can be calculated using Eq. (1):

$$q_e = (C_i - C_e) \frac{V}{m} \quad (1)$$

where: q_e ($\text{mg}\cdot\text{g}^{-1}$) is the amount of adsorbate per mass unit of adsorbent at equilibrium, C_i and C_e ($\text{mg}\cdot\text{L}^{-1}$) are the initial and equilibrium concentration of adsorbate respectively, V (L) is the volume of the solution and m (g) is the mass of adsorbent.

No universal isotherm model was found to describe all experimental isotherm curves with the same accuracy and most of the single-solute isotherms were originally developed for gas or vapour adsorption [95]. The most commonly used isotherms for application in water and wastewater treatment are Freundlich and Langmuir models (Table 2). In order to select

isotherm model that adequately describes the adsorption mechanism, experimental isotherm curve have to be fitted to mathematical equations of these isotherms models [96].

Table 2. Freundlich and Langmuir isotherm models

| Model | Non-linear form | Parameters |
|------------|---|---|
| Langmuir | $q_e = \frac{q_{max} k_L C_e}{1 + k_L C_e}$ | q_{max} (mg.g ⁻¹): Maximum amount of solute adsorbed. q_e (mg.g ⁻¹): Amount of solute adsorbed at equilibrium. k_L (L.mg ⁻¹): Constant related to the energy of sorption. |
| Freundlich | $q_e = k_F C_e^n$ | C_e (mg.L ⁻¹): The equilibrium concentration. k_F : Constant related to the adsorption capacity n : Constant related to the adsorption intensity |

Kinetics

Adsorption kinetics present the time progress of the adsorption process (Figure 5). Investigations into kinetics are necessary to clarify the possible mechanisms and rate-limiting step of the process [60].

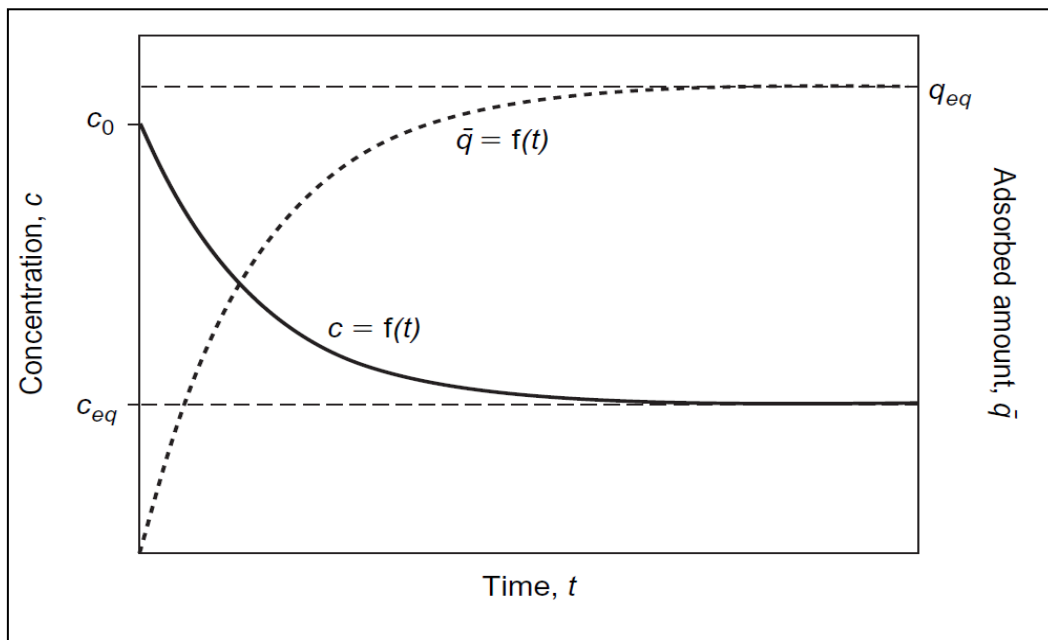


Figure 5. General aspect of kinetics of adsorption process [68]

In order to identify kinetics that adequately describe the adsorption process, adsorption data has to be fitted to existing kinetics models. Several kinetic models can be tested such as pseudo-first (PFO), pseudo-second order (PSO), Elovich, and Intra-particle diffusion as shown in Table 3.

Table 3. Kinetic models and their equations

| Model | Non-linear form | Parameters |
|--------------------------|---|---|
| Pseudo-first order | $\frac{dq_t}{dt} = k_1(q_e - q_t)$ | q_t (mg.g ⁻¹): amount of solute adsorbed per unit weight of solid at time (t). q_e (mg.g ⁻¹): Amount of solute adsorbed at equilibrium t (min): time K_1 (min ⁻¹): PFO rate constant K_2 (g.mg ⁻¹ .min ⁻¹): PSO rate constant α (mg.g ⁻¹ .min ⁻¹): Rate of chemisorption at zero coverage β (g.mg ⁻¹): Extent of surface coverage k_3 : Intra-particle diffusion constant |
| Pseudo-second order | $\frac{dq_t}{dt} = k_2(q_e - q_t)^2$ | |
| Elovich | $\frac{dq_t}{dt} = \alpha \cdot \exp(-\beta q_t)$ | |
| Intra-particle diffusion | $q_t = k_3\sqrt{t}$ | |

Kinetics of adsorption process can be divided in four consecutive steps as shown in Figure 6.

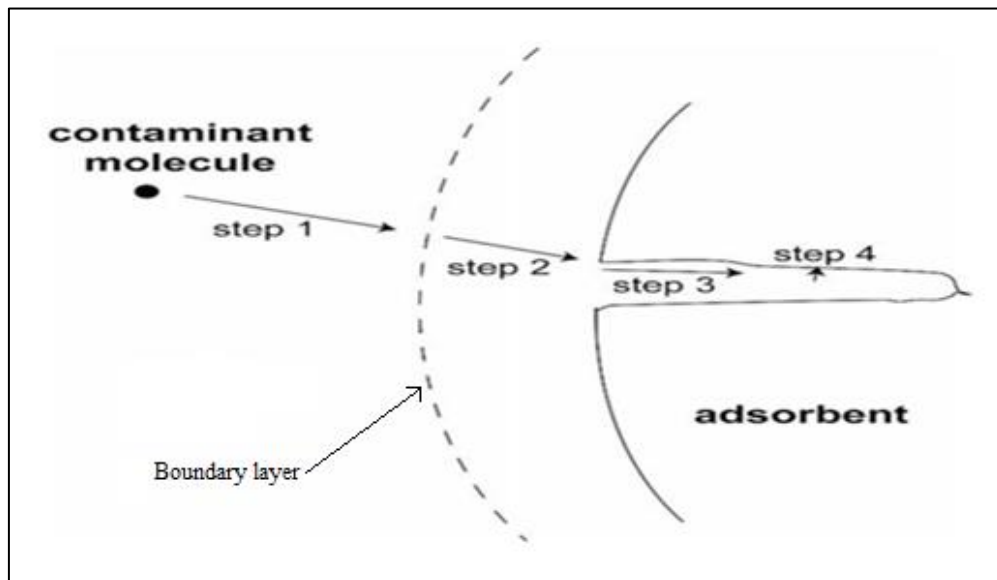


Figure 6. Steps of adsorption kinetics

- Step 1: Transport of the adsorbate from the bulk liquid phase to the boundary layer localized around the bio-adsorbent particle.
- Step 2: Transport through the boundary layer to the external surface of the bio-adsorbent, termed film diffusion or external diffusion.
- Step 3: Transport into the interior of the bio-adsorbent particle (termed intra-particle diffusion or internal diffusion) by diffusion in the pore liquid (pore diffusion) and/or by diffusion in the adsorbed state along the internal surface (surface diffusion)
- Step 4: Energetic interaction between the adsorbate molecules and the final adsorption sites present in the surface of the bio-adsorbent.

Thermodynamics

Thermodynamic is the consequence of the adsorption process, it can help to identify whether the sorption process follows physisorption or chemisorption mechanisms and whether it is spontaneous or non-spontaneous. It investigates also the range of temperature at which the adsorption process is favourable or unfavourable. Further, investigations of thermodynamic parameters are also helpful in the adsorption process optimization and alteration [97]. For these purposes, thermodynamic parameters such as free energy change (ΔG°), enthalpy change (ΔH°) and entropy change (ΔS°) should be calculated. It is possible to calculate these parameters by using Eq. (2) and Eq. (3):

$$\Delta G^\circ = -R T \ln K_d \quad (2)$$

$$\ln K_d = \frac{\Delta H^\circ}{RT} + \frac{\Delta S^\circ}{R} \quad (3)$$

where: T is the absolute temperature in kelvin and R is the gas constant ($8.314 \text{ J}\cdot\text{mol}^{-1}\cdot\text{K}^{-1}$).

K_d presents the distribution coefficient for the adsorption and it was obtained by plotting $\ln(q_e/C_e)$ against C_e , and extrapolating C_e to zero, then the value obtained was multiplied by 1000 as proposed by Milonjić [98]. Values of ΔH° and ΔS° can be determined from slope and intercept of the linear plot of ($\ln K_d$) versus ($1/T$) as shown in (Figure 7).

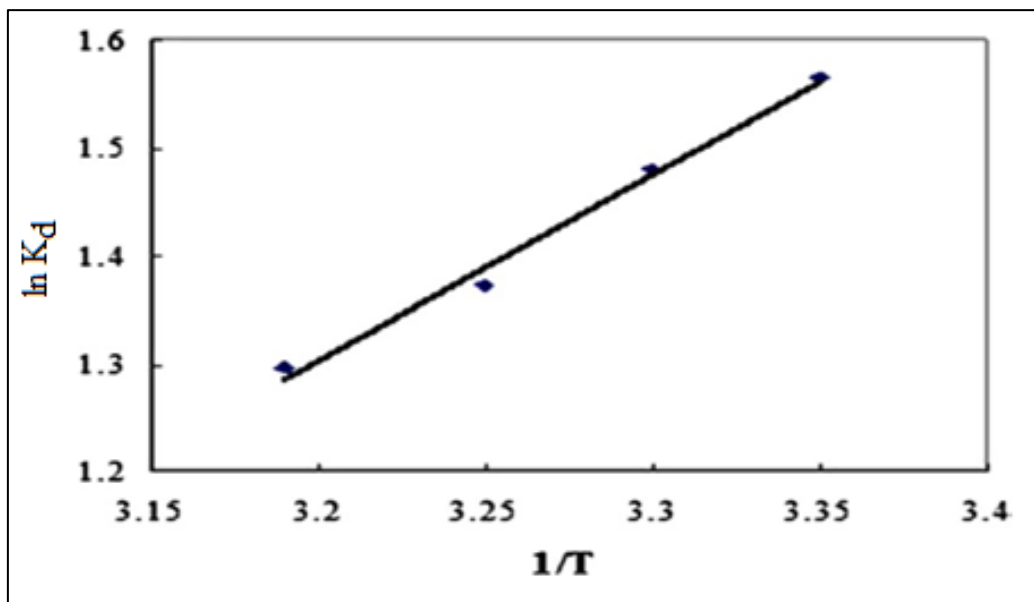


Figure 7. Example of linear plot of $\ln(k_d)$ versus ($1/T$).

The sign of ΔG° helps to predict either if the adsorption process is thermodynamically feasible or non-feasible, if $\Delta G^\circ < 0$, then the adsorption process is always feasible and spontaneous, while if the $\Delta G^\circ > 0$, then the adsorption process is non-feasible and non-spontaneous. On the

other hand, if ΔH^0 is positive then the process is endothermic in nature and if it is negative then the process is exothermic. The positive value of ΔS^0 indicates an increase in the degree of freedom (or disorder) of the adsorbed species [99].

2.3 Pomegranate peel as bio-adsorbent

The pomegranate (*Punica granatum*) is one of the most widely consumed and cultivated fruit in the world thanks to its pleasant taste, high nutritional content and health benefits [100]. The estimated world production of pomegranate was around 3.8 million metric tons in 2017. It is expected that this volume will increase continuously because of the greater interest for increasing the cultivation and industrialization of this fruit, especially in countries known as the most important producers including India, Iran, Turkey, China, United States of America, Egypt, Spain, Italy, Tunisia, Morocco, Argentina, Brazil, Australia and others [101]. This fruit is popularly consumed either fresh or processed into new products such as juice, jams, wines, flavouring and colouring agent, concentrates and jellies [102]. In view of the huge world production of pomegranate and considering that pomegranate peel (PP) comprises between 35 to 50% of the total fruit weight, approximately 1.5 million tons of PP is produced annually which presents an environmental burden [103,104]. However, PP is recognised as an important source of minerals especially potassium, calcium, phosphorus, magnesium, sodium, complex polysaccharides in addition to diverse bioactive chemical compounds such as phenolics, flavonoids, proanthocyanidin compounds, ellagitannins, punicalin, gallic acid, ellagic acid and glycosides [105]. Therefore, PP is considered as one of the most valuable by-product in the food processing industry [106].

As shown in Table 4, PP holds several valuable compounds, therefore, development of an appropriate valorisation approach would not only protect the environment but also promote a “win-win” solution by creating a bio-economy under sustainable development principles [107]. Various valorisation methods have been developed for full exploitation and use of PP in various fields. Traditional methods are mainly the direct use as animal feed [108,109], bio-fertilizer [110] and compost [111]. While most of recent researches have focused on the phenolic content and antioxidant activity of PP. Therefore, It was exploited for recovery of several beneficial compounds such as essential oils [112,113], food additives [114,115] as well as cosmetic and medicinal products [116,117]. In addition, PP was converted into energy and value-added products such as bioethanol [118] and biogas [119,120], however, process complexity and elevated costs limit these methods.

Table 4. Chemical composition of PP [121]

| Element or compound | Amount |
|--|---------------|
| C (g.kg ⁻¹) | 400.9 |
| N (g.kg ⁻¹) | 11 |
| C/N | 39.1 |
| Moisture (g water/ g dry weight) (%) | 7.06±0.07 |
| Proteins (%) | 3.26 ± 0.14 |
| Fat (%) | 3.31 ± 0.05 |
| Minerals (mg.g ⁻¹) | 30.96 |
| Crude fibres (%) | 34 |
| Ash (%) | 3.31 ± 0.05 |
| Carbohydrates (%) | 86.52±0.18 |
| <u>Phenolic acids (µg.g⁻¹)</u> | |
| Gallic | 6208 |
| Chlorogenic | 24659 |
| Caffeic | 228 |
| Catechol | 2423 |
| Hydrolysable tannins (g.kg ⁻¹) | 27-172 |
| Pectin (%) | 8.1 ± 3.5 |
| Essential oils (% w/w) | 0.20 |
| Glucose (% Dry matter) | 27.94 |
| Fructose (% Dry matter) | 32.29 |

Nowadays, there is a trend toward using PP as bio-adsorbent for heavy metals, dyes and other contaminants removal due to several advantages that present this management method [122]. Numerous studies have investigated the use of PP as bio-adsorbent due to the large extent of functional groups present in its surface, namely –OH and –COOH groups [123]. In most of these studies, PP can be effectively used either in raw and modified form or as activated carbons (AC) to eliminate contaminants such as heavy metals and dyes. However, it is believed that the potential application of PP as bio-adsorbent has not been fully explored. Table 5 summarizes the most relevant studies on the use of PP as bio-adsorbent.

Table 5. Possible applications of PP for heavy metals and/or pollutants removal from wastewaters / process waters

| PP form | Target pollutant | Adsorption capacity | Reference |
|------------------|-------------------------------|----------------------------|-----------|
| Raw PP | Cd (II) | 0.075 mmol.g ⁻¹ | [124] |
| | Cu (II) | 0.074 mmol.g ⁻¹ | |
| | Zn (II) | 0.073 mmol.g ⁻¹ | |
| | NI (II) | 0.068 mmol.g ⁻¹ | |
| | Cr (VI) | 0.042 mmol.g ⁻¹ | |
| | Pb (II) | 19.23 mg.g ⁻¹ | [125] |
| | Cu(II) | 30.12 mg.g ⁻¹ | [123] |
| | Cu(II) | 103 mg.g ⁻¹ | [126] |
| | ReactiveYellow 145 | 209.7 mg.g ⁻¹ | |
| | 2,4 dichlorophenol | 65.7 mg.g ⁻¹ | [127] |
| | malachite green | 31.45 mg.g ⁻¹ | [128] |
| crude oil | 92 % removal | [129] | |
| Modified PP | Pb (II) | 27.5 mg.g ⁻¹ | [130] |
| | Cr(VI) | 22.28 mg.g ⁻¹ | [131] |
| | PO ₄ ³⁻ | 40.21 mg.g ⁻¹ | [132] |
| PP active carbon | Cd (II) | 22.72 mg.g ⁻¹ | [133] |
| | Fe (II) | 18.52 mg.g ⁻¹ | [134] |
| | Zn (II) | 89 % removal | [135] |
| | direct blue-106 dye | 90 % removal | [136] |
| | blue reactive dye | 94 % removal | [137] |
| | NI (II) | 10.82 mg.g ⁻¹ | [138] |
| | Ni (II) | 52 mg.g ⁻¹ | [139] |
| | Pb(II) Cu(II) | >90 % removal | [140] |

2.4 Application of nutrient-loaded bio-adsorbents for soil fertilization:

The direct use of nutrient-loaded AFW as fertilizers present an innovative and eco-friendly approach for the sustainable management of nutrients sources and the cost-effectivity of the adsorption technology. This strategy ensure the valorization of AFW as an alternative to chemical fertilizers due to their widespread availability, biodegradability, and nutrient adsorption capacity. Furthermore, AFW are already used to improve soil fertility [141], therefore, they are a suitable substrate to be loaded with nutrients, and compared to conventional fertilizers, they offer several advantages such as soil-deliverability, controlled nutrient release, fewer adverse effects, biocompatibility, and excellent nutrient use efficiency [142]. However, despite the aforementioned advantages, few researchers investigated the application of AFW as fertilizer after adsorption of nutrients. For this purpose, nutrient-loaded

AFW need to be explored further upon their relevant properties, such as nutrient loading capacity, nutrient release rate, adaptability to soil conditions and more importantly their potential toxicity before they can be applied successfully and safely as fertilizer [142]. Robalds and coworkers have used a peat-based biosorbent for phosphate removal and then they tested the phytotoxicity of the spent sorbent as organic fertilizer for further use in agricultural land application [143]. Wheat straw was used by three different researchers for ammonium and phosphate recovery and then it was tested as slow-release fertilizer [144–146]. Tuhy and coworkers have investigated the use of spent mushroom for the same aim [147]. In addition to the above materials, biochars prepared from AFW were also tested as fertilizer after adsorption of nutrients. Shang and coworkers used biochar derived from sawdust as an effective N-fertilizer after adsorption of ammonium [148]. Biochar derived from corn cobs was also examined as a soil conditioner after ammonia adsorption [149]. In another study, Yao and coworkers prepared an engineered biochar from tomato tissue for removal of phosphate and then they regenerated the biochar for use as soil P fertilizer [150].

3 Aims

The overarching aim of this Ph.D. thesis is to produce an efficient bio-adsorbent from AFW for NH_4^+ and PO_4^{3-} removal and recovery from aqueous solutions. Such study can potentially open up the door for a sustainable and green wastewater treatment technology that involves wastewater recycling, nutrients recovery and AFW revalorization.

In order to attain this goal, the following specific objectives have been drawn:

- Conducting a preliminary screening experiments using batch adsorption method in order to test the ability of several AFW to remove NH_4^+ from model solution.
- The focus will be laid on the material that will show the most promising results among AFW tested.
- Investigating the physicochemical properties of the selected AFW using the appropriate techniques and methods.
- Identification of the influencing parameters on NH_4^+ biosorption from model solution by the selected AFW using batch adsorption method.
- Determination of kinetic and isotherm models that adequately describe mechanisms and properties of NH_4^+ biosorption from model solution by the selected AFW.
- Verification of the efficiency of the selected AFW to remove NH_4^+ from a real wastewater using batch adsorption method.
- Identification of the influencing parameters on NH_4^+ biosorption from real wastewater by the selected AFW.
- Determination of kinetic and isotherm models that adequately describe mechanisms and properties of NH_4^+ biosorption from real wastewater by the selected AFW.
- Searching for suitable activation method able to enhance the adsorptive characteristics of the selected AFW for PO_4^{3-} removal and recovery.
- Investigating the new physicochemical properties of the activated AFW.
- Identification of the influencing parameters on PO_4^{3-} biosorption from model solution by the activated AFW using batch adsorption method.
- Determination of kinetics, isotherm and thermodynamics of PO_4^{3-} biosorption by the activated AFW.
- Investigation on the use of nutrient-loaded AFW as fertilizer.

4 Materials and methods

4.1 Bio-adsorbents preparation

Seven AFW were collected, including pomegranate peel, banana peel, wheat husk, compost, poplar bark, wheat bran and sugar beet pulp. Samples were cut into small pieces and washed with distilled water several times to remove dust and impurities, then they were oven dried at 110 °C for two hours. Finally, dried materials were crushed and grinded to desired particle size (< 250 µm).

4.2 Activation of PP

The activation of PP was done using an approach similar to that of Nguyen and coworkers based on iron loading method in order to improve PO_4^{3-} removal ability [151]. The first step of this activation method was the base treatment or saponification, where 40 g of PP was stirred with 1 L of a NaOH solution (0.05 M) at room temperature for 24 h and then washed several times with distilled water until the pH of washing solution became neutral. The saponification step aimed to improve the cationic exchange capacity of PP and promote the incorporation of iron ions (Fe^{3+}) on its surface. The second step was the iron loading, where the saponified PP was stirred with 500 mL of iron chloride (FeCl_3) solution (0.25 M) at room temperature for 24 h. Finally, the iron-loaded PP (IL-PP) was carefully washed with distilled water again and oven-dried at 105°C for 8 h, and then, it was mechanically milled with a planetary ball mill to the desired size (< 250 µm) before use in the adsorption experiments. The NaOH and FeCl_3 solutions were prepared by dissolving specific amounts of NaOH and $\text{FeCl}_3 \cdot 6\text{H}_2\text{O}$ in deionized water.

4.3 Preparation of stock solutions

Stock solution of NH_4^+ was prepared by dissolving 1000 mg of anhydrous ammonium chloride (NH_4Cl) in 1L of deionized water then it was diluted to desired concentrations using distilled water. The same method was followed for PO_4^{3-} stock solution preparation using anhydrous di-sodium hydrogen phosphate (Na_2HPO_4). Initial pH value of solutions was adjusted using NaOH or HCl (0.1 M). All the chemicals used in this thesis were A.C.S certified and obtained from Merck Company (Germany).

4.4 Screening experiments

The screening experiments were performed according to the batch method (appendix 2) using 100 mg of each sample and 60 mL of NH_4Cl solution with initial $\text{NH}_4\text{-N}$ concentration of 30 $\text{mg}\cdot\text{L}^{-1}$. The system was shaken at 100 rpm and at room temperature until equilibrium. To

compare the efficiency of AFW tested for NH_4^+ removal, residual solutions were filtered using 0.45 μm microporous membrane filters. $\text{NH}_4\text{-N}$ concentration was determined by spectrophotometer Spectroquant Nova 60 (Merck, Germany), using test kits that are automatically identified and the measurement value can be immediately read off from the display. NH_4^+ removal rate can be calculated as shown in Eq. (4).

$$\text{Removal \%} = \frac{C_i - C_f}{C_i} * 100 \quad (4)$$

where C_i and C_f are the initial and final $\text{NH}_4\text{-N}$ concentrations in solution, respectively.

4.5 Characterization of PP

4.5.1 Particle size distribution and porosity

The particle size distribution of PP were determined using laser particle size analyzer in dry mode Horiba LA-950V2 (Horiba, Japan). From the measured data, the computer calculated the particle size distribution according to the Fraunhofer theory. Measurement range of the analyzer is between 10 nm and 3 mm.

Porosity is a term that is often used to indicate the porous nature of solid material and is more precisely defined as the ratio of the volume of accessible pores and voids to the total volume occupied by a given amount of the solid. Porosity of PP was determined using automated mercury porosimeter AutoPore IV 9500 Series (Micromeritics, USA). This device characterizes material's porosity by applying various levels of pressure to a sample immersed in mercury then the pressure readings are converted to pore diameter by means of the Washburn equation or by another model. This method is called mercury porosimetry or often "mercury intrusion."

4.5.2 Zeta potential

Zeta potential measurement is a widely used technique for the quantification of the electric double layer charge responsible for electrostatic interactions between the adsorbent's surface and the adsorbate. Zeta potential of PP and IL-PP were determined using 10 mg suspensions mixed in bottles containing 30 ml of NH_4Cl , sodium chloride (NaCl) and Na_2HPO_4 solutions at different concentrations and pH values. After mixing, equilibrium pH of samples was measured and adjusted then zeta potential was measured by zetasizer Nano Zs, (Malvern, UK) using electrophoretic light scattering (ELS). All samples were prepared in triplicates and the average of measurements was used for data analysis.

4.5.3 FT-IR ATR analysis

PP and IL-PP surfaces were investigated using FTIR-ATR analysis. This technique is widely used to observe functional groups present in the material's surface. The instrument for recording the spectra was spectrophotometer Bio-Rad Digilab Division FTS-65A/896 (Bio-Rad, USA) with 4cm^{-1} resolution. The $4000\text{--}400\text{ cm}^{-1}$ wavenumber range was recorded and 256 scans were collected for each spectrum. In addition to the spectra of each sample, single reflection of diamond ATR accessory measurements were taken.

4.5.4 Scanning electron microscope SEM

SEM was used for imaging the microstructure of PP and IL-PP to observe the variations on their surface morphology. For this purpose, samples were analysed using Hitachi S-4700 type II scanning electron microscope (Hitachi, Japan). For the production and acceleration of the electron beam, a cold field emission gun and 10 kV acceleration voltage were applied, respectively. The micrographs were recorded by collecting secondary electrons with an Everhart–Thornley detector.

4.5.5 Batch adsorption studies

Batch adsorption method was used in order to study the equilibrium characteristics of NH_4^+ adsorption by PP from NH_4Cl solution and milking parlour wastewater (MPWW). The first series of experiments were carried out to assess the effect of parameters such as initial NH_4^+ concentration, pH, adsorbent dose, stirring speed, temperature and contact time using the one factor at a time method (OFAT). For the measurement of $\text{NH}_4\text{-N}$ concentration, method used in the screening experiments was followed and NH_4^+ removal rate was calculated using Eq. (4). The adsorbed amount of $\text{NH}_4\text{-N}$ was calculated using Eq. (1) cited in the literature review section where C_i (mg.L^{-1}) and C_e (mg.L^{-1}) are the initial and equilibrium $\text{NH}_4\text{-N}$ concentrations in solution, respectively. V (L) is the solution volume and m (g) is the mass of PP.

For isotherm and kinetics modelling, data were fitted to the existing models using linear method and the best-fit models were selected based on the highest correlation coefficient (R^2) and agreement of experimental data with calculated parameters.

Batch adsorption method was also used for studying the adsorption of PO_4^{3-} from model solution by IL-PP. However, to identify the influencing and optimum parameters for higher PO_4^{3-} removal, factorial design using Minitab19 software was applied.

Spectrophotometry method using Spectroquant Nova 60 (Merck, Germany) was also used for the determination of (PO₄-P) concentration. Before measurements, samples were filtered through 0.45µm microporous membrane.

Removal rate of PO₄³⁻ was calculated using Eq. (4) where C_i (mg.L⁻¹) and C_f (mg.L⁻¹) are initial and final PO₄-P concentrations in solution, respectively. Similarly, the adsorbed amount of PO₄-P was calculated using Eq. (1) where C_i (mg.L⁻¹) and C_e (mg.L⁻¹) are initial and equilibrium concentrations of PO₄-P in solution respectively; V (L) represents the solution volume, and m (g) represents the mass of IL-PP.

Optimum results obtained from batch adsorption experiments series were used for adsorption isotherm and kinetics determination. In order to identify isotherm and kinetic models that adequately describe PO₄³⁻ adsorption by IL-PP, non-linear method was performed using the Solver add-in, Microsoft Excel [152]. Application of this method instead of the linear one is highly recommended because it provides accurate fitting results based on values of non-linear correlation coefficients (R^2) and chi-square (χ^2) that can be calculated using Eq. (5) and Eq. (6), respectively:

$$\chi^2 = \sum \frac{(q_{e,exp} - q_{e,cal})^2}{q_{e,cal}} \quad (5)$$

$$R^2 = \frac{\sum (q_{e,cal} - q_{e,mean})^2}{\sum (q_{e,cal} - q_{e,mean})^2 + \sum (q_{e,cal} - q_{e,exp})^2} \quad (6)$$

Where: $q_{e,exp}$ (mg.g⁻¹) is the amount of PO₄-P uptake at equilibrium, $q_{e,cal}$ (mg.g⁻¹) is the amount of PO₄-P uptake achieved from the model using the Solver add-in, and $q_{e,mean}$ (mg.g⁻¹) is the mean of the $q_{e,exp}$ values.

Selection of best-fitted kinetic and isotherm model is mainly based on the value of R^2 , however, statistics of χ^2 confirm this selection. When χ^2 is close to zero, data obtained using a model are similar to the experimental data while high value of χ^2 is a sign of inappropriate model [153].

For describing thermodynamic properties of PO₄³⁻ adsorption by IL-PP, thermodynamic parameters including ΔG° , ΔH° and standard ΔS° were calculated using the method and appropriate equations described in literature review section; Eq. (2) and Eq. (3).

4.6 Milking parlour wastewater (MPWW)

Wastewater used for NH₄⁺ biosorption study was sampled from a milking parlour unit near the city of Szeged, Hungary on 13/04/2019. A volume of 20L of MPWW was generated from washing operations discharges and it consists of water, cleaning chemicals, manure, and urine

thus this wastewater contains high levels of nutrients mainly NH_4^+ , along with other ions such as potassium (K^+), calcium (Ca^{2+}), magnesium (Mg^{2+}), sodium (Na^+) and heavy metals [154]. The collected volume was stored in the laboratory's freezer before characterization and use for the adsorption experiments. Chemical oxygen demand (COD) was measured using the colorimetric method (APHA 5220D 2005). 5 days biochemical oxygen demand (BOD_5) was determined by respirometric method at a controlled temperature of 20 °C for a 5-day-long period using Lovibond Oxidirect (Germany). Total nitrogen (TN) content was determined by Torch (Teledyne Tekmar, U.S.) combustion (HTC) type analyzer equipped with pressurized NDIR detector. Ammonium content was determined using spectrophotometry method by Spectroquant Nova 60 (Merck, Germany). Table 6 presents the main characteristics of MPWW used.

Table 6. Characteristics of MPWW.

| Parameter | value |
|--|----------|
| pH | 7±1 |
| COD ($\text{mg O}_2\cdot\text{L}^{-1}$) | 4850±500 |
| BOD_5 ($\text{mg O}_2\cdot\text{L}^{-1}$) | 1200±300 |
| Total Nitrogen TN ($\text{mg}\cdot\text{L}^{-1}$) | 120±10 |
| $\text{NH}_4\text{-N}$ ($\text{mg}\cdot\text{L}^{-1}$) | 80±10 |

4.7 Application of nitrogen-loaded PP and phosphorus-loaded IL-PP as fertilizer

In order to evaluate the potential use of nitrogen-loaded PP (N-PP) and phosphorus-loaded IL-PP (P-IL-PP) as fertilizer, their suitability to provide necessary nitrogen and phosphorus in soil without causing toxicity to plants has to be investigated. Since the wastewater used for nitrogen and phosphorus recovery (MPWW in our case) contain toxic compounds such as heavy metals, phytotoxicity tests were performed using N-PP and P-IL-PP prior that they can be cycled back directly to the soil as an effective fertilizer. PP loaded with nitrogen (0.5 to 10 $\text{mg}\cdot\text{N}\cdot\text{g}^{-1}$), and IL-PP loaded with phosphorus (0.5 to 5 $\text{mg}\cdot\text{P}\cdot\text{g}^{-1}$) were tested for their phytotoxicity using germination and pot bioassays. The difference in the amount of nitrogen and phosphorus laden in the material is due to the fact that MPWW used for the adsorption experiments was taken at different time intervals.

4.7.1 Germination test

In this study, the phytotoxicity effect of Raw-PP, N-PP and P-IL-PP was studied in terms of relative seed germination (RSG), relative root elongation (RRE), and germination index (GI) using rapeseed (*Brassica napus* L.), which is commonly used in phytotoxicity studies. Ten seeds of *Brassica napus* L. were placed and equally distributed on filter paper in 9-cm diameter Petri dishes. Raw-PP, N-PP and P-IL-PP were suspended in 20 mL of distilled water for use as a medium for seeds germination, and then 3 mL of each of the following treatments was added in triplicate:

- Distilled water for the control
- Raw-PP (0.05 %, 0.5% and 5% of dry matter)
- N-PP (0.05 %, 0.5% and 5% of dry matter)
- P-IL-PP (0.05 %, 0.5% and 5% of dry matter)
- Mixture of N-PP and P-IL-PP (Mix) (0.05 %, 0.5% and 5% of dry matter)

The petri dishes were incubated at 25°C in a dark incubator for 4 days. Seeds with visible roots after 4 days were counted as germinated. Root lengths were measured from the transition points among the hypocotyl to their extremities based on their digital images using ImageJ software. Then, RSG, RRE and GI were calculated using the following equations.

$$\text{RSG}(\%) = \frac{\text{Number of seeds germinated in the sample extract}}{\text{Number of seeds germinated in the control}} \times 100 \quad (7)$$

$$\text{RRE}(\%) = \frac{\text{Mean root elongation in the sample extract}}{\text{Mean root elongation in the control}} \times 100 \quad (8)$$

$$\text{GI}(\%) = \frac{(\% \text{ Seed germination}) \times (\% \text{ Root elongation})}{100} \quad (9)$$

4.7.2 Pot experiments

An outdoor pot experiment was conducted at the Department of Biotechnology of the University of Szeged to examine the effects of N-PP and P-IL-PP on both vegetative and reproductive growth *Brassica napus* L. For this purpose, treatments used in the germination test were used also for this experiment namely: control, Raw-PP, N-PP, P-IL-PP and Mix at 3 different doses: 0.05, 0.5 and 5% of dry matter. 15 treatments with 3 replicates were included so that a total of 45 pots were cultivated. The treatments were manually mixed into Mr. Garden flower soil (pH: 5.5, N: 0.1% (m/m), P₂O₅: 0.01% (m/m), K₂O: 0.03% (m/m), organic matter: 75% (m/m) and 70% initial water content) using a wooden stick. Then, a 2 L

polypropylene pot (15 cm diameter) was filled with 600 g of the prepared soil medium. *Brassica napus* L. seeds were pre-germinated for 24 h at 26 °C. Then, the germinated seeds were transplanted uniformly in pots (7 seeds each). Pots were then placed in a bright area protected from direct sunlight under natural weather conditions. Plants were watered only if necessary. After 32 days, plant habits of rapeseed seedlings were recorded and harvested. Then, the basic morphological parameters were measured including the number of leafs in addition to fresh and dry weights of roots and shoots.

5 Results and discussion

5.1 Screening results

Results of screening experiments presented in Table 7 show that most of AFW tested have low efficiency in NH_4^+ removal from NH_4Cl solution. The removal rates using wheat bran, wheat husk, sugar beet pulp and bark were only 6.7%. Moreover, removal rates using banana peel and compost were negative; -6% and -2%; respectively. As the compost purchased from the market and the banana peel contain nitrogen [155,156], we can assume that these biomaterials release nitrogen in solution that combines with H^+ to form NH_4^+ . Therefore, final concentration of $\text{NH}_4\text{-N}$ in solution is higher than its initial concentration resulting in a negative removal rate. However, removal of NH_4^+ using PP was 36.7% effective, therefore, the focus will be laid on this potential bio-adsorbent.

Table 7. Removal rates of NH_4^+ by AFW tested

| AFW tested | NH_4^+ removal at equilibrium (%) |
|------------------|--|
| Compost | - 2 |
| Wheat bran | 6.7 |
| Wheat husk | 6.7 |
| Pomegranate peel | 36.7 |
| Sugar beet pulp | 6.7 |
| Poplar bark | 4.2 |
| Banana peel | - 6 |

5.2 Characterization of PP and IL-PP

5.2.1 Particle size distribution and porosity

The particle size of the adsorbent is an important parameter indicating its surface accessibility [68]. PP used in this study has a particle size ranged from 10 μm to 750 μm (Figure 8a). When particle size decreased, the specific surface area increased, leading to better bioavailability and absorptivity due to the fast dissolution of functional ingredients [157].

On the other hand, the porosity of a material affects its physical properties and subsequently its behaviour in its surrounding environment, especially its adsorptive characteristics. Pore size distribution of PP is illustrated in Figure 8b, and it shows that PP has a low porosity (=22.89 %), therefore, the nature of functional groups present on its surface will play a major role in its NH_4^+ adsorption capacity [158].

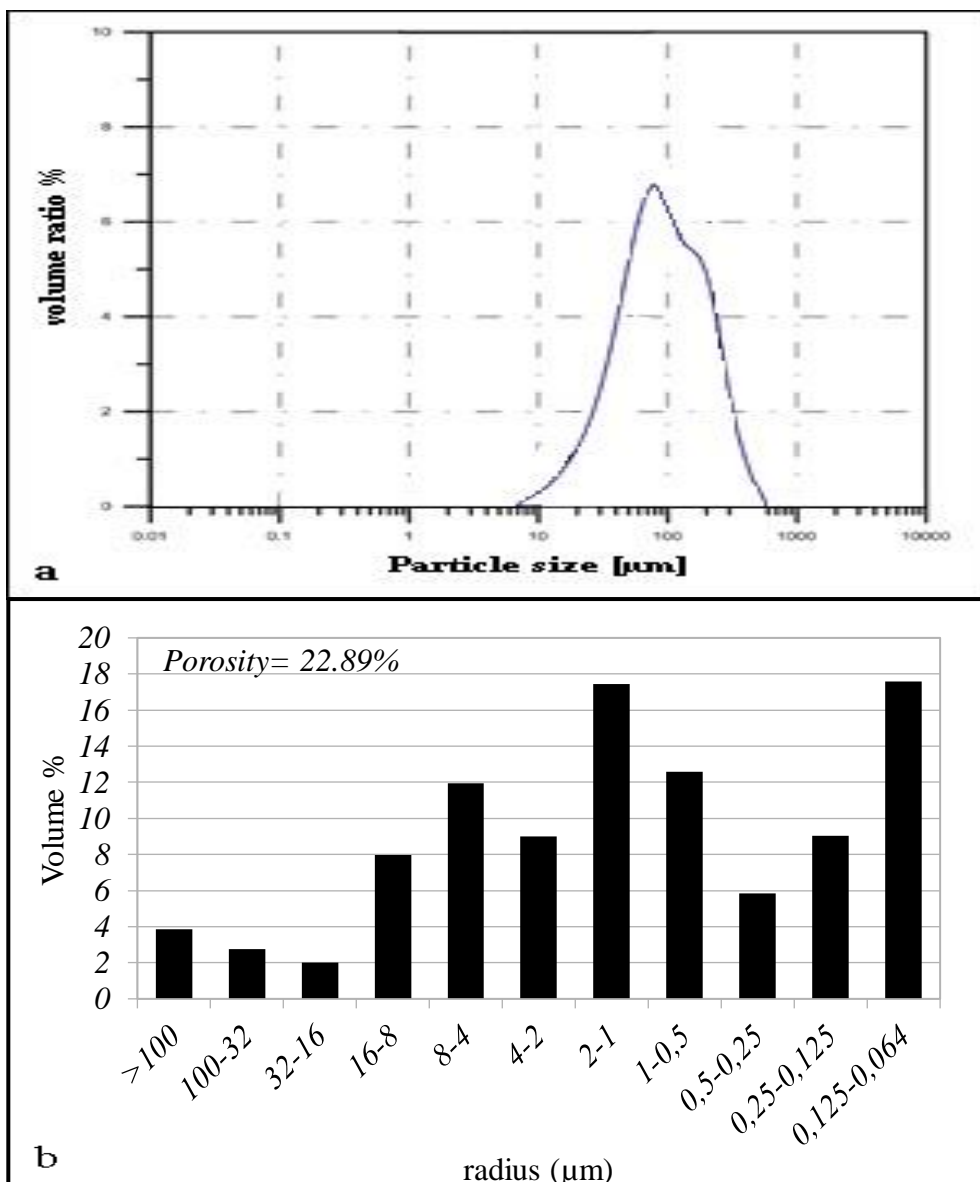


Figure 8. **a.** Particle size distribution of PP, **b.** Pore size distribution of PP

5.2.2 Zeta potential

Determination of zeta potential of the adsorbent at various solutions with different pH values and ionic strength (IS) is of high importance because it gives insights on the adsorbent's surface chemistry and possible interactions with the adsorbate [159]. Zeta potential measurement showed that PP's surface is negatively charged in the studied range of pH and NH_4Cl concentrations. The value of zeta potential decreases from -10.4 mV to -16.5 mV when pH increased from 3 to 7 (Figure 9a). This negatively charged surface represents the driving force for electrostatic interaction with cations present in the solution thus it contributes to the ability of PP to attach NH_4^+ . Similar observations were made on the adsorption of ammonium on wetland-plant derived biochars [160]. In addition, zeta potential

increases from -21.1 mV to -6.2 mV when NH_4Cl concentration increased from 1 to 75 mmol.L^{-1} as shown in (Figure 9b). This behaviour can be explained by the accumulation of NH_4^+ on PP's surface and thus negatively charged functional groups are neutralized. These results suggest that electrostatic interaction is one of the mechanisms involved in the sorption of NH_4^+ by PP.

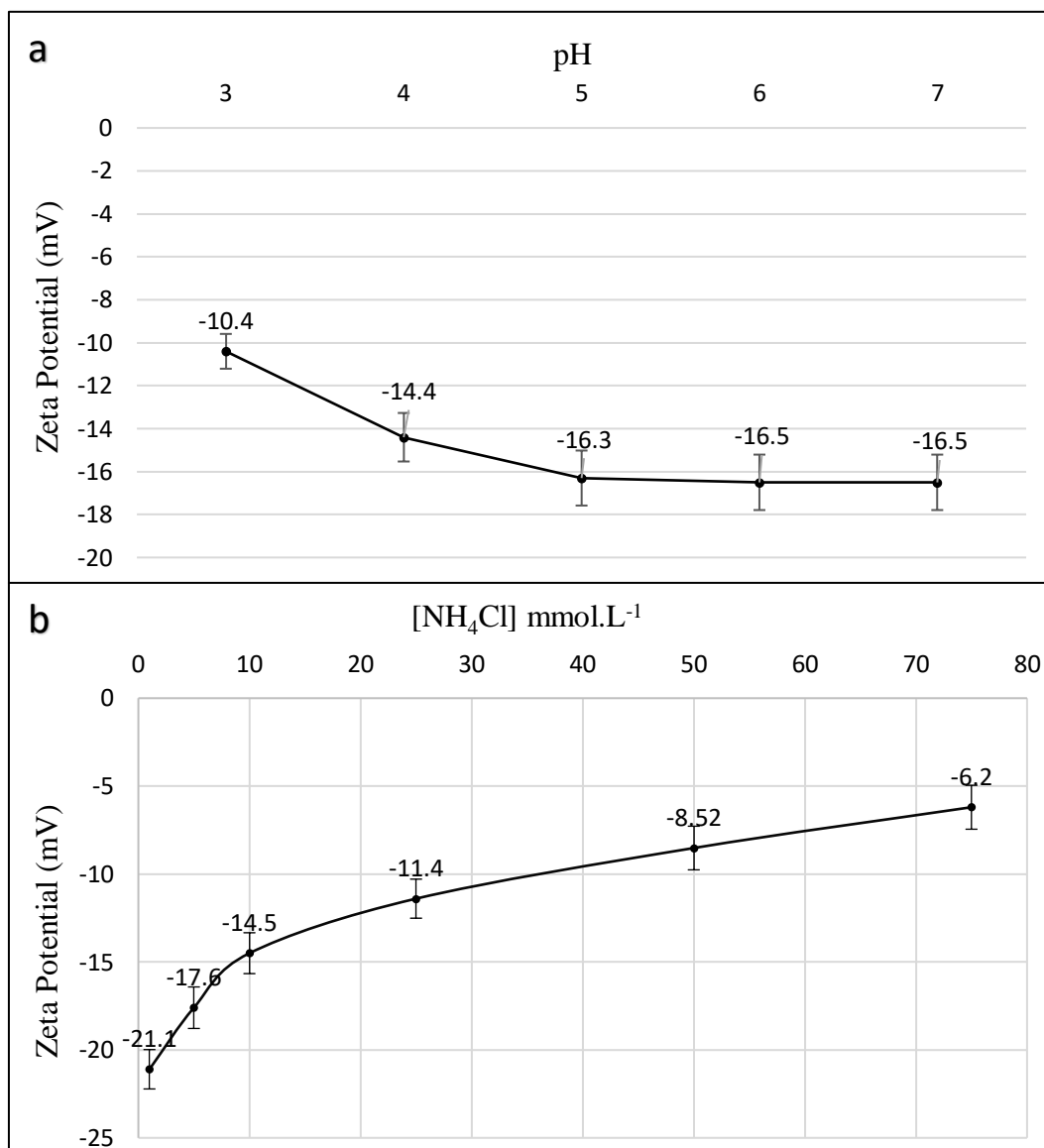


Figure 9. **a.** Zeta Potential of PP as function of pH (NH_4Cl Concentration= 10 mmol.L^{-1}), **b.** Zeta potential of PP as function of NH_4Cl concentration (pH=4).

On the other hand, IL-PP showed a positive zeta potential in NaCl solution (IS=10) over the entire studied pH range (from +5.8 mV at pH 3 to +16.1 mV at pH 9) compared to PP that showed negative values (from -26.7 mV at pH 3 to -30.6 mV at pH 9) as illustrated in Figure 10a. These results indicated that PP's surface became positively charged after incorporation of Fe^{3+} . Moreover, zeta potential of IL-PP in Na_2HPO_4 solution (IS=10) decreased from +11.3

mV to -31.8 mV when pH increased from 3 to 9 and the isoelectric point can be interpolated at pH 5.4 meaning that IL-PP surface has excess negative charge for pH > 5.4 and excess positive charge for pH < 5.4. The decrease in surface charge can be explained by the neutralization of Fe³⁺ present in IL-PP surface by PO₄³⁻. However, in NaCl solution, Cl⁻ cannot neutralize IL-PP surface because there is no chemical interaction between Cl⁻ and Fe³⁺ [161], therefore, specific adsorption mechanism rather than a simple electrostatic attraction is expected between IL-PP surface and PO₄³⁻. On the other hand, zeta potential of IL-PP decreased when Na₂HPO₄ concentration increased as shown in Figure 10b, which can be explained by the compression of the diffuse layer and as a result more PO₄³⁻ anions are attached to this layer. These results are in agreement with findings of Nechifor and coworkers in a study investigating the adsorption kinetics and zeta potential of phosphate and nitrate ions on a cellulosic membrane [162].

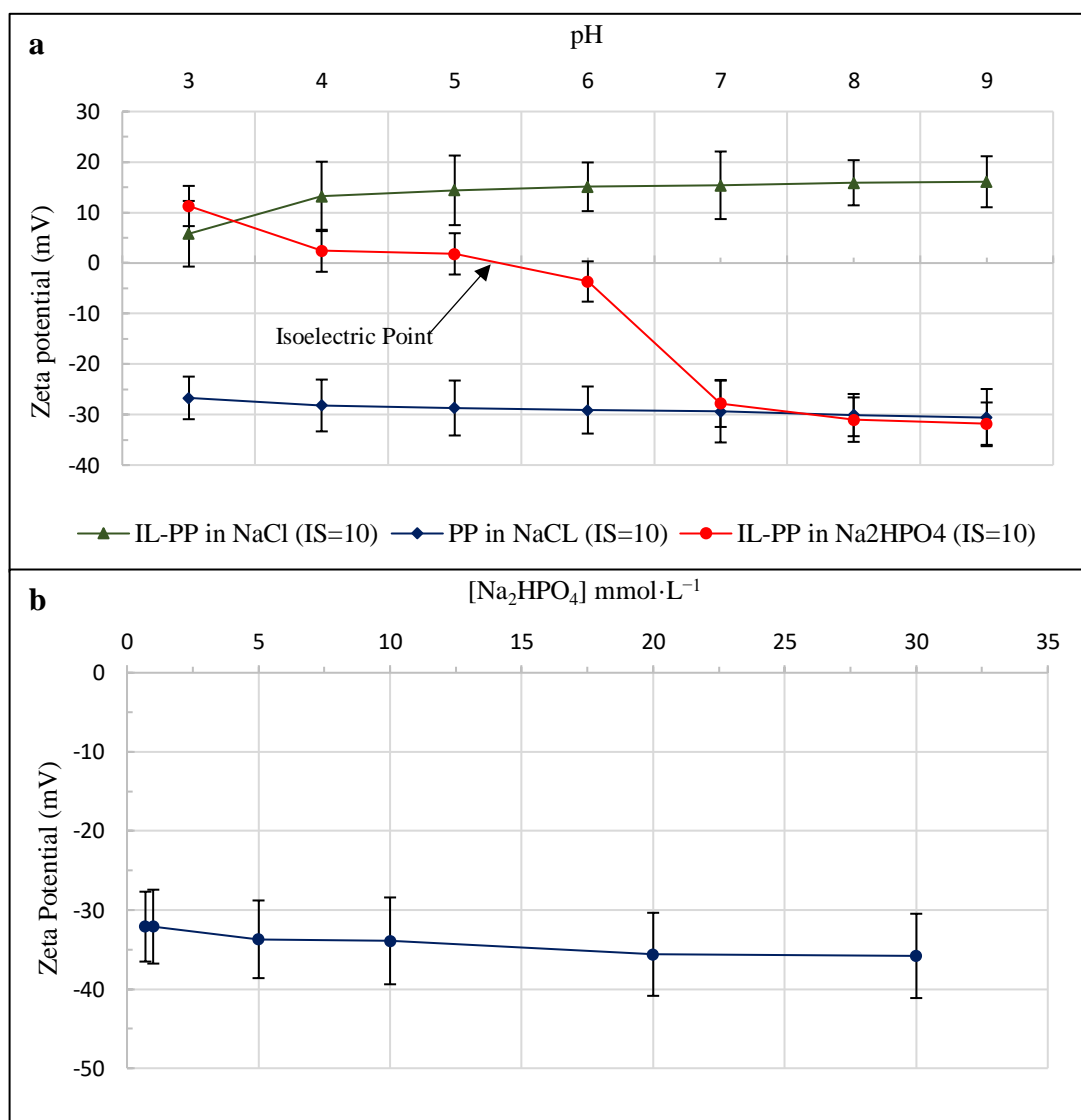


Figure 10. **a.** Zeta potential of PP and IL-PP in NaCl and Na₂HPO₄ solution as function of pH, **b.** Zeta potential of IL-PP in different Na₂HPO₄ solution concentrations

5.2.3 FTIR- ATR analysis

FTIR spectra of PP before and after adsorption of NH_4^+ were used to investigate the functional groups present on PP's surface and to assess the occurred changes after adsorption of NH_4^+ . As illustrated in Figure 11a and Table 8, FTIR spectra of PP display a number of absorption peaks ranging from 400 to 4000 cm^{-1} , indicating the complex nature of this biomaterial. The observed bands in PP's surface agree with similar FTIR studies on functional groups present in PP [163,164]. Two significant differences can be seen between the spectrums of PP before and after NH_4^+ adsorption. These changes are presented by two new well-separated peaks ν_2 and ν_4 appeared at 1656 cm^{-1} and 1370 cm^{-1} , respectively. These variations belong to the stretching vibrations of N-H [165], which confirms the uptake of NH_4^+ by PP.

Table 8. FTIR analysis of PP (before and after NH_4^+ adsorption) and IL-PP (before and after PO_4^{3-} adsorption).

| Adsorption band (cm^{-1}) | | | | Assignment |
|--------------------------------------|-------------------------------------|-------|---|---|
| PP | PP after NH_4^+ adsorption | IL-PP | IL-PP after PO_4^{3-} adsorption | |
| 3323 | 3310 | 3306 | 3327 | –OH and N–H |
| 2931 | 2920 | 2918 | 2924 | C–H, –CH ₃ , or –CH ₂ |
| 1719 | 1720 | – | – | C=O and C–C |
| – | 1656 | – | – | N-H |
| 1615 | – | 1617 | – | C=C, C=O, or N–H |
| – | – | – | 1601 | Fe-P |
| 1442 | – | – | – | –OH |
| – | 1370 | – | – | N-H |
| 1320 | – | 1313 | 1318 | C–H, –CH ₃ , or –CH ₂ |
| 1223 | 1215 | – | – | O–H |
| 1031 | 1030 | 1030 | – | C-O and C-O–C |
| 876 | – | – | – | O–H, C=O, and O–H |
| – | – | 801 | – | Fe–OH |
| 747 | – | – | – | C–N |

Likewise, FT-IR spectra of IL-PP before and after PO_4^{3-} adsorption were also analyzed to confirm the incorporation of Fe^{3+} onto PP's surface and the adsorption of PO_4^{3-} by IL-PP (Figure 11b). Spectra of IL-PP showed important changes characterized mainly by the appearance of a new peak at 801 cm^{-1} , which was previously assigned to (Fe–OH) band by Li and coworkers [154], in addition to disappearance of several bands (1724 cm^{-1} , 1440 cm^{-1} , 1225 cm^{-1} , 875 cm^{-1} and 748 cm^{-1}), which confirms the incorporation of Fe^{3+} onto PP's

surface. On the other hand, spectra of IL-PP after PO_4^{3-} adsorption shows the appearance of a new peak at 1601 cm^{-1} , that was attributed by Carvalho and coworkers to the bending vibration of Fe-P [166], and therefore confirms PO_4^{3-} adsorption by IL-PP.

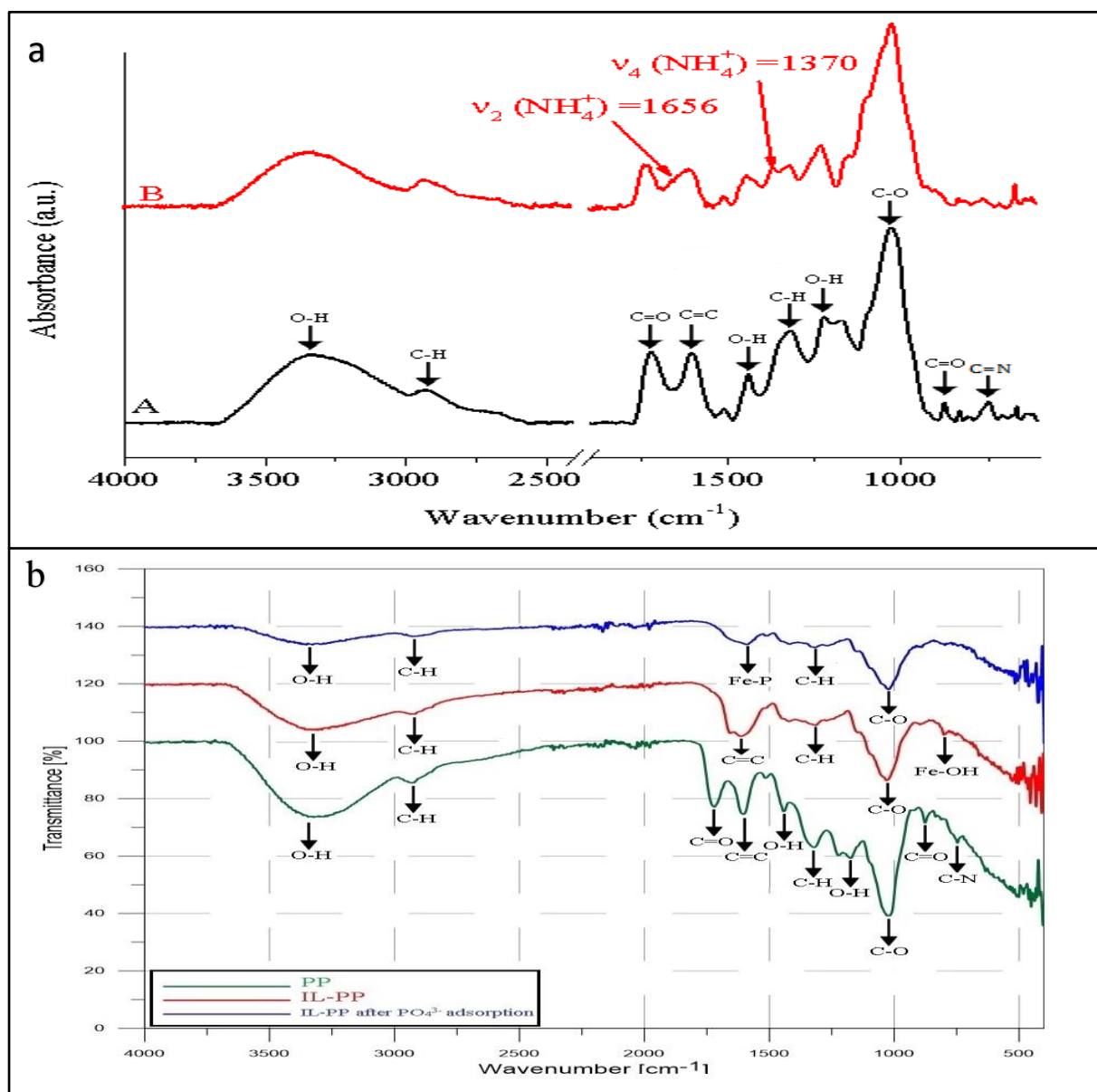


Figure 11. **a.** FTIR of PP before (A) and after adsorption of NH_4^+ (B), **b.** FTIR spectrum of PP and IL-PP before and after PO_4^{3-} adsorption

5.2.4 SEM results

SEM micrographs shows the surface morphology of PP and IL-PP at the same magnification power ($50,000\times$). The texture of PP's surface was flat and smooth (Figure 12a), however, IL-PP showed much rougher surface with coarser texture (Figure 12b). Apparently, inner surface of PP was changed after modification, which is in accordance with the results of FT-IR analysis and proves that Fe^{3+} was successfully incorporated in PP's surface.

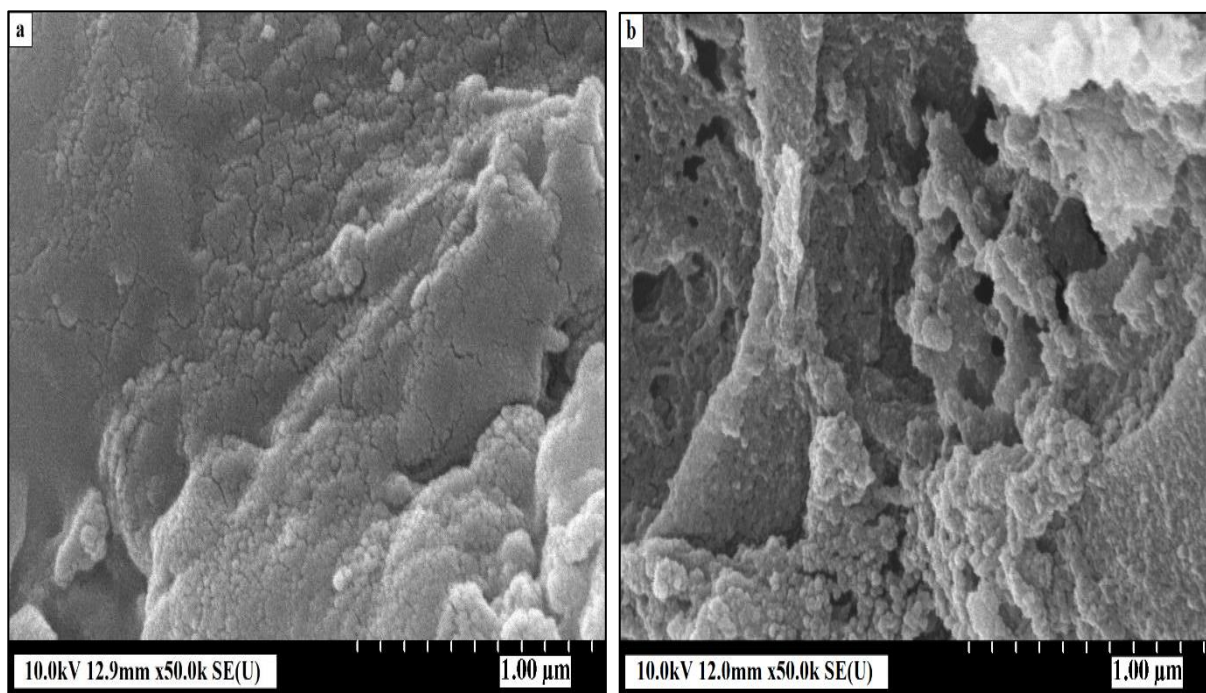


Figure 12.a. SEM of PP, b. SEM of IL-PP

5.3 Biosorption of NH_4^+ from NH_4Cl solution using PP

Among AFW tested, PP showed the most promising results, and as we have seen in literature review section, there are many studies investigating the use of PP for the removal of contaminants from aqueous solutions such as heavy metals and dyes, but no study was conducted before on the application of PP for NH_4^+ removal. Therefore, this study focused on the use of PP to remove NH_4^+ from model solution in order to understand general aspects of NH_4^+ biosorption by determining the influencing parameters, kinetic, and isotherm of the process.

5.3.1 Effect of initial $\text{NH}_4\text{-N}$ concentration

The effect of initial $\text{NH}_4\text{-N}$ concentration on NH_4^+ removal by PP was studied employing different initial concentrations (5, 30, 60, and 90 mg.L^{-1}) while other parameters were kept constant (pH 4, 100 mg of PP, stirring rate of 100 rpm and contact time of 120 min). It is clear from Figure 13 that the removal rate decreased by increasing initial $\text{NH}_4\text{-N}$ concentration. Maximum removal rate was 88% at an initial concentration of 5 mg.L^{-1} , indicating a high affinity of active sites present in PP's surface for NH_4^+ . Low concentration gives enough time for NH_4^+ to bind to active sites present in PP's surface with a slower mass transfer coefficient, while increasing $\text{NH}_4\text{-N}$ concentration leads to an increase in the adsorption driving force, therefore, active sites are rapidly occupied and PP's surface became saturated which in turn leads to a fast breakpoint. However, the amount of $\text{NH}_4\text{-N}$ adsorbed per unit

mass of adsorbent (q_e) decreased due to its low concentration in solution. Similar results were found for NH_4^+ removal by zeolite [167].

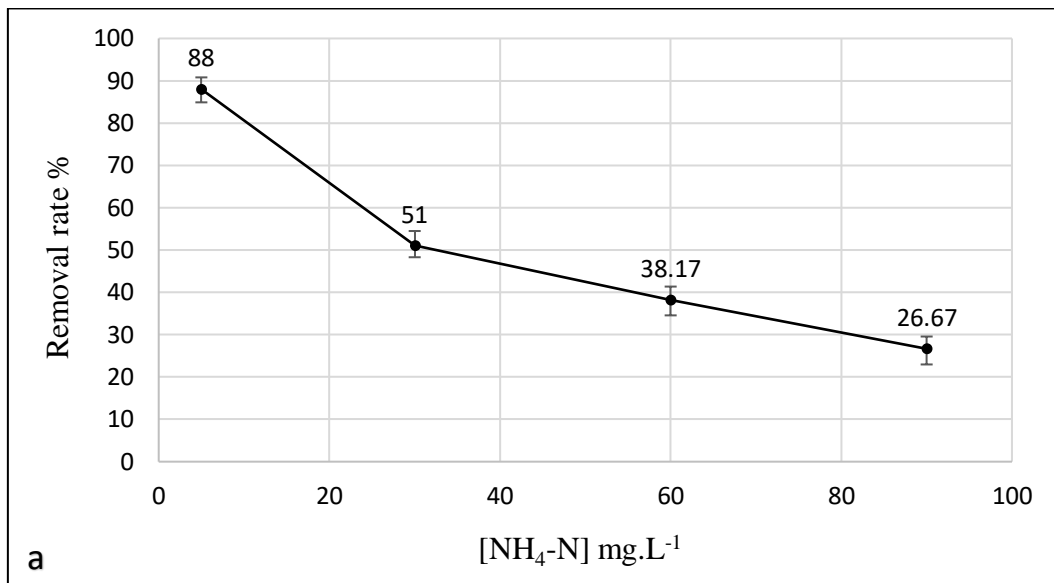


Figure 13. Effect of initial $\text{NH}_4\text{-N}$ concentration (pH 4, 100 mg of PP, stirring rate of 100 rpm and contact time of 120 min).

5.3.2 Effect of solution pH

To study the effect of pH, experiments were performed in solutions with different pH values (3, 4, 5, 6 and 7) and fixed values of other parameters (100 mg of PP, stirring rate of 100 rpm, contact time of 120 min and initial $\text{NH}_4\text{-N}$ concentration of 30 mg.L⁻¹). The initial solution pH plays a critical role in the adsorption processes as it affects both adsorbate and adsorbent characteristics and behaviours, especially in adsorption involving charge–charge interactions [95].

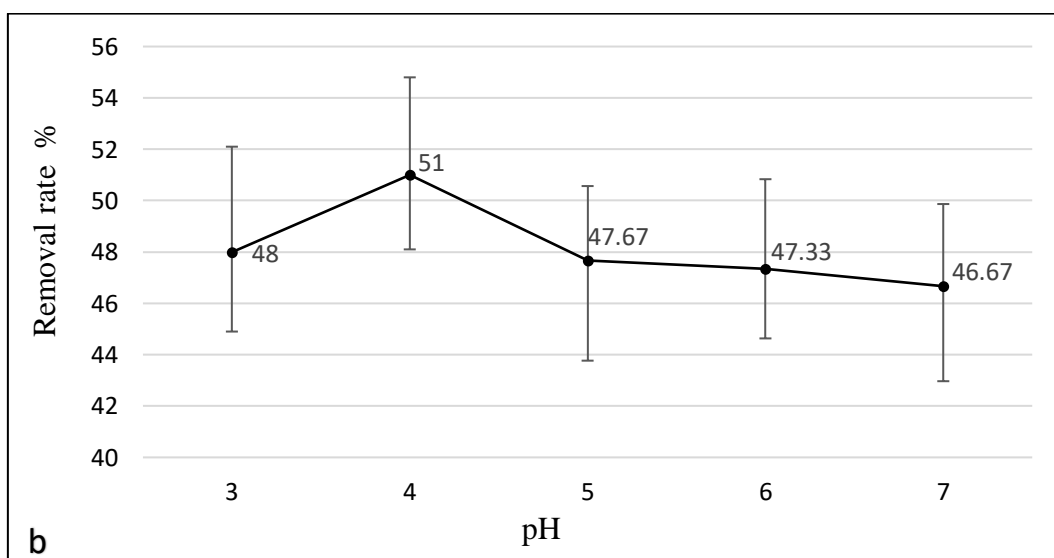


Figure 14. Effect of pH (initial $\text{NH}_4\text{-N}$ concentration of 30 mg.L⁻¹, 100 mg of PP, stirring rate of 100 rpm and contact time of 120 min)

In acidic solutions, more protons H^+ are present and they compete effectively with NH_4^+ to be adsorbed by active sites present in PP's surface, however, this study shows negligible effect of pH with maximum removal at pH 4 (=51%) as shown in Figure 14. This negligible effect could be explained by the large extent of -COOH and -OH groups in PP surface leading to a large number of possible interactions with NH_4^+ and H^+ . Results obtained in this study are in a good agreement with those reported in a previous study using PP for heavy metals removal [168].

5.3.3 Effect of PP dose

The effect of adsorbent dose was studied by varying the used mass of PP and keeping other parameters constant (pH 4, initial NH_4 -N concentration of 30 mg.L^{-1} , stirring rate of 100 rpm and contact time of 120 min). Increasing PP dose from 100 to 400 mg shows a remarkable increase in NH_4^+ removal rate from 47.67% to 97.33%, respectively (Figure 15). This effect can be explained by the fact that increasing the amount of PP provides more active sites for NH_4^+ binding [86].

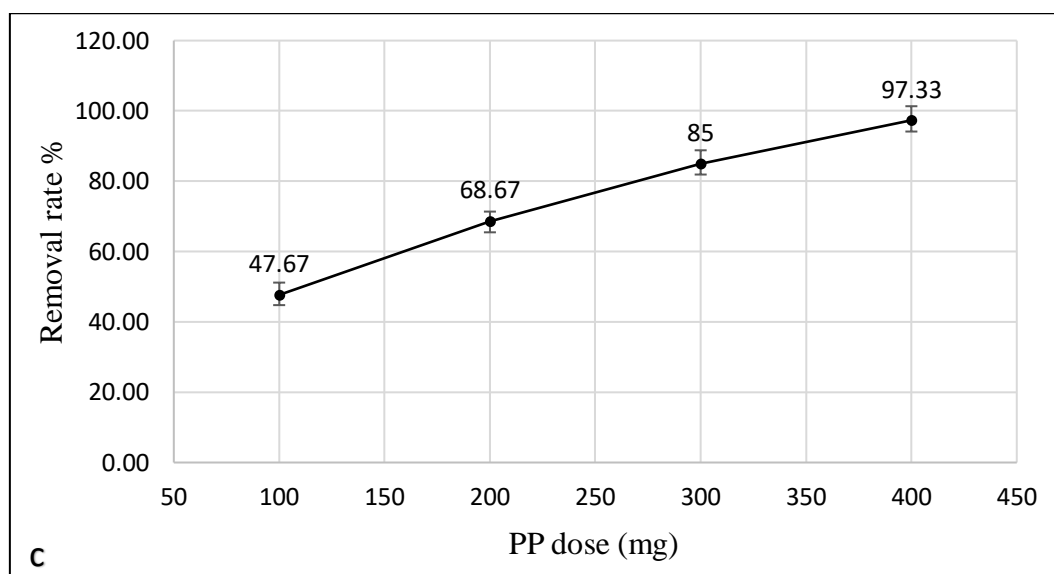


Figure 15. Effect of PP dose (pH 4, initial NH_4 -N concentration of 30 mg.L^{-1} , stirring rate of 100 rpm and contact time of 120 min)

5.3.4 Effect of stirring rate

Stirring rate present the physical driving force in the batch adsorption method. The removal rate of NH_4^+ by PP at different stirring rate (from 100 to 500 rpm) and fixed values of other parameters (pH 4, initial NH_4 -N concentration of 30 mg.L^{-1} , 100 mg of PP and contact time of 120 min) is shown in Figure 16. The maximum removal rate was 47.67% at 100 rpm and decreased slightly to 43% when the stirring rate was increased to 500 rpm. This reduction is due to the turbulence produced by high stirring rate, which does not give enough time to all

NH_4^+ present in solution to meet active sites present in PP's surface and led bound NH_4^+ to be released again. Similar effect was observed by Fauzia and coworkers for the adsorption of tatrazine by using *Annona muricata* L seeds [169].

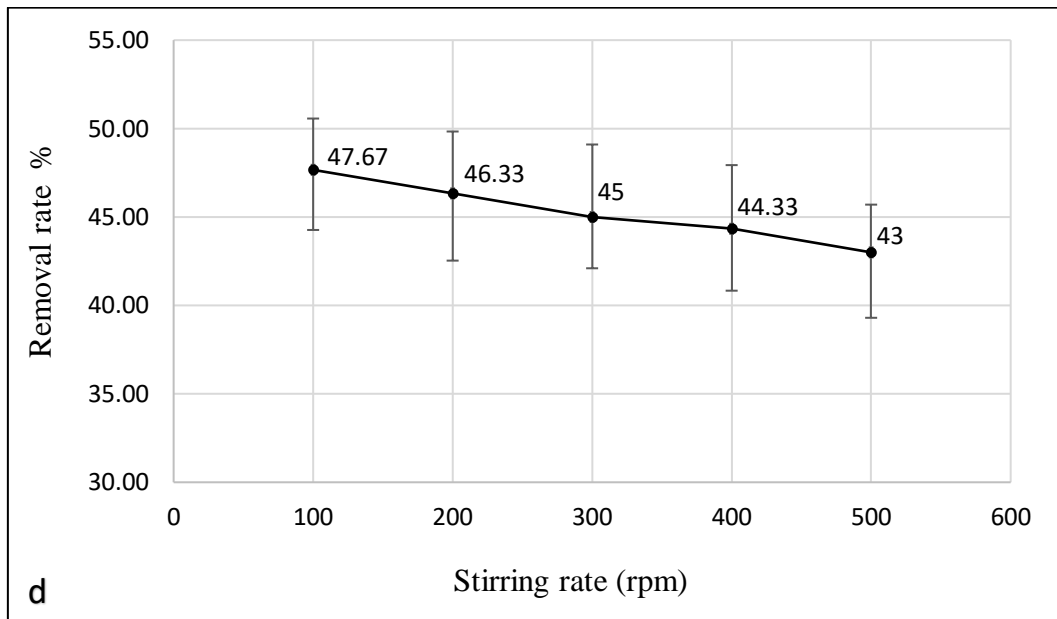


Figure 16. Effect of stirring rate (pH 4, initial $\text{NH}_4\text{-N}$ concentration of 30 mg.L^{-1} , 100 mg of PP and contact time of 120 min)

5.3.5 Effect of contact time

The effect of contact time was measured in a system with an initial $\text{NH}_4\text{-N}$ concentration of 30 mg.L^{-1} , pH 4, 400 mg of PP and stirring rate of 150 rpm. The time progress of NH_4^+ adsorption by PP can be divided on three phases as shown in Figure 17.

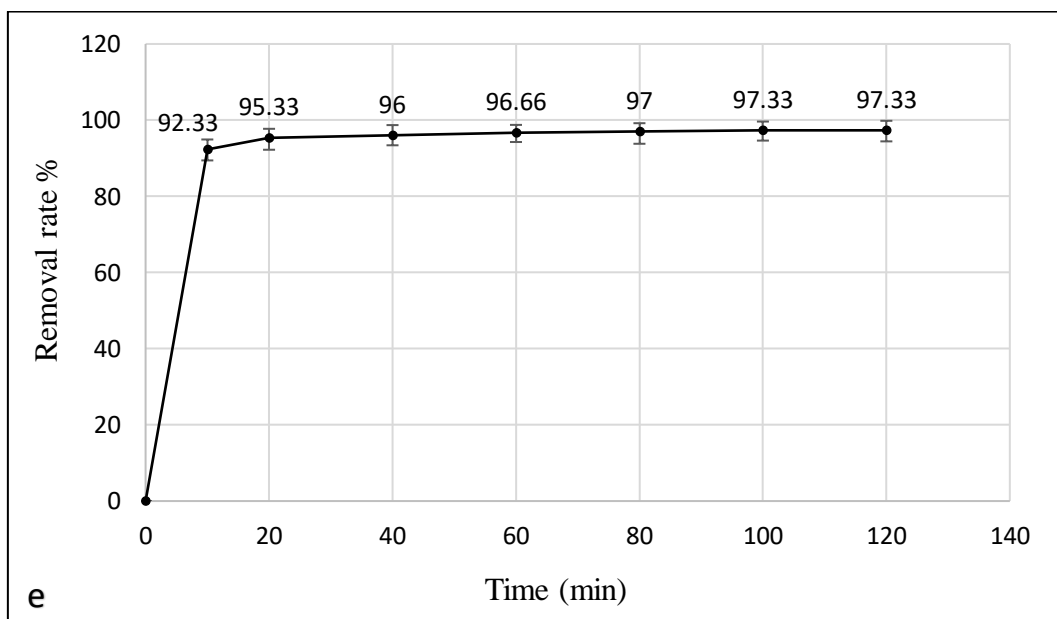


Figure 17. Effect of contact time (initial $\text{NH}_4\text{-N}$ concentration of 30 mg.L^{-1} , pH 4, 400 mg of PP and stirring rate of 150 rpm)

The process starts with an initial phase which is rapid and characterized by high removal rate (92.33% within 10 min) due to the large availability of free active sites, mainly -COOH and -OH groups. Then, as the contact time increases, the removal rate gradually becomes slower (from 95.33% at 20 min to 97.33% at 100 min) because of the slow transfer of NH_4^+ to the internal structure of PP, this phase is known as the intermediate phase. Finally, the removal rate reached a constant value (97.33%) after 120 min where no more NH_4^+ was removed from the solution because of the saturation of free active sites, this phase is known by equilibrium phase.

5.3.6 Process modeling

Isotherm

Isotherm of NH_4^+ biosorption by PP was evaluated through series of batch adsorption experiments using different doses of PP and a constant initial $\text{NH}_4\text{-N}$ concentration. The resulting data was interpreted through a curve relating the adsorbed amount of $\text{NH}_4\text{-N}$ on PP's surface (q_e) to its equilibrium concentration in the solution (C_e) (Figure 18).

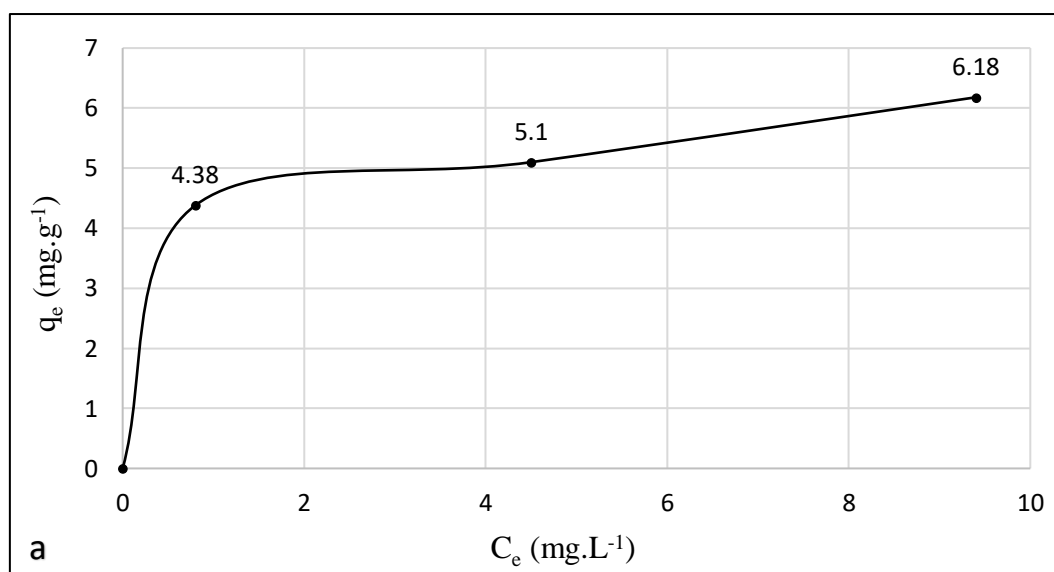


Figure 18. Isotherm of NH_4^+ biosorption by PP

Langmuir and Freundlich models were tested to identify the model that adequately describes the biosorption of NH_4^+ by PP. Table 9 presents parameters and R^2 values of both models. According to the value of R^2 , Langmuir isotherm fits the best with the experimental data (Figure 19). This model assumes that the adsorption process is localized and controlled by monolayer coverage of the adsorbent surface and all adsorption sites possess equal affinity for the adsorbate [95]. Furthermore, intermolecular attractive forces diminish rapidly with distance in absence of interaction between adsorbed molecules on neighbouring sites [170].

Table 9. Parameters and properties of Langmuir and Freundlich models

| Model | Linear form | Parameters | R ² |
|------------|---|---|----------------|
| Langmuir | $\frac{C_e}{q_e} = \left(\frac{1}{q_{max}}\right)C_e + \frac{1}{k_L q_{max}}$ | k _L = 3.01 (L.mg ⁻¹) q _{max} = 6.18 (mg.g ⁻¹) R _L = 0.01 | 0.98 |
| Freundlich | $\ln(q_e) = \ln(k_F) + \left(\frac{1}{n}\right)\ln(C_e)$ | k _F = 4.04 1/n = 0.13 | 0.91 |

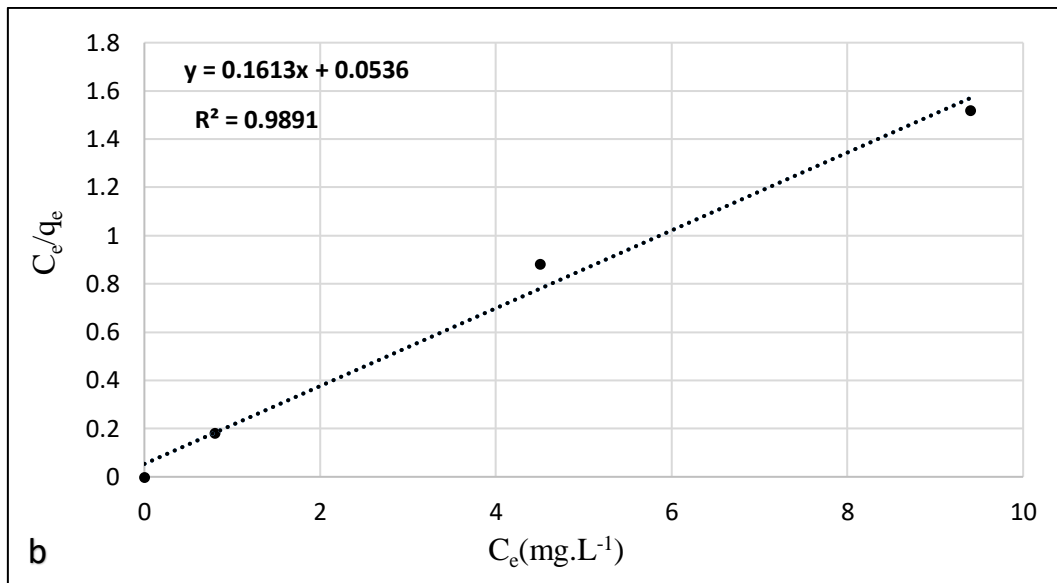


Figure 19. Langmuir model

The constant k_L of Langmuir model can be obtained from Langmuir graph and it is an index of affinity between the adsorbent and adsorbate [171]. In this case, $k_L = 3.01$ which means that PP has a high affinity towards NH_4^+ . While, the parameter R_L which is recognized as the separation factor can be calculated using Eq. (10).

$$R_L = 1/(1 + k_L C_i) \quad (10)$$

Value of R_L obtained is 0.01 which is very low and indicates that the biosorption of NH_4^+ by PP is favourable [172].

Kinetics

In order to study kinetics of NH_4^+ biosorption by PP, the change in $\text{NH}_4\text{-N}$ concentration over time was followed and measured by taking samples at defined time intervals. The resulting kinetic curve is shown in Figure 20. This curve provides data for fitting with existing kinetic models. Selecting the best-fit model is based on the value of R^2 and the calculated equilibrium

adsorption capacity ($q_{e,cal}$). Among models tested, pseudo-second order model fits the best to NH_4^+ biosorption by PP as shown in Table 10.

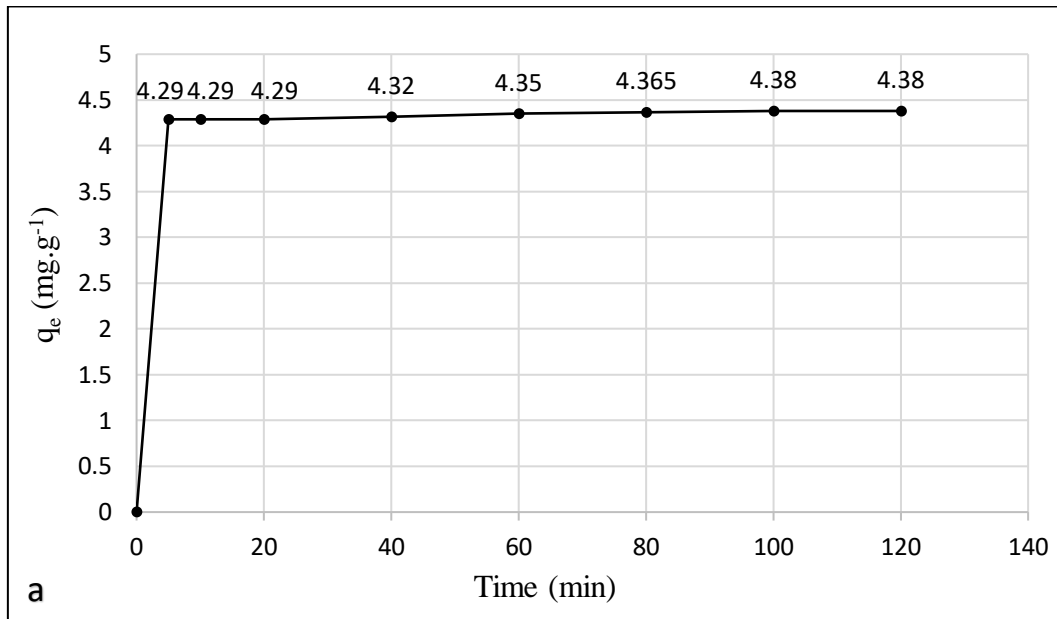


Figure 20. Kinetics of NH_4^+ biosorption by PP (400 mg PP, 30 mg.L⁻¹ NH_4 -N, pH 4, stirring rate 100 rpm, contact time 120 min)

Table 10. Kinetic models properties and parameters of NH_4^+ adsorption by PP

| Kinetics | Linear form | Parameters | R ² |
|-------------------------|---|---|----------------|
| Pseudo-first order | $\frac{q_t}{q_e} + \ln(q_e - q_t) = \ln(q_e) - K_1 t$ | $k_1 = 1.01$ (L.min ⁻¹) $q_{e,cal} = 4.28$ (mg.g ⁻¹) | 0,95 |
| Pseudo-second order | $\frac{t}{q_t} = \frac{1}{k_2 q_e^2} + \frac{t}{q_e}$ | $k_2 = -3.09$ (L.min ⁻¹) $q_{e,cal} = 4.36$ (mg.g ⁻¹) | 0.99 |
| Intraparticle diffusion | $q_t = k_p \sqrt{t} + C$ | $k_3 = 0.29$ (mg.g ⁻¹ .min ⁻¹) $q_{e,cal} = 3.17$ (mg.g ⁻¹) $C = 1.86$ | 0.53 |

Pseudo-second order which is a plot of (t/q_t) against (t) (Figure 21), assumes that the adsorption process is governed by chemical sorption and involves sharing and exchange of electrons between the adsorbent and adsorbate [173].

Intra-particle diffusion model which is a linear plot of (q_t) versus (\sqrt{t}) was employed to identify the governing step in the adsorption process. As illustrated in Figure 22, the linear plot is not passing through the origin with low value of R², indicating that intra-particle diffusion is not the rate limiting step in the biosorption of NH_4^+ by PP [174].

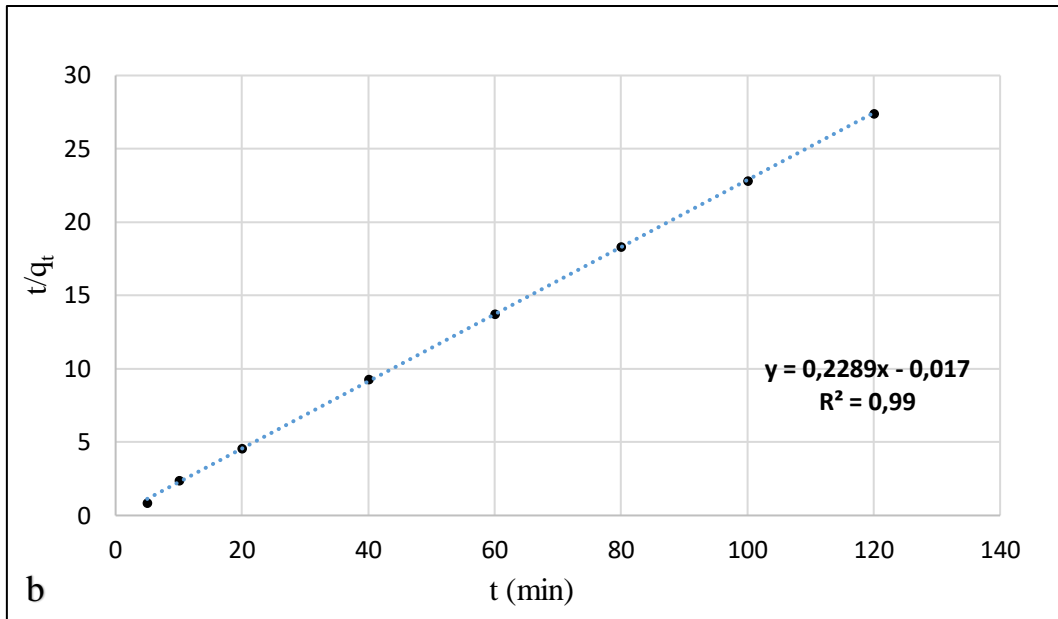


Figure 21. Pseudo-second order model

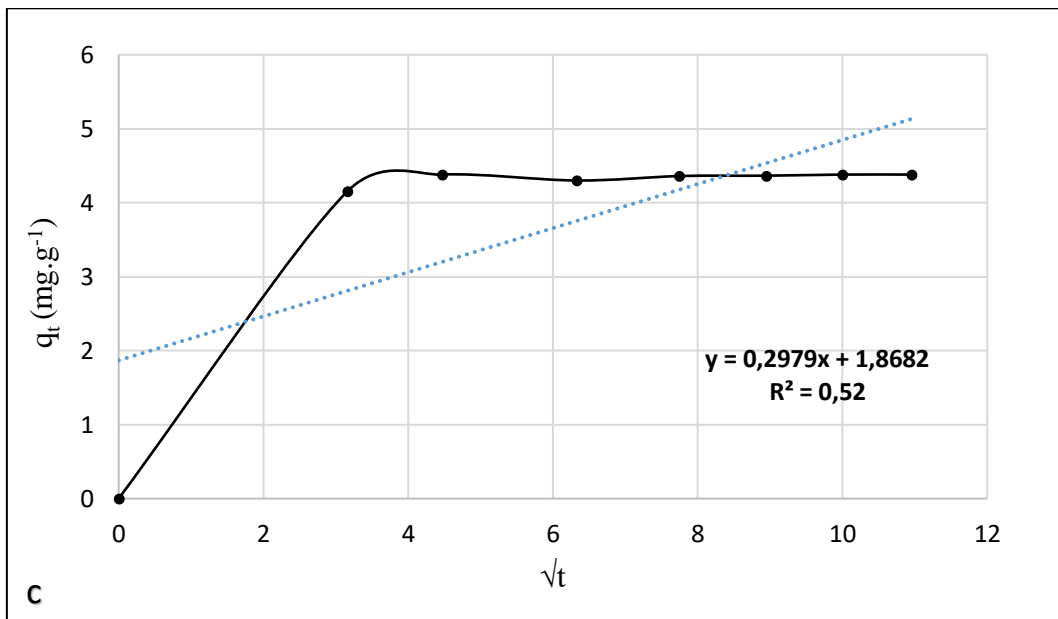


Figure 22. Intra-particle diffusion model

Based on all of this, it can be said that PP showed a promising NH_4^+ removal of 97% within 120 min using batch method. Maximum $\text{NH}_4\text{-N}$ uptake was 6.18 mg.g^{-1} as calculated by Langmuir isotherm. However, investigating the biosorption of NH_4^+ by PP under real conditions is highly required.

5.4 Biosorption of NH_4^+ from MPWW using PP

The promising efficiency of PP to remove NH_4^+ from model solution has to be proven under real conditions using a real wastewater. For this purpose, batch adsorption experiments using MPWW were performed. MPWW is a multi-solute system characterised by high $\text{NH}_4\text{-N}$ content along with different interfering ions that can compete with NH_4^+ to be adsorbed by PP. The initial $\text{NH}_4\text{-N}$ concentration in MPWW used in this study was $80 \text{ mg}\cdot\text{L}^{-1}$. A detailed study of NH_4^+ biosorption from MPWW by PP would help in scaling up this method and presenting PP as an alternative of NH_4^+ conventional adsorbents.

5.4.1 Effect of PP dose

The effect of adsorbent dose on the removal of NH_4^+ from MPWW by PP was studied by using different doses of PP (1 g, 1.5 g and 2 g) while other parameters were kept constant (pH 6, stirring rate of 300 rpm, temperature 25°C and contact time of 120 min). Generally, NH_4^+ removal rate increased by increasing adsorbent dose, however, the amount of $\text{NH}_4\text{-N}$ adsorbed per unit mass of adsorbent (q_e) decreased [61]. As illustrated in Figure 23, NH_4^+ removal rate by PP increased significantly (from 53.9% to 88.7%) when PP dose was increased from 1 g to 2 g due to the increase of free active sites capable for NH_4^+ binding. Adsorbed amount of $\text{NH}_4\text{-N}$ (q_e) using 1.5 g of PP was $2.49 \text{ mg}\cdot\text{g}^{-1}$, however this amount was only $2.02 \text{ mg}\cdot\text{g}^{-1}$ when using 2 g of PP. Therefore, 1.5 g of PP was used for the following experiments.

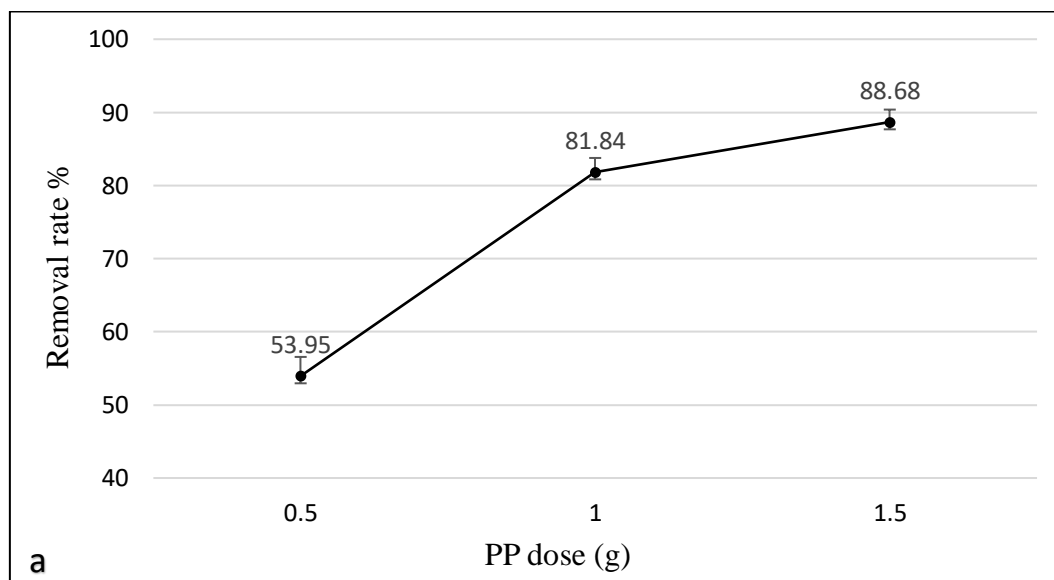


Figure 23. Effect of PP dose (pH 6, stirring rate of 300 rpm, 25°C temperature and contact time of 120 min)

5.4.2 Effect of solution pH

The effect of pH on the biosorption of NH_4^+ from MPWW by PP was investigated by varying the pH of MPWW to different values (3, 4, 5, 6 and 7) and keeping other parameters constant (1.5 g PP, stirring rate of 300 rpm, 25 °C temperature and contact time of 120 min). Optimum NH_4^+ removal was around 81% at pH 6, as shown in Figure 24. This removal decreased by decreasing pH because of the presence of more protons H^+ in acidic solutions. These protons competed effectively with NH_4^+ and led to the protonation of PP's surface, as a result, NH_4^+ uptake by electrostatic forces decreased. However, the slight decrease in the removal rate at pH 7 could be attributed to the deprotonation of NH_4^+ .

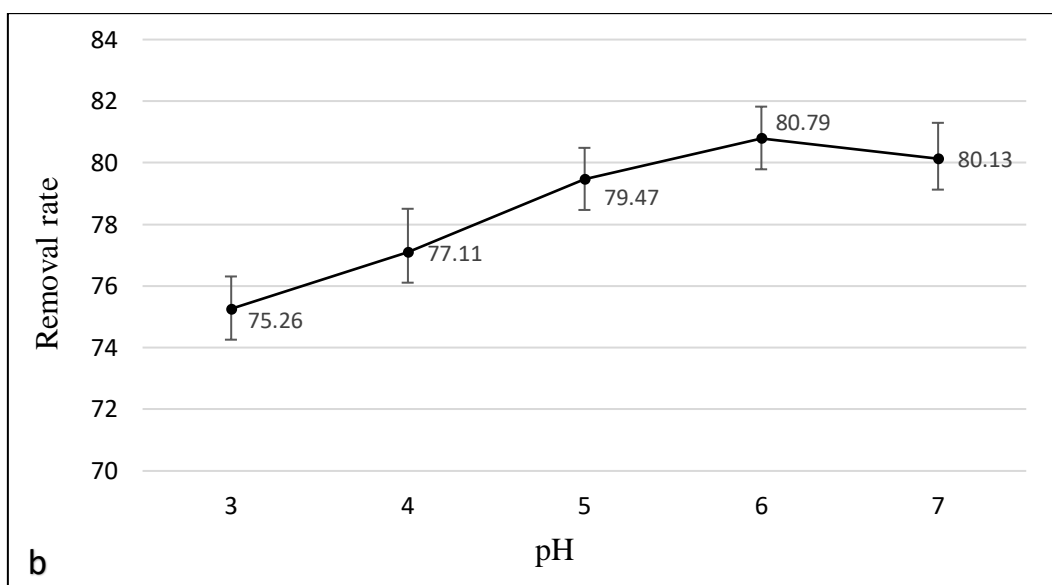


Figure 24. Effect of pH (1.5g PP, stirring rate of 300 rpm, 25 °C temperature and contact time of 120 min)

5.4.3 Effect of stirring rate

Results of investigation on the effect of stirring rate using fixed parameters (1.5 g PP, pH 6, 25 °C temperature and contact time of 120 min) showed that the removal of NH_4^+ from MPWW by PP varies by varying the stirring rate. The optimal removal was 80.79 % at 300 rpm as shown in Figure 25. The increase of stirring rate to 450 rpm led to a decrease in the removal rate because it created turbulence that perturbs NH_4^+ uptake. Likewise, lower stirring rate was not enough for that all NH_4^+ ions encounter available active sites present in PP's surface, which resulted in low NH_4^+ uptake as well [169]. Therefore, a moderate stirring rate is required to improve the diffusion of NH_4^+ to active sites present in PP's surface.

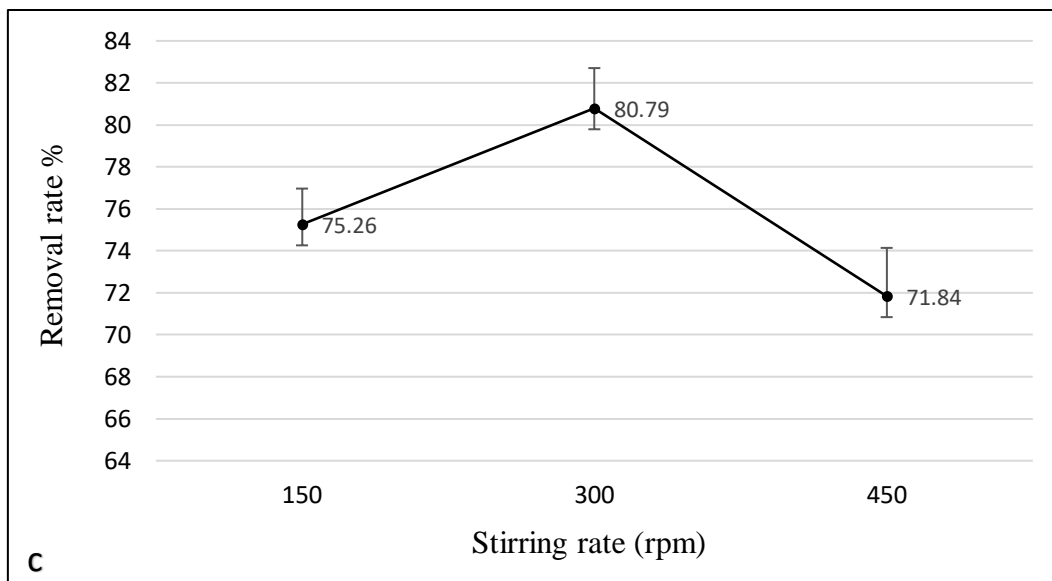


Figure 25. Effect of stirring rate (1.5g PP, pH 6, 25 °C temperature and contact time of 120 min)

5.4.4 Effect of temperature

The effect of temperature on the removal of NH_4^+ from MPWW by PP was investigated using three different temperatures (25, 35 and 45 °C) and fixed values of other parameters (1.5 g PP, pH 6, stirring rate of 300 rpm and a contact time of 120 min).

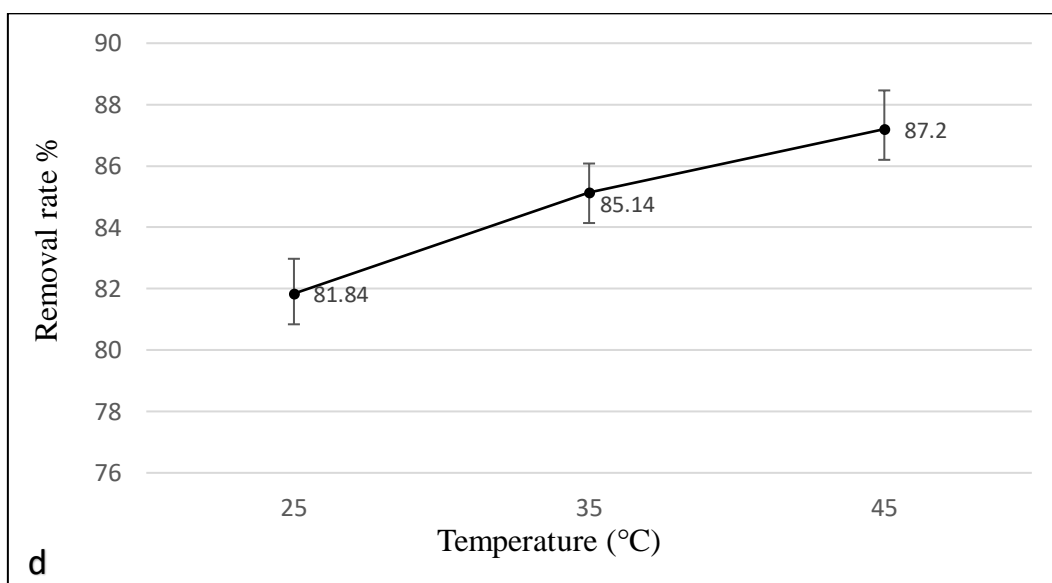


Figure 26. Effect of temperature (1.5g PP, pH 6, stirring rate of 300 rpm and a contact time of 120 min)

The removal rate increased slightly from 81.8% to 87.2% when temperature raised from 25 to 45°C as illustrated in Figure 26. Generally, increasing temperature of the solution improves the mobility of ions and the availability of active sites present in the adsorbent's surface, thus, it facilitates the diffusion of the adsorbate to this surface. However, the effect of increasing

temperature in this study was not of high significance. Similar assumption was reported in a study investigating NH_4^+ biosorption by *posidonia oceanica* fibers [74].

5.4.5 Effect of contact time

The effect of contact time was studied using optimum parameters (1.5 g PP, pH 6, 25 °C temperature and 300 rpm stirring rate). The graph illustrated in Figure 27 showed that biosorption of NH_4^+ from MPWW by PP started with a rapid initial phase which was characterized by a high removal rate (71% within 5 min) due to the large initially available active sites in PP surface that mainly comprised of $-\text{COOH}$ and $-\text{OH}$ groups. Then, as the contact time increased, the removal rate slowed down due to the slow diffusion of NH_4^+ into the internal structure of PP; this phase is known as the intermediate phase. Finally, the removal rate achieved a constant value (81.8% within 120 min) where no more NH_4^+ was removed from the solution due to the saturation of free active sites known as the equilibrium phase.

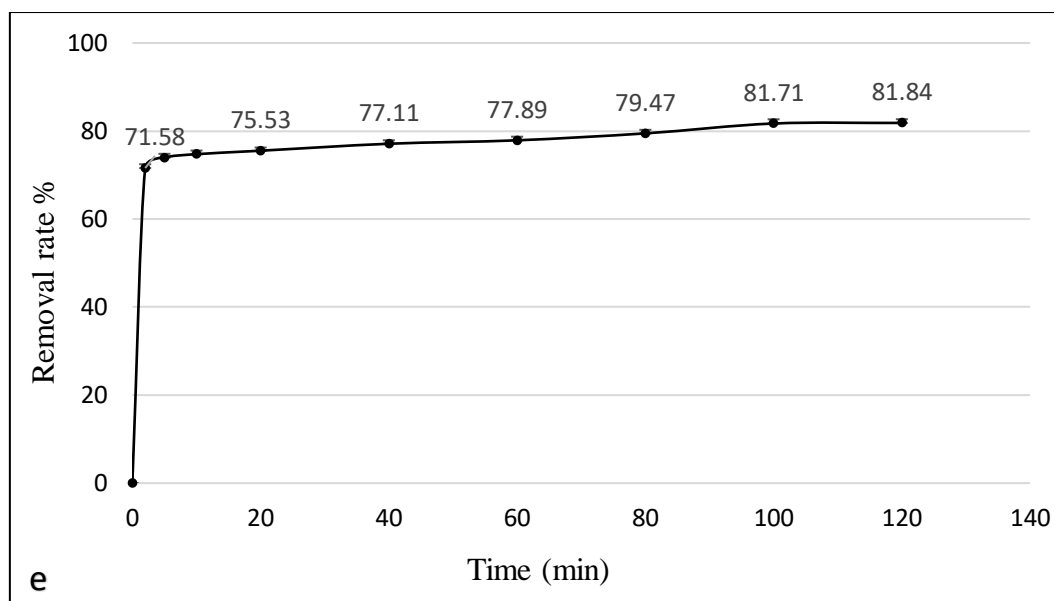


Figure 27. Effect of contact time (1.5g PP, pH 6, 25 °C temperature and 300 rpm stirring rate).

5.4.6 Process modeling

Isotherm

Isotherm curve of NH_4^+ biosorption from MPWW by PP is shown in Figure 28. Fitting isotherm data to mathematic functions of existing models helps to understand the interactions between PP's surface and NH_4^+ and offer details about the chemistry of binding.

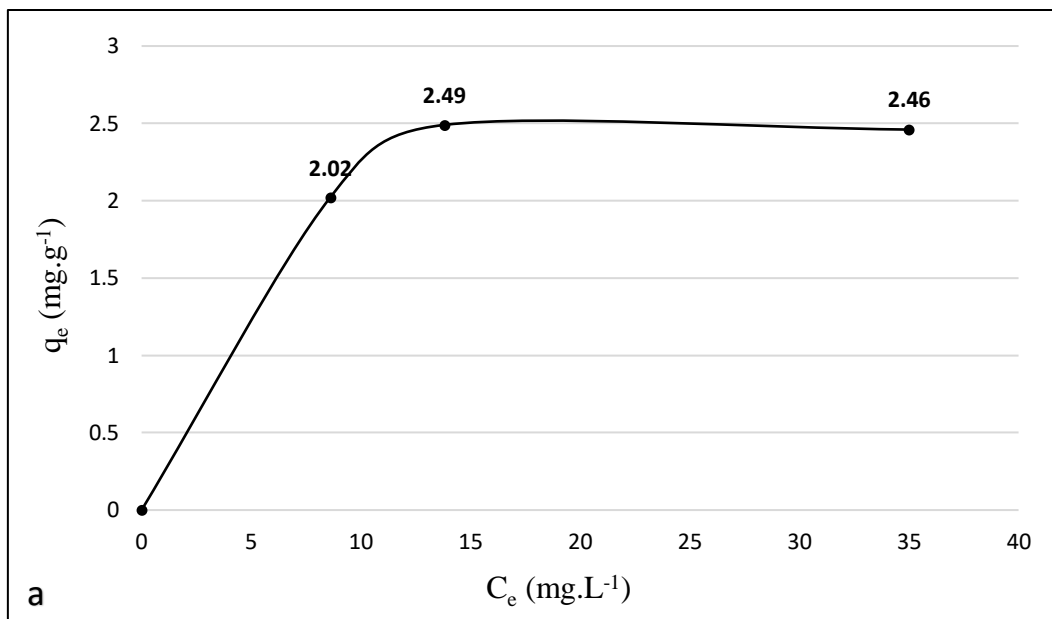


Figure 28. Isotherm of NH_4^+ biosorption from MPWW by PP

Similarly to adsorption of NH_4^+ from NH_4Cl model solution, Langmuir isotherm offered the best fit to experimental adsorption curve according to the value of R^2 (> 0.99), as shown in Table 11 and Figure 29. Therefore, assumptions made in the previous study about the adsorption extent and the interactions between PP's surface and NH_4^+ can be certified.

Table 11. Parameters of Langmuir model for NH_4^+ biosorption from MPWW by PP

| Isotherm | q_{\max} (mg.g ⁻¹) | k_L | R_L | R^2 |
|----------------|----------------------------------|-------|-------|-------|
| Langmuir model | 2.49 | 0.42 | 0.02 | 0.99 |

Value of R_L obtained ($=0.02$) was very low and close to the value obtained for the adsorption of NH_4^+ from NH_4Cl model solution (0.01), which indicated that NH_4^+ biosorption from MPWW by PP remain favourable. However, competition from other cations present in MPWW have decreased the value of k_L from 3.01 for NH_4Cl model solution to 0.42 for MPWW, which indicates a decrease in the affinity of PP towards NH_4^+ . This competitive effect can be also recognized by the decrease of q_{\max} value from 6.18 mg.g⁻¹ in NH_4Cl model solution to only 2.49 mg.g⁻¹ in MPWW and therefore other cations were adsorbed on PP's surface.

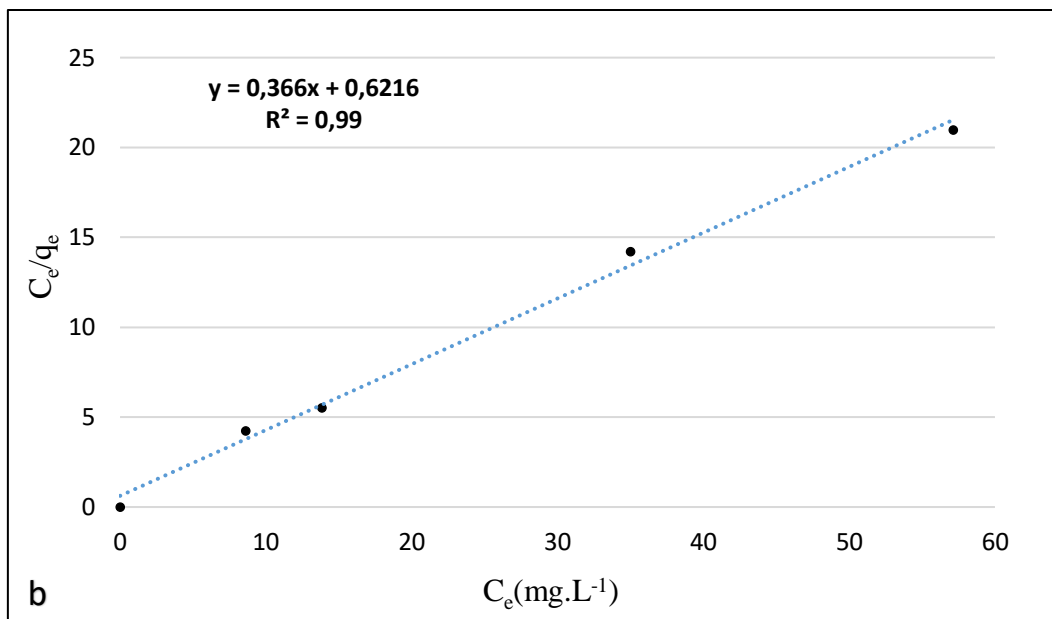


Figure 29. Langmuir isotherm

Kinetics

Kinetics determines the required time to reach the state of equilibrium and describes the mass transfer of NH_4^+ from MPWW to the active sites present in PP's surface (Figure 30).

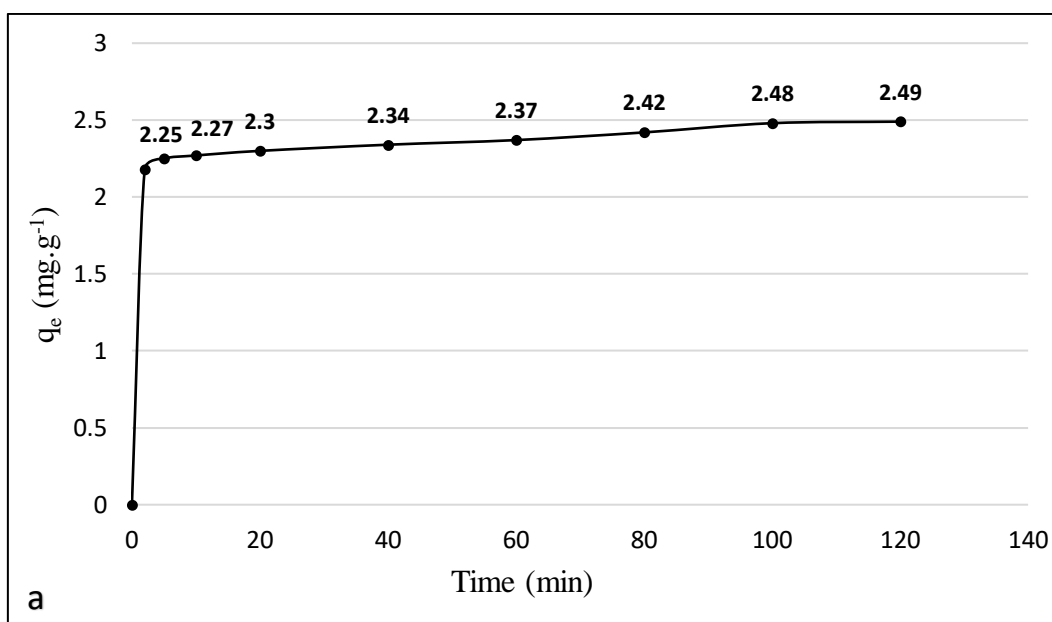


Figure 30. Kinetics of NH_4^+ biosorption from MPWW by PP. (1.5g PP, 80 mg.L⁻¹ $\text{NH}_4\text{-N}$, pH 6, 300 rpm stirring rate and 25°C temperature)

Similarly to kinetics of NH_4^+ adsorption by PP from NH_4Cl model solution, pseudo-second order kinetic model fits well with the adsorption of NH_4^+ from MPWW by PP according to the value of R^2 (> 0.99) as shown in Table 12 and Figure 31.

These results approve the governance of chemisorption mechanism on the process with sharing and exchange of electrons between PP's surface and NH_4^+ .

Table 12. Parameters of kinetic models for NH_4^+ biosorption from MPWW by PP

| Kinetics | Parameters | R^2 |
|---------------------------|---|-------|
| Pseudo-second order model | $k_2 = 0.37 \text{ (L}\cdot\text{min}^{-1})$ $q_{e,\text{cal}} = 2.49 \text{ (mg}\cdot\text{g}^{-1})$ | 0.99 |
| Intraparticle diffusion | $k_3 = 0.12 \text{ (mg}\cdot\text{g}^{-1}\cdot\text{min}^{-1})$ $q_{e,\text{cal}} = 2.76 \text{ (mg}\cdot\text{g}^{-1})$ | 0.38 |

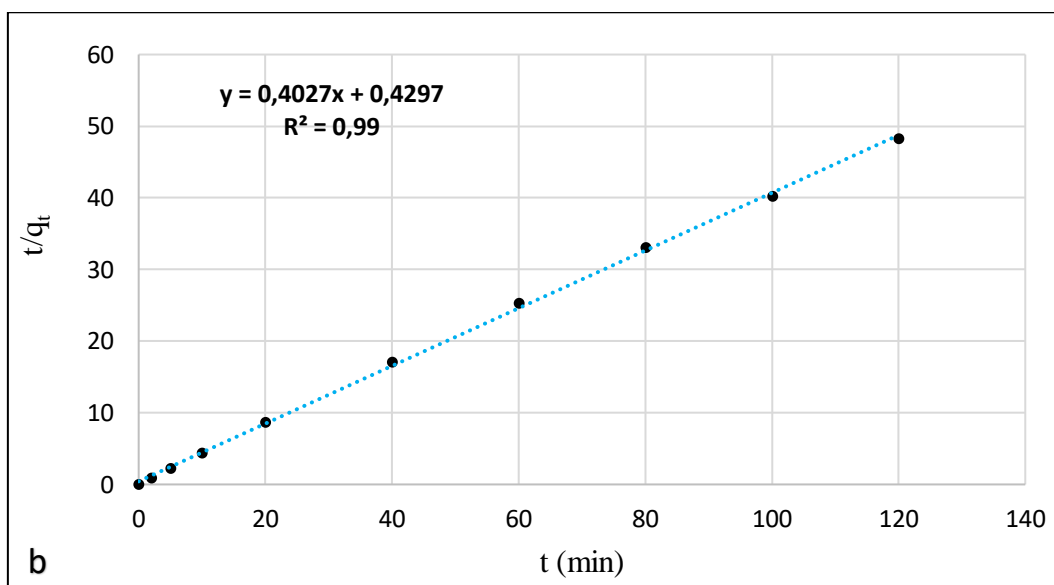


Figure 31. Pseudo second-order kinetic model

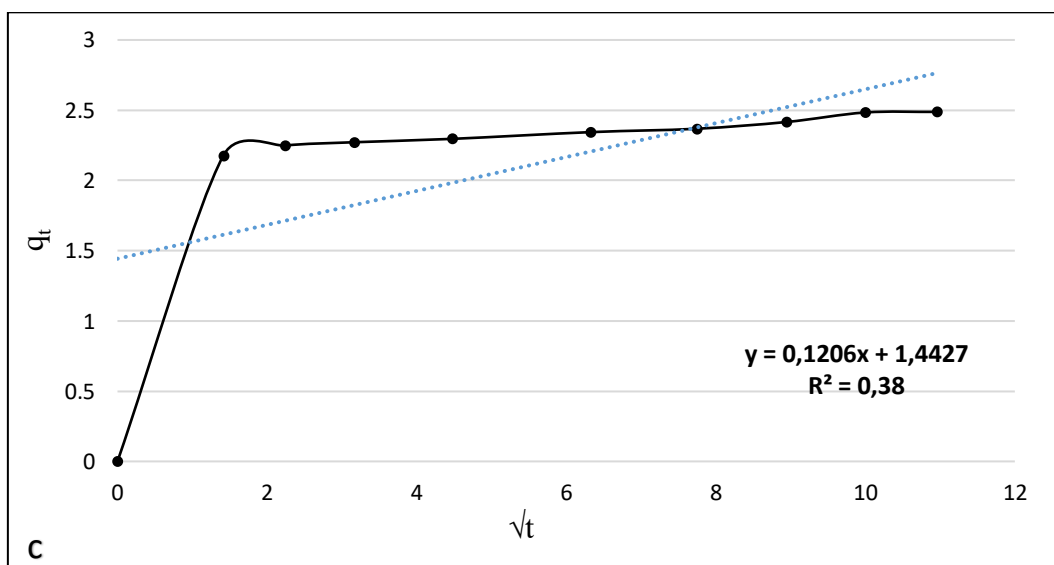


Figure 32. Intra-particle diffusion model

For intra-particle diffusion model, the linear plots at all studied concentrations do not pass through the origin with a low value of R^2 ($=0.38$) indicating that intra-particle diffusion is not the rate-limiting step (Figure 32). This finding is similar to results of the previous study using NH_4Cl model solution and to another study investigating the biosorption of NH_4^+ from aqueous solutions onto *Posidonia oceanica* fibers [173].

The results of this study have showed that using PP for NH_4^+ biosorption from MPWW can achieve 81.8% removal and $\sim 2.5 \text{ mg.g}^{-1}$ of $\text{NH}_4\text{-N}$ uptake within 120 min. Factor with the highest impact on the removal efficiency was adsorbent dose, while the effects of other factors, such as pH, stirring rate, and temperature, were almost negligible. Therefore, PP provides the advantage of working in a wide range of pH levels, temperatures, and stirring rates. Furthermore, $\text{NH}_4\text{-N}$ adsorption capacity of PP can increase if MPWW was suitably pre-treated, since this study was performed using untreated wastewater rich in suspensions that potentially limited the uptake of NH_4^+ .

5.5 Biosorption of PO_4^{3-} from Na_2HPO_4 solution using IL-PP

In this study, I investigated the removal of PO_4^{3-} from model solution using PP. However, unlike NH_4^+ biosorption, activation of PP was highly required to incorporate active sites on its surface able to bind PO_4^{3-} . For this purpose, PP which originally had a negative zeta potential was activated using iron-loading method in order to adsorb negatively charged ions, i.e. PO_4^{3-} . The new physicochemical properties of IL-PP were characterized before it was used in batch adsorption experiments. The next chapter gives insight into the properties and mechanisms of PO_4^{3-} biosorption from model solution using IL-PP.

5.5.1 Effect of solution pH

Depending on the solution pH, phosphate can exist in four species: H_3PO_4 (pH ~ 2.15), H_2PO_4^- ($2.15 < \text{pH} < 7.20$), HPO_4^{2-} ($7.20 < \text{pH} < 12.33$) and PO_4^{3-} (pH ~ 12.33) [175]. As shown in Figure 33, removal of PO_4^{3-} by using 100 mg of IL-PP increased from 43.5% to 64.25 % when pH was increased from 3 to 9. At pH lower than 4, the dominant specie H_2PO_4^- is weakly favoured for adsorption by available active sites present in IL-PP's surface and therefore low removal rate occurs. While, at pH values between 4 and 9 the predominant species are H_2PO_4^- and HPO_4^{2-} and it is found that Fe^{3+} has strong affinity toward HPO_4^{2-} in alkaline medium [90]. The interaction between HPO_4^{2-} and Fe^{3+} can take place in three different ways: monodentate and mononuclear; bidentate and mononuclear; monodentate and binuclear leading to high PO_4^{3-} uptake by IL-PP. On the other hand, the unique possibility of interaction for H_2PO_4^- anion is monodentate and mononuclear [176]. These results are in

accordance with the decrease in the zeta potential of IL-PP's surface in Na_2HPO_4 solution when the pH was increased, which indicates that more PO_4^{3-} ions were attached to this surface. For each sample, the equilibrium pH value was lower than the initial pH value, which indicates that large quantities of hydrogen ions were produced by Fe^{3+} hydrolysis and reduced the equilibrium pH [177].

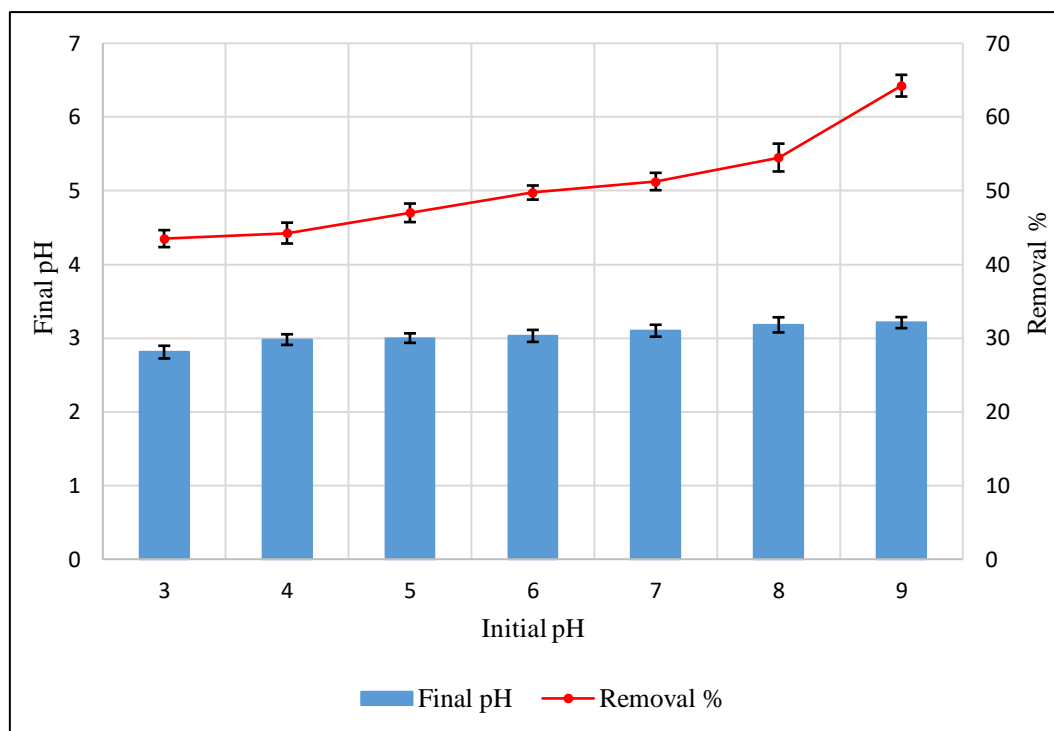


Figure 33. Effect of pH on PO_4^{3-} removal by IL-PP ($\text{PO}_4\text{-P}$ concentration: $40 \text{ mg}\cdot\text{L}^{-1}$, adsorbent dose 100 mg , temperature: $25 \text{ }^\circ\text{C}$, stirring speed: 150 rpm)

5.5.2 Determination of equilibrium time

Figure 34 shows the equilibrium time for PO_4^{3-} removal by IL-PP, which was studied using two different doses of IL-PP (100 and 150 mg) and fixed values of $\text{PO}_4\text{-P}$ concentration ($40 \text{ mg}\cdot\text{L}^{-1}$), pH (9), and temperature (25°C). Within the first 2 min , rapid PO_4^{3-} uptake took place with removal rates of 51% and 76.5% for 100 and 150 mg , respectively, of IL-PP. This fast uptake can be explained by the presence of a large number of active sites to which a large amount of PO_4^{3-} anions could attach. Afterward, the removal rate decreased as equilibrium was approached because of the saturation of available active sites [36]. The equilibrium state for PO_4^{3-} removal was reached within 60 min . Removal rates of 64.25% and 90% were achieved with 100 and 150 mg , respectively, of IL-PP.

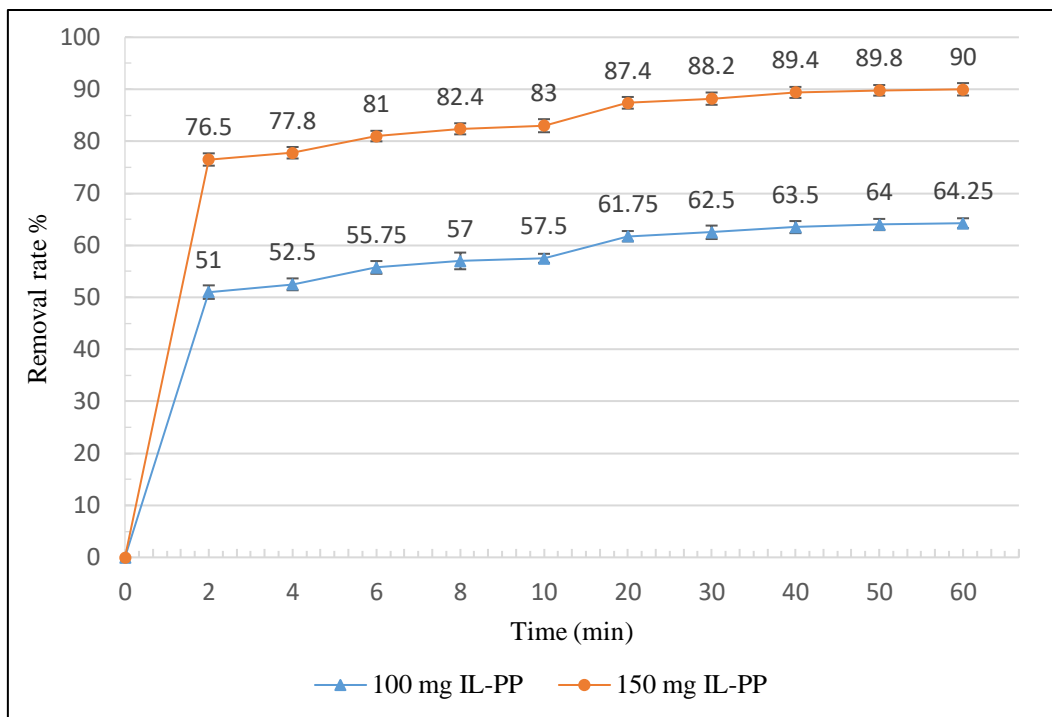


Figure 34. Effect of contact time on PO₄³⁻ removal by IL-PP (PO₄-P concentration: 40 mg.L⁻¹, temperature: 25 °C, stirring speed: 150 rpm)

5.5.3 Factorial design study

For the determination of optimum working parameters, 2³ full factorial design (three factors each, at two levels) was employed evaluating the effect of pH, adsorbent dosage, temperature and their interactions on PO₄³⁻ removal by IL-PP. Factorial design plots such as plots for the main effects and interactions, Pareto chart, and normal plot for the standardized effects describe how the effect of one factor varies with the level of the other factors [178]. This technique investigates all possible combinations and verifies the accuracy of the obtained mathematical model through the analysis of variance (ANOVA) to achieve optimum removal of PO₄³⁻. For this purpose, parameters such as initial PO₄-P concentration (40 mg.L⁻¹), contact time (60 min) and stirring speed (150 rpm) were kept constant and the three factors pH, adsorbent dose, and temperature of solution were varied at two levels as given in (Table 13). A centre point was duplicated and added to matrix in order to verify the curvature of the studied model.

Table 13. Factors and levels used in the factorial design for PO₄³⁻ removal by IL-PP

| Factor | Coded symbol | Low level (-1) | High level (+1) | Centre point (0, 0, 0) |
|----------------|--------------|----------------|-----------------|------------------------|
| pH | A | 3 | 9 | 6 |
| Adsorbent dose | B | 100 | 150 | 125 |
| Temperature | C | 25 | 45 | 35 |

Factorial design matrix of parameters coded values and average of three replicates of PO_4^{3-} removal rate measured in each factorial experiment are shown in Table 14. The mean of the experimental results for the respective high and low levels of pH, adsorbent dose and temperature are shown in Figure 35.

Table 14. Design matrix and results of 2^3 full factorial design for PO_4^{3-} removal by IL-PP

| Runs | pH (A) | Adsorbent dose (B) | Temperature (C) | Removal rate (average %) |
|------|-----------|-----------------------|--------------------|-----------------------------|
| 1 | 1 | -1 | -1 | 61.08 |
| 2 | -1 | 1 | 1 | 87.5 |
| 3 | 1 | 1 | -1 | 90 |
| 4 | -1 | 1 | -1 | 81.66 |
| 5 | 0 | 0 | 0 | 71 |
| 6 | -1 | -1 | -1 | 41.16 |
| 7 | 1 | 1 | 1 | 90.75 |
| 8 | 1 | -1 | 1 | 68.25 |
| 9 | -1 | -1 | 1 | 49.16 |
| 10 | 0 | 0 | 0 | 71.5 |

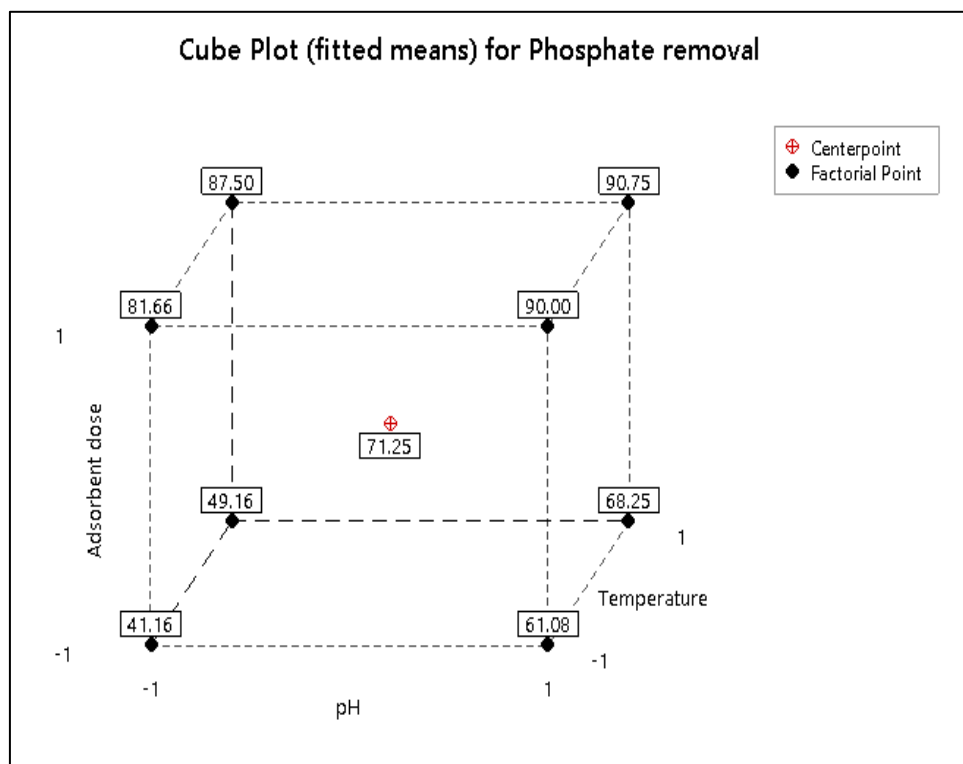


Figure 35. Cube plots for PO_4^{3-} removal by IL-PP

Table 15 presents the main and interaction effects, model coefficients, standard deviation of each coefficient, standard errors, Fisher test value (F-value), and probability value (P-value). Results showed that the effects of pH, adsorbent dosage, temperature, and (pH × Adsorbent dose) were significant at a 5% probability level ($P < 0.05$). However the effects of (pH × Temperature), (Adsorbent dose × Temperature) and (pH × Adsorbent dose × Temperature) were not significant ($P > 0.05$). Furthermore, the adjusted square correlation coefficient R^2 (adj) had a value of 99.96%, which indicates that the presented model perfectly fit the statistical model [179].

Table 15. Estimated effects and coefficients for PO_4^{3-} removal by IL-PP

| Term | Effect | Coef | SE coef | t-value | p-value | VIF |
|-----------------------------------|----------|--------|---------|---------|---------|------|
| Constant | | 71.195 | 0.125 | 569.56 | 0.001 | |
| pH | 12.650 | 6.325 | 0.125 | 50.60 | 0.013 | 1.00 |
| Adsorbent dose | 32.565 | 16.282 | 0.125 | 130.26 | 0.005 | 1.00 |
| Temperature | 5.440 | 2.720 | 0.125 | 21.76 | 0.029 | 1.00 |
| pH × Adsorbent dose | -6.855 | -3.428 | 0.125 | -27.42 | 0.023 | 1.00 |
| pH × Temperature | -1.480 | -0.740 | 0.125 | -5.92 | 0.107 | 1.00 |
| Adsorbent dose × Temperature | -2.145 | -1.072 | 0.125 | -8.58 | 0.074 | 1.00 |
| pH × Adsorbent dose × Temperature | -1.065 | -0.533 | 0.125 | -4.26 | 0.147 | 1.00 |
| Ct Pt | | 0.055 | 0.280 | 0.2 | 0.876 | 1.00 |
| S | 0.135015 | | | | | |
| R^2 | 100.00% | | | | | |
| R^2 (Adj) | 99.96% | | | | | |

In this way, PO_4^{3-} removal by IL-PP could be expressed using Eq. (11).

$$\text{Phosphate removal\%} = 71.195 + 6.325 A + 16.282 B + 2.720 C - 3.428 A \cdot B + 0.740 A \cdot C - 1.072 B \cdot C - 0.533 A \cdot B \cdot C + 0.055 Ct Pt \quad (11)$$

where: A (pH), B (adsorbent dose), C (temperature), AB, AC and BC (their 2- way interaction) and ABC (their 3-way interaction). ($3 < \text{pH} < 9$, $100 \text{ mg} < \text{Adsorbent dose} < 150 \text{ mg}$, $25 \text{ }^\circ\text{C} < \text{temperature} < 45^\circ\text{C}$).

This equation describes how the experimental parameters and their interactions influence the response variable and thus can be used to predict responses for given levels of each parameter [180]. Positive values in the equation indicate that the PO_4^{3-} removal increases when this effect increases. By contrast, negative values indicate that the removal rate decreases when this effect increases [178].

An analysis of variance was performed to investigate the significance of parameters affecting PO_4^{3-} removal to ensure the accuracy of the model. Table 16 presents the sum of the squares used to estimate the effect of factors, the F-ratio (i.e., the ratio of individual mean square effects to the mean square error) and the P-value (i.e., the level of significance leading to the rejection of the null hypothesis). The results showed are in accordance with the estimated effects shown in Table 15 and thus confirm the accuracy of the factorial design model.

Table 16. Analysis of variance (ANOVA) for PO_4^{3-} removal by IL-PP

| Source | DF | Adj SS | Adj MS | F-Value | P-Value |
|-------------------------------|----|---------|---------|----------|---------|
| Model | 8 | 2610.03 | 1118,32 | 2610.03 | 0.015 |
| Linear | 3 | 2500.19 | 2499.60 | 6667.18 | 0.009 |
| pH | 1 | 320.05 | 959.50 | 2560.36 | 0.013 |
| Adsorbent dose | 1 | 2120.96 | 6361.90 | 16967.67 | 0.005 |
| Temperature | 1 | 59.19 | 177.40 | 473.50 | 0.029 |
| 2-Way Interactions | 3 | 107.56 | 107.54 | 286.84 | 0.043 |
| pH*Adsorbent dose | 1 | 93.98 | 281.88 | 751.86 | 0.023 |
| pH*Temperature | 1 | 4.38 | 13.13 | 35.05 | 0.107 |
| Adsorbent dose*Temperature | 1 | 9.20 | 27.63 | 73.62 | 0.074 |
| 3-Way Interactions | 1 | 2.27 | 6.77 | 18.15 | 0.147 |
| pH*Adsorbent dose*Temperature | 1 | 2.27 | 6.77 | 18.15 | 0.147 |
| Curvature | 1 | 0.00 | 0.00 | 0.04 | 0.876 |
| Error | 1 | 0.13 | 0.02 | | |
| Total | 9 | 2610.15 | | | |

Figure 36 shows the main effects of each parameter on PO_4^{3-} removal by IL-PP by giving the deviations between high and low levels of each parameter, which can help with identifying which parameters affect the response variable the most. A larger deviation is synonymous with a large effect [181]. Accordingly, adsorbent dose appears to have the greater effect on PO_4^{3-} removal by IL-PP, followed by pH and then temperature that has an almost negligible effect.

Figure 37 plots the interactions of the studied parameters. If the interaction lines are not parallel, this implies that the interaction has a strong effect, whereas parallel interaction lines indicate a weak effect. Interpretation of interaction plot implies that if the interactions lines are not parallel, the interaction under control is strong and vice versa [182]. The most important interaction for PO_4^{3-} removal by IL-PP appears to be (pH \times adsorbent dose), followed by (adsorbent dose \times temperature). The least important interaction was (pH \times temperature), which had almost parallel interaction lines.

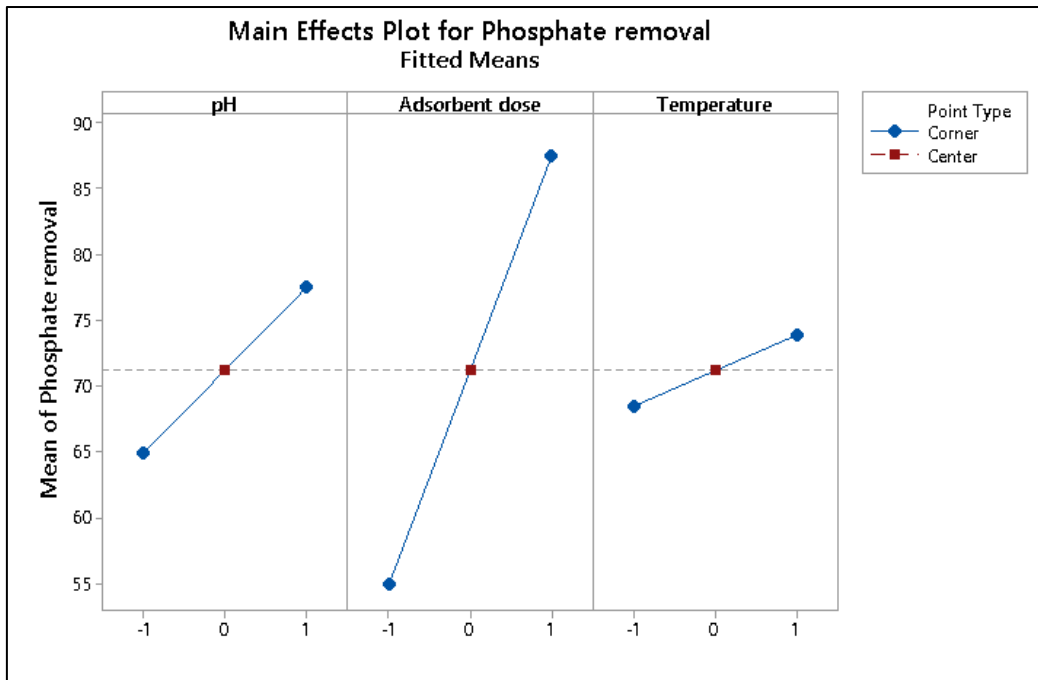


Figure 36. Main effects plot for PO_4^{3-} removal by IL-PP

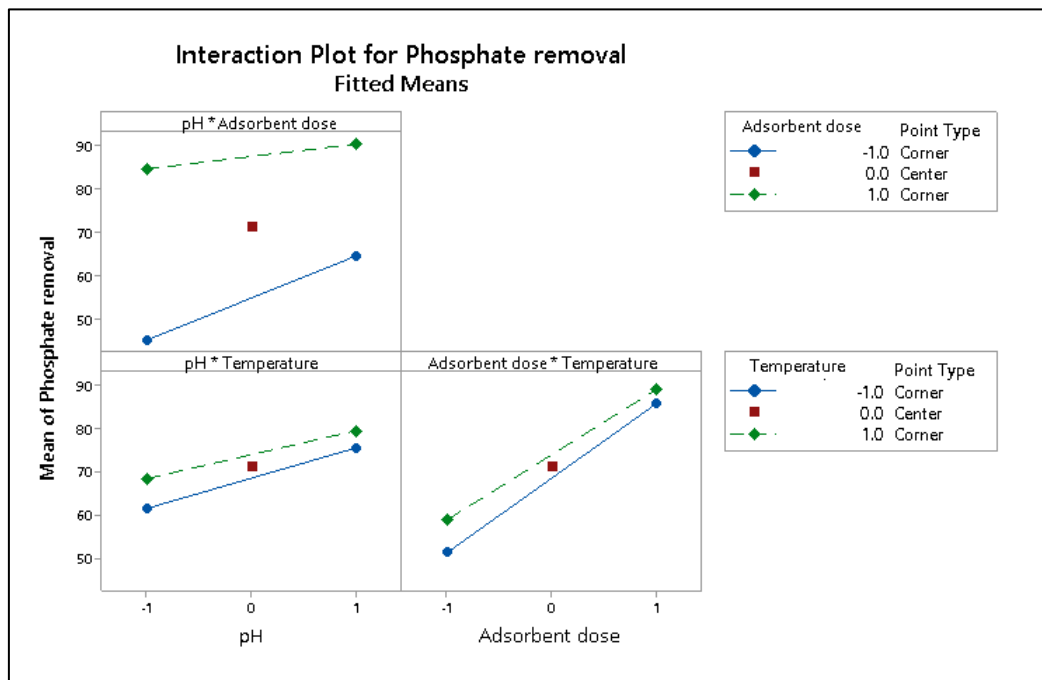


Figure 37. Interaction plot for PO_4^{3-} removal by IL-PP

A Pareto chart is helpful for observing the relative importance of the main effects of parameters and their interactions. This chart can be used to evaluate the significance of effects on the basis of how much they exceed the reference line [183]. Figure 38 shows that adsorbent dose, pH, their interaction, and temperature had a significant effect because their

values exceeded that of the reference line (12.7, in red). However, the effects of interactions (adsorbent dose \times Temperature), (pH \times Temperature) and (pH \times Adsorbent dose \times Temperature) are not significant as their values didn't exceed the red line.

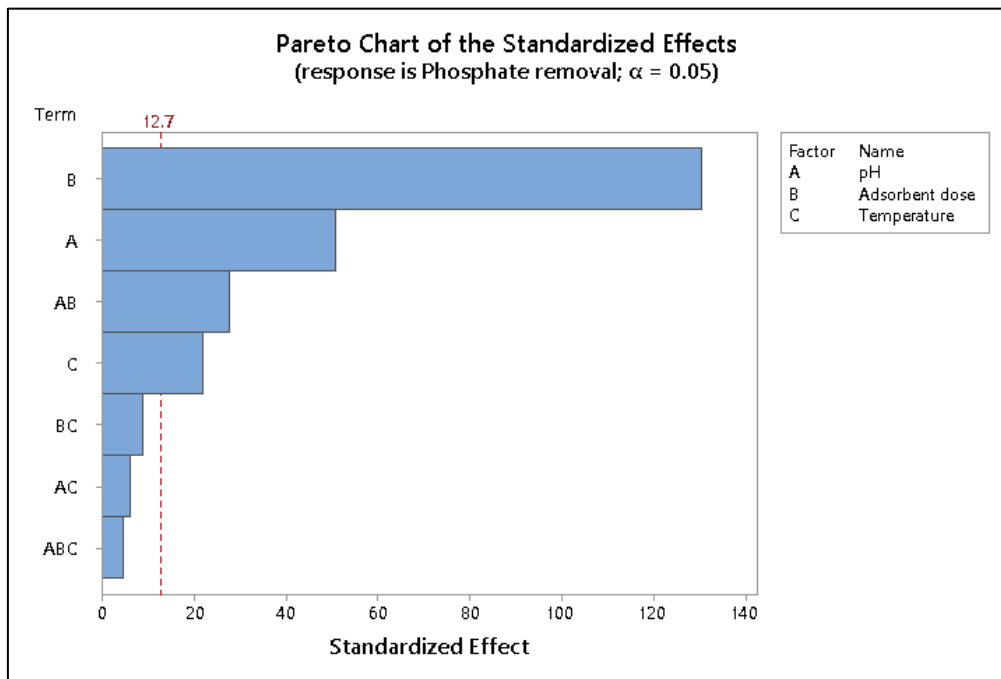


Figure 38. Pareto chart of the standardized effects for PO_4^{3-} removal by IL-PP

Figure 39 shows the normal plot of the standardized effects, which was used to identify the “real” effects. Each point on this plot was assigned to an effect. Points far from the reference line likely represent the greatest effect and vice versa [183].

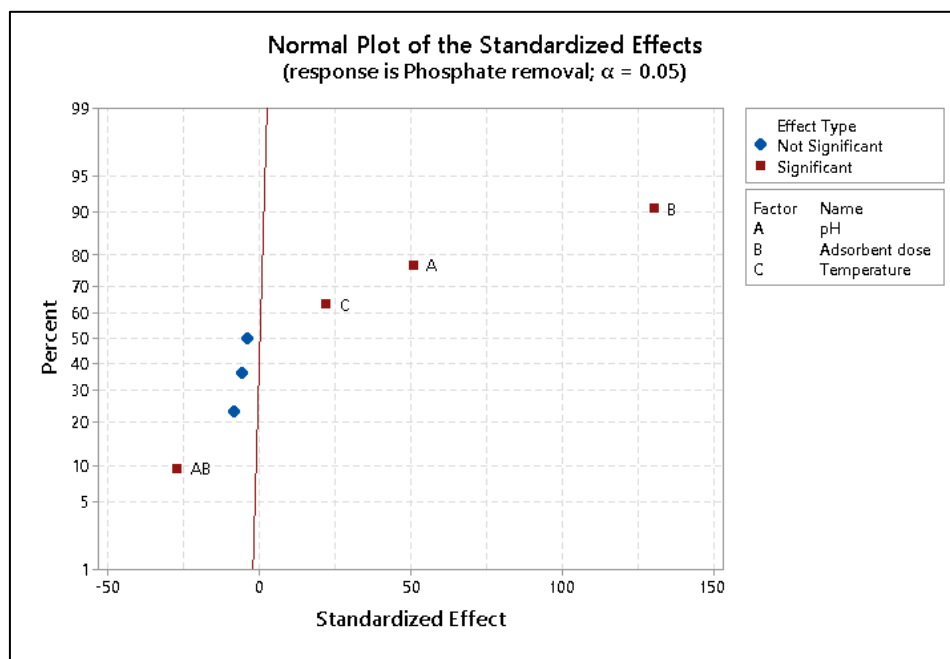


Figure 39. Normal plot of the standardized effects for PO_4^{3-} removal by IL-PP

The adsorbent dose (B) had the largest effect because its point was farthest from the reference line (in red), followed by pH (A), their interaction (AB), and temperature (C), while the interactions BC, AC and ABC were not significant. The adsorbent dose (B), pH (A) and temperature (C) had positive effects because their points are on the right side of the line, whereas their interaction (AB) had a negative effect because it is on the left side [179].

- **Reduced factorial design model for biosorption of PO₄³⁻ from Na₂HPO₄ solution using IL-PP**

The results of 2³ factorial design have showed that pH (A), adsorbent dose (B), their interaction (AB), and temperature (C) are the factors with significant effect on the biosorption of PO₄³⁻ from Na₂HPO₄ solution using IL-PP. On the other hand, the effect of temperature on removal rate between high and low level was very weak and tends to be negligible (0.25%) when using optimum pH (9) and adsorbent dose (150 mg), therefore for technical and cost-effectivity reasons, a reduced model that take in consideration only the significant factors and neglect temperature is suggested. The new model is 2² factorial model with two factors (pH, and adsorbent dose) at two levels and can be described using Eq.(12):

$$\text{Phosphate removal\%} = 71.19 + 6.33 A + 16.28 B - 3.43 A \cdot B + 0.06 C t P t \quad (12)$$

5.5.4 Process modelling

For isotherm and kinetics modelling, optimum parameters for higher PO₄³⁻ removal (pH (9), adsorbent dose (150 mg)) were used, however 25 °C temperature was preferred.

Isotherm

In order to select the isotherm model that adequately describes mechanisms of PO₄³⁻ biosorption by IL-PP, batch adsorption results were fitted to Langmuir and Freundlich models. The best-fitted model was selected based on R² and χ² values. According to results shown in Table 17, biosorption of PO₄³⁻ by IL-PP can be described by both Langmuir (R² = 0.98, χ² = 0.78) and Freundlich (R² = 0.94, χ² = 2.62) isotherms, but the former fits better than the latter.

Table 17. Isotherm models and parameters of PO₄³⁻ biosorption by IL-PP

| Isotherm model | Parameters | R ² | χ ² |
|----------------|--|----------------|----------------|
| Langmuir | k _L = 0.09 (L.mg ⁻¹) q _{max} = 49.12 (mg.g ⁻¹) R _L = 0.21 | 0.98 | 0.78 |
| Freundlich | k _F = 6.88 1/n = 2.04 | 0.94 | 2.62 |

Langmuir model assumes that the adsorption occurs on a homogenous surface through monolayer coverage, and conversely, Freundlich model assumes that adsorption occurs on a heterogeneous surface through multilayer adsorption and the adsorbed amount increases with increasing equilibrium concentrations. The applicability of both Langmuir and Freundlich models indicates the homogeneous and heterogeneous distribution of active sites on IL-PP's surface and consequently the adsorption properties are likely to be complex and involve more than one mechanism [132]. On the other hand, Langmuir separation factor ($R_L=0.21$) is between 0 and 1 and the Freundlich adsorption affinity constant ($n=2.04$) is between 1 and 10 which implied a favourable biosorption of PO_4^{3-} by IL-PP [177]. Furthermore, the value of $1/n$ was below unity implying that chemisorption is the governing mechanism [172]. Experimental isotherm model and Langmuir and Freundlich models fitting for PO_4^{3-} biosorption by IL-PP are shown in Figure 40.

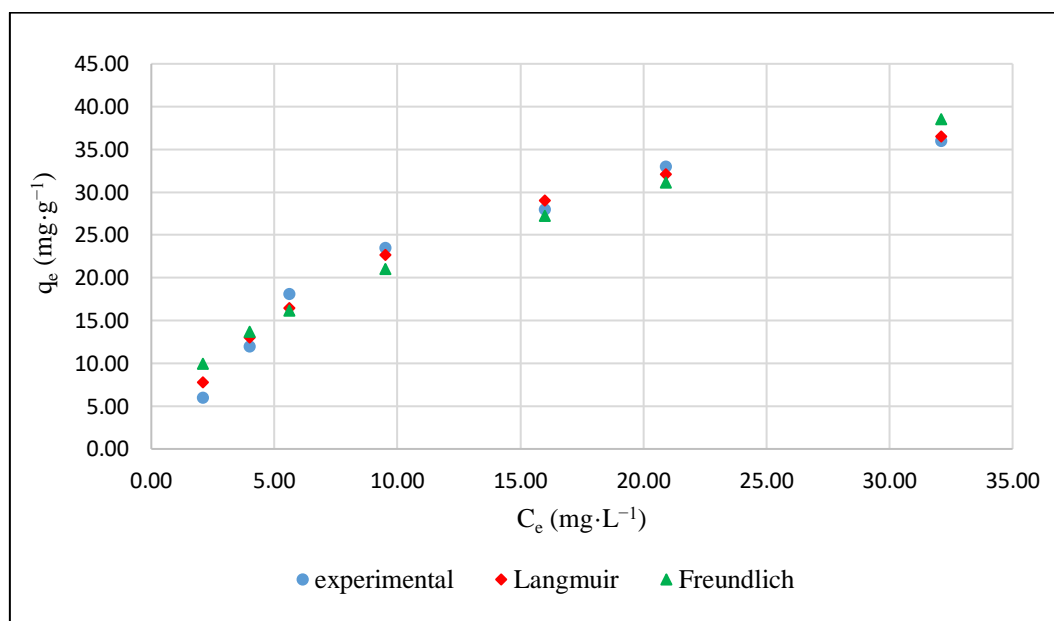


Figure 40. Langmuir and Freundlich isotherm fitting for PO_4^{3-} biosorption by IL-PP

Kinetics

In order to predict mechanisms and potential rate controlling step of PO_4^{3-} biosorption by IL-PP, four kinetic models were applied namely, pseudo-first-order, pseudo-second-order, Elovich equation and intra-particle diffusion. Calculated and experimental q_e values, adsorption constant of each model as well as R^2 and χ^2 values are given in Table 18. Based on R^2 and χ^2 values and comparison between calculated and experimental q_e , it was found that PO_4^{3-} biosorption by IL-PP can be best described by Elovich model ($R^2 = 0.97$, $\chi^2 = 0.007$, $q_{e,\text{cal}} = 12.11$). This kinetic model describes chemical adsorption mechanism and suggests that

IL-PP's surface is heterogeneous [184]. Elovich kinetics model was also postulated for PO_4^{3-} adsorption by various types of adsorbents [185–187]. Experimental kinetics and Elovich fitting model for PO_4^{3-} biosorption by IL-PP are illustrated in Figure 41.

Table 18. Kinetic models and parameters of PO_4^{3-} biosorption by IL-PP.

| Kinetics model | $q_{e,\text{cal}}$ ($\text{mg}\cdot\text{g}^{-1}$) | Parameters | R^2 | χ^2 | $q_{e,\text{exp}}$ ($\text{mg}\cdot\text{g}^{-1}$) |
|--------------------------|---|--|-------|----------|---|
| Pseudo-first order | 11.44 | $K_1 = 1.01$ ($\text{L}\cdot\text{min}^{-1}$) | 0.39 | 0.22 | 12 |
| Pseudo-second order | 11.85 | $K_2 = 0.19$ ($\text{g}\cdot\text{mg}^{-1}\cdot\text{min}^{-1}$) | 0.83 | 0.05 | |
| Elovich equation | 12.11 | α ($\times 10^6$) = 11.88 ($\text{mg}\cdot\text{g}^{-1}\cdot\text{min}^{-1}$) $\beta = 1.72$ ($\text{mg}\cdot\text{g}^{-1}$) | 0.97 | 0.007 | |
| Intra-particle diffusion | 12.22 | $K_3 = 0.28$ ($\text{mg}\cdot\text{g}^{-1}\cdot\text{min}^{-1}$) $C = 10.04$ | 0,91 | 0.03 | |

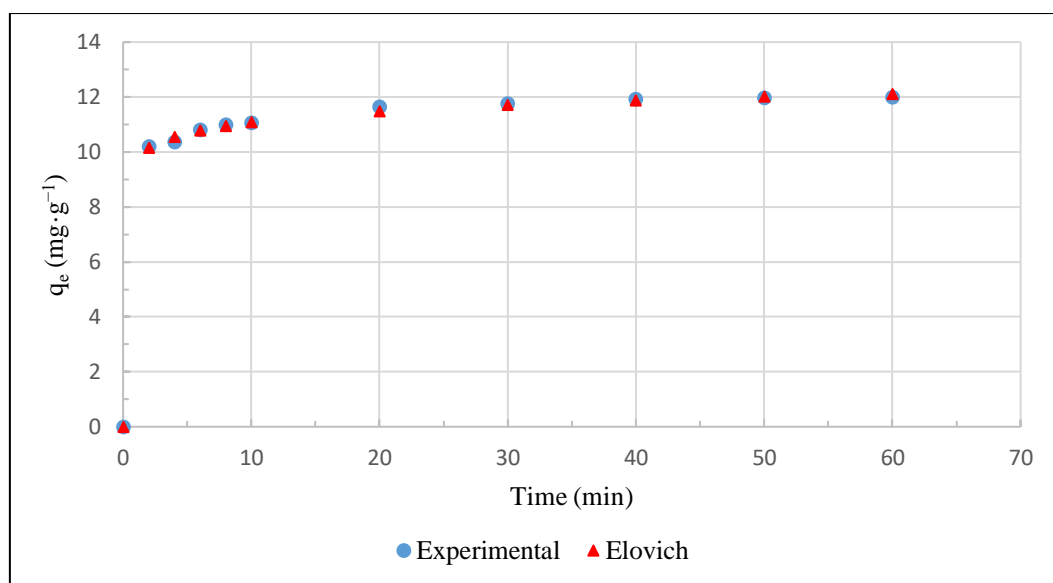


Figure 41. Experimental kinetics and Elovich model fitting for PO_4^{3-} biosorption by IL-PP

Thermodynamics

Thermodynamics study determines whether the adsorption process is favourable, spontaneous exothermic or endothermic [188]. The change in Gibbs free energies ΔG° was calculated using Eq.(2) while ΔH° and ΔS° were calculated from the slope and intercept of the plot of $\ln K_d$ versus $1/T$ (Fig. 42).

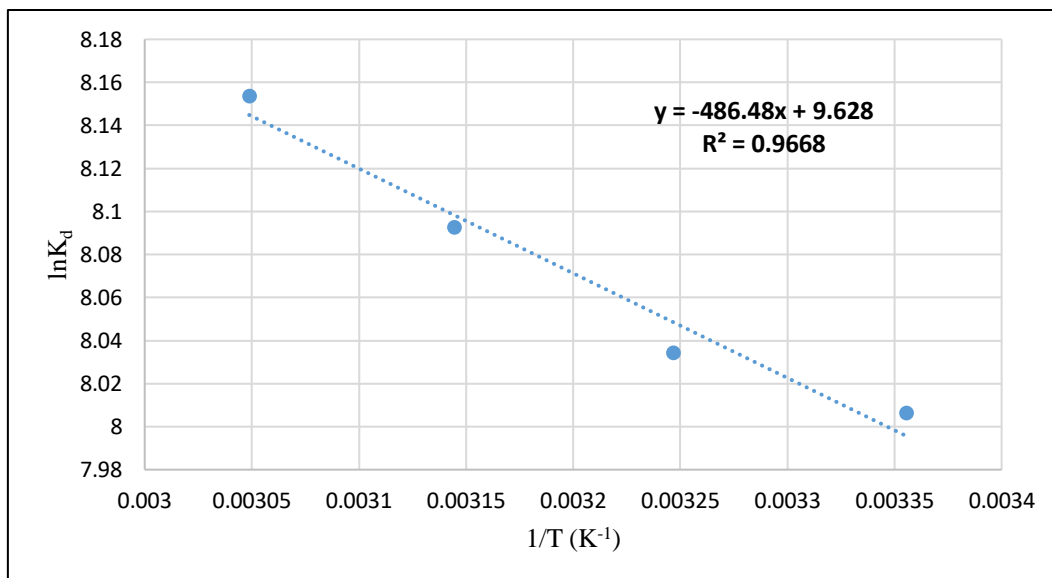


Figure 42. Van't Hoff plot for PO_4^{3-} biosorption by IL-PP

As illustrated in Table 19, ΔG° value was found to decrease from -19836 to -22235 $\text{J}\cdot\text{mol}^{-1}$ when temperature increased from 298 to 328K suggesting a higher driving force and more spontaneous adsorption at high temperature [189]. Positive ΔH° value indicates that PO_4^{3-} biosorption by IL-PP is endothermic in nature due to the enlargement of pore sizes and/or activation of the sorbent surface [190]. Positive ΔS° value (77.87 $\text{J}\cdot\text{K}^{-1}\cdot\text{mol}^{-1}$) indicates that PO_4^{3-} has good affinity to IL-PP [191].

Table 19. Thermodynamics parameters of PO_4^{3-} adsorption by IL-PP.

| Temperature (K) | ΔG ($\text{J}\cdot\text{mol}^{-1}$) | ΔH ($\text{J}\cdot\text{mol}^{-1}$) | ΔS ($\text{J}\cdot\text{K}^{-1}\cdot\text{mol}^{-1}$) |
|-----------------|---|---|---|
| 298 | -19836 | 3384 | 77.87 |
| 308 | -20573 | | |
| 318 | -21395 | | |
| 328 | -22235 | | |

The efficiency of IL-PP to remove PO_4^{3-} from aqueous solution was evaluated in this chapter. Results of this study present IL-PP as an efficient bio-adsorbent which could be used in a green technology for wastewater treatment, waste biomass management and phosphate recovery. However, deep investigations on the efficiency in real operating system present a pivotal issue.

5.6 Application of N-PP and P-IL-PP as fertilizer

After the successful biosorption of N and P nutrients by PP, and taking into account the principles of circular farming, I found that it is important to investigate the utilization of N-PP and P-IL-PP as a soil replacement agent, i.e. fertilizer. This approach seems to be the most

expedient given the need for a suitable nutrient-loaded bio-adsorbent deposit and the high N and P requirements of certain cultivated plants. The key issue that determines the applicability of this approach is related to the toxicity of the nutrient-loaded bio-adsorbents, followed by the determination of their effect on the growth vigor. To answer these queries, I performed the germination and pot tests.

5.6.1 Germination test

Seeds germination is a widely used phytotoxicity test, which integrates all the potentially harmful effects of the substances present in the sample. The RSG % recorded in *Brassica napus* L. of all treatments were high and close to control (100%) assuming no inhibitory effect on seed germination as shown in Figure 43. The slight reduction of RSG compared to control may have been due to the availability of such as phenolic compounds, ethylene, ammonia, organic acids and excess accumulation of salts that may have a low phytotoxicity effect [192].

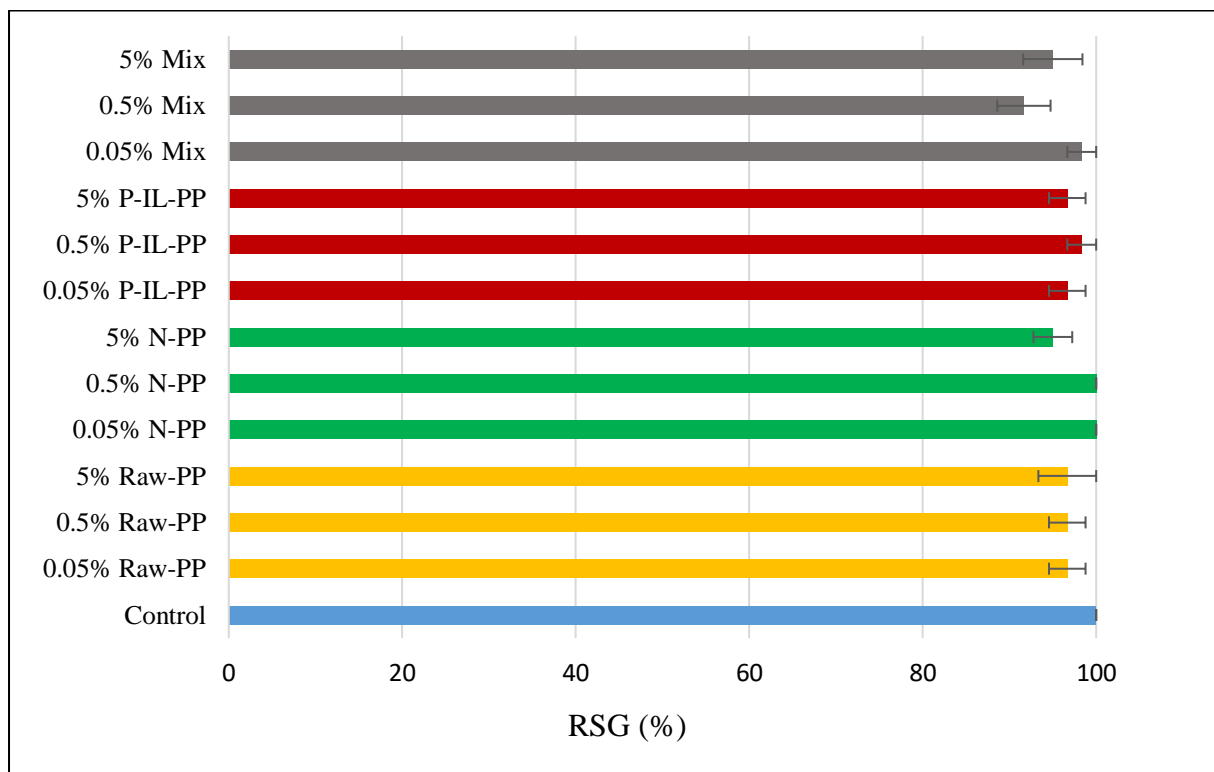


Figure 43. RSG of *Brassica napus* L. using tested treatments.

On the other hand RRE% of most germinated seeds were above the control (100%) and they can be ordered as follow: 0.05% Mix (123%) > 0.05% and 0.5% P-IL-PP and 0.05% N-PP (121%) > 0.5% N-PP (114%) > 0.05% Raw-PP (113%) > 0.5% Mix (112%) (Figure 44). This can be explained by the uptake of nitrogen and phosphorus by *Brassica napus* L. seeds

for use in various metabolic activities, including cell division, differentiation and elongation [193].

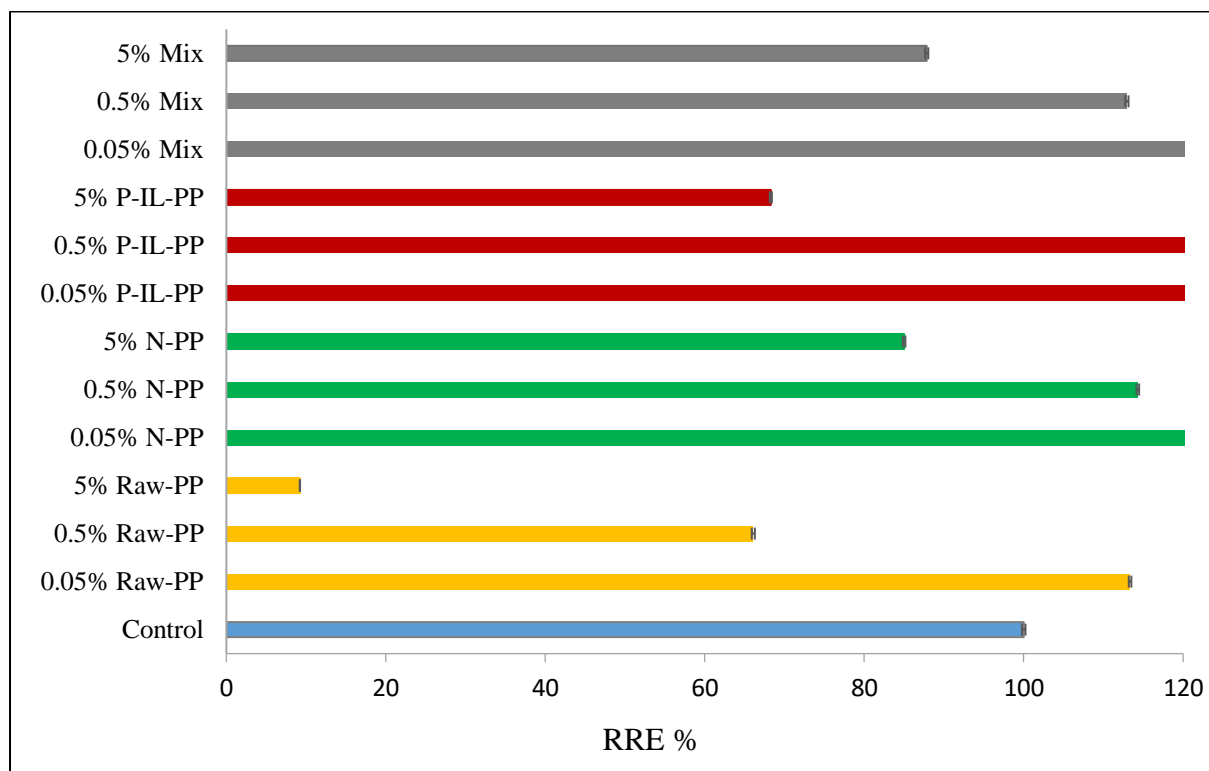


Figure 44. RRE of Brassica napus L. using tested treatments.

The germination index (GI%) of Brassica napus L was used to evaluate the ecotoxicological effects of N-PP and P-IL-PP based on the rate of seed germination during the assay period and thus verify their suitability for agricultural purposes. A GI above 80% indicates a non-phytotoxicity of the studied material and below 50% reveals toxicity [143,193]. The calculated germination indexes for all treatments studied are shown in Figure 45. The results showed that 5% Raw-PP significantly inhibited the seed germination (GI=8.91%), while GI of 0.5% Raw-PP was above 50 assuming the non-toxicity of the Raw-PP at low doses. Moreover GI of 0.05 Raw-PP has significantly stimulated the germination rate (GI=109%) compared to control (100%) indicating the beneficial use of Raw-PP as fertilizer with moderate concentrations. The efficiency of Raw-PP as fertilizer was investigated and proven in different studies [194,195]. On the other hand, calculated GI of all N-PP, P-IL-PP and Mix treatments were above 80% except 5% P-IL-PP that showed a GI of 66% indicating the non-phytotoxicity of these treatments. Furthermore, higher GI values were recorded for 0.05% N-PP (GI=121%), 0.5% N-PP (GI=114%), 0.05% P-IL-PP (117%), 0.5% P-IL-PP (119%), 0.05% Mix (121%) and 0.5 Mix (103%) indicating a favorable response Brassica napus L. to the application of the use of these materials as fertilizers during the germination phase.

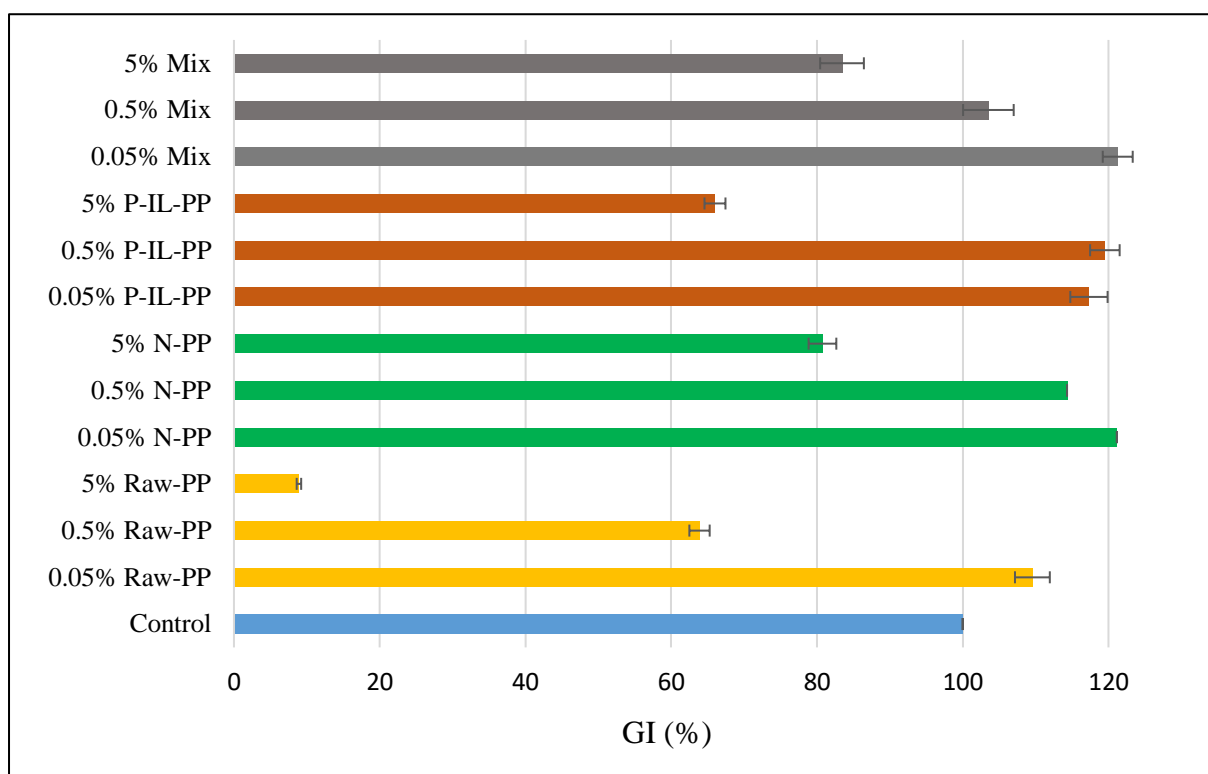


Figure 45. GI of Brassica napus L. using tested treatments.

5.6.2 Pot experiments

Pregerminated seeds of Brassica napus L. were sowed in soil for phytotoxicity measurements in order to obtain a broader view of the phytotoxicity of N-PP and P-IL-PP and to further understand their effects on the morphological characteristics of Brassica napus L. seedlings. The treatments evaluated in this pot study were the same as those used in the germination study.

Plant habit which is the height of the plant from the surface of the pot soil to the top of the highest point of the plant for every treatment was recorded as shown in Figure 46. No significant inhibition can be observed for plant habits compared to control (27 cm). Treatments with a decreased plants habits are: 0.05 Raw-PP (22cm), 0.5 Raw-PP (26 cm), 0.05 N-PP (25 cm), 0.5 N-PP (25 cm), 0.05 P-IL-PP (23 cm) and 5% P-IL-PP (24 cm). However, the other treatments have positively affect the plants habits including 5% Raw-PP (32cm), 0.05% Mix (28cm), 0.5% Mix (29cm), 5% Mix (30cm). These results are in line with another study of Kangning and coworkers reporting no inhibited root elongation of maize treated by nutrient-loaded biochar [196].

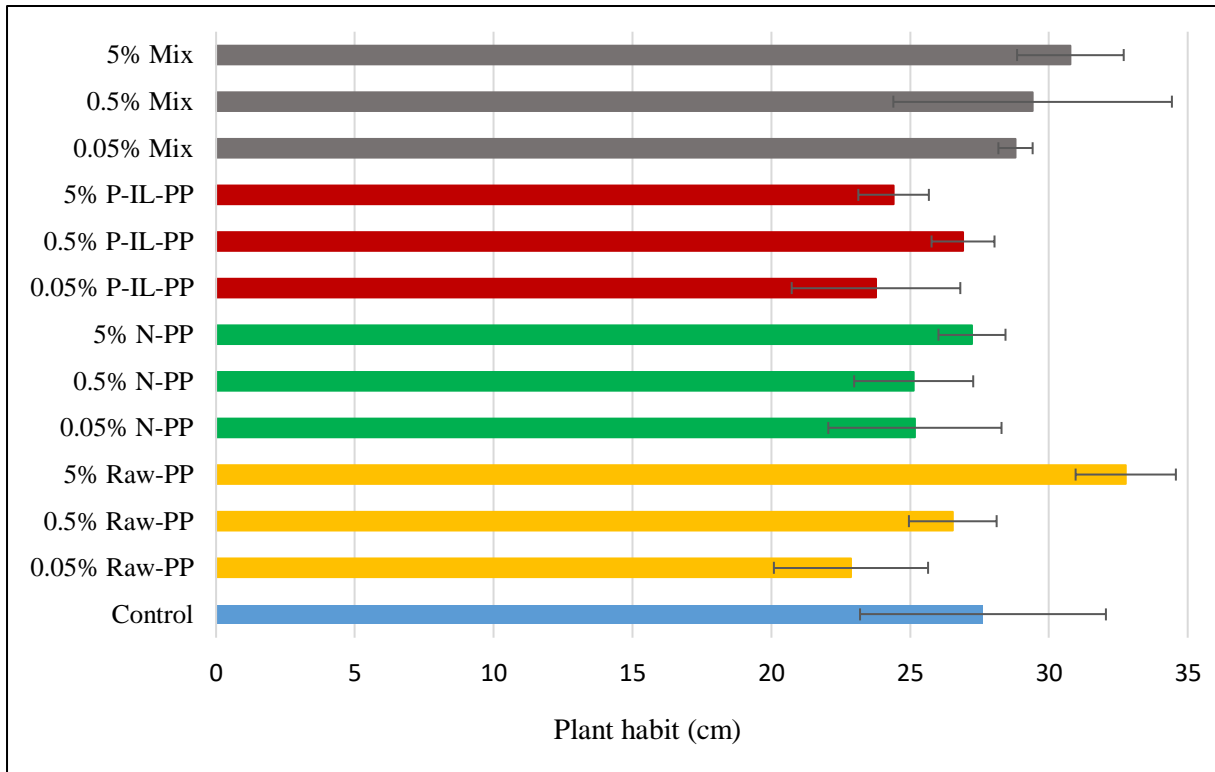


Figure 46. Plant habits of Brassica napus L. using tested treatments

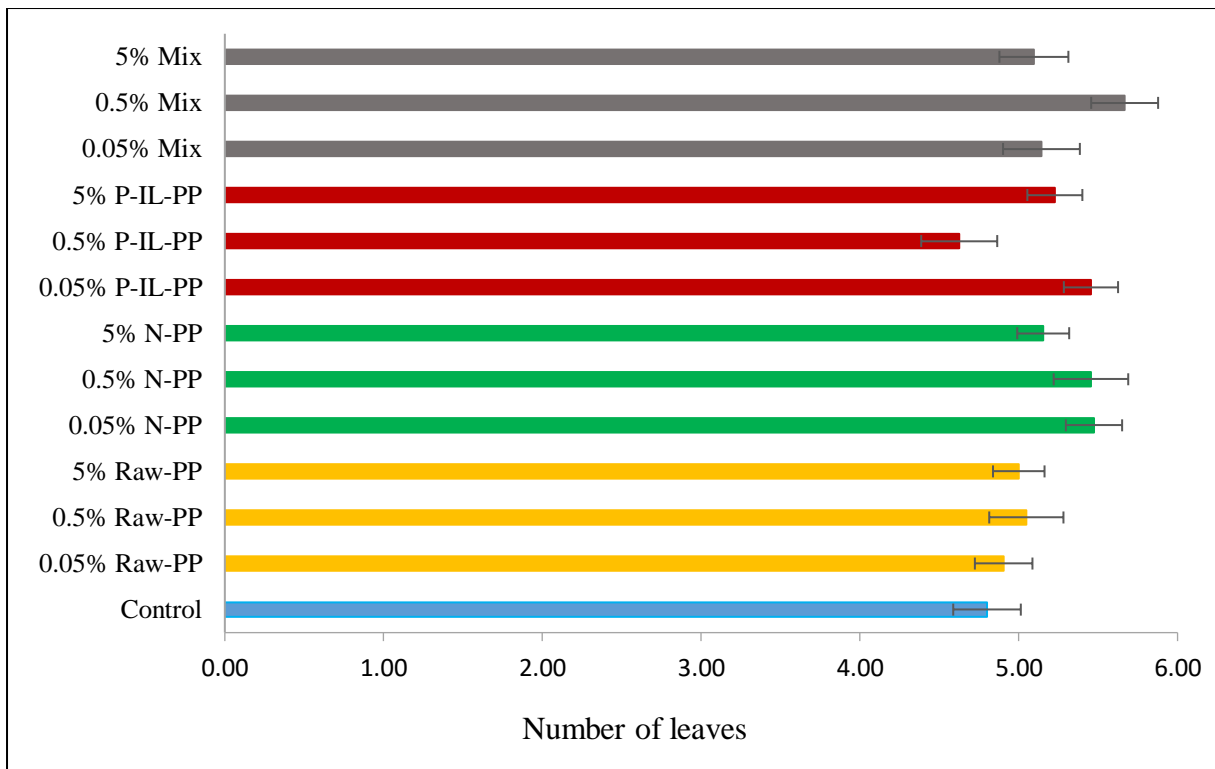


Figure 47. Number of produced leaves of Brassica napus L. using tested treatments

On the other hand, Figure 47 showed that the number of produced leaves have been stimulated for all the treatments except 0.5% P-IL-PP that showed an average number of

leaves equal to 4.63 which is lower than control (4.80) . The number of leaves for the studied treatments can be ordered as follow: 0.5% Mix (5.67) > 0.05% N-PP (5.47) > 0.5% N-PP and 0.05% P-IL-PP (5.45) > 5% P-IL-PP (5.23) > 5% N-PP (5.15) > 0.05% Mix (5.14) > 5% Mix (5.10) > 0.5% Raw-PP (5.05) > 5% Raw-PP (5.00) > 0.05% Raw-PP (4.90) > control (4.80).

Brassica napus L. seedlings were also assessed in terms of root and shoot fresh weight (g). For this purpose, Brassica napus L. seedlings were harvested. Roots and shoots were weighted (roots were gently washed in order to remove all the possible soil particles, then dried using paper towel to avoid biases). Results presented in Figure 48 showed that all treatments have negatively affected the root weight except 0.5 P-IL-PP treatment that shows a root weight of 0.55g which is higher than control (0.52g). It was expected that nitrogen and phosphorus involved in the bio-adsorbent will promote the weight of roots [197], however, an inhibitory effect of N-loaded PP and P-loaded-IL-PP on fresh root weight was observed and can be explained by the imbalances in the metabolism of reactive molecules, such as reactive oxygen- and nitrogen-species which may influence the root growth responses [198].

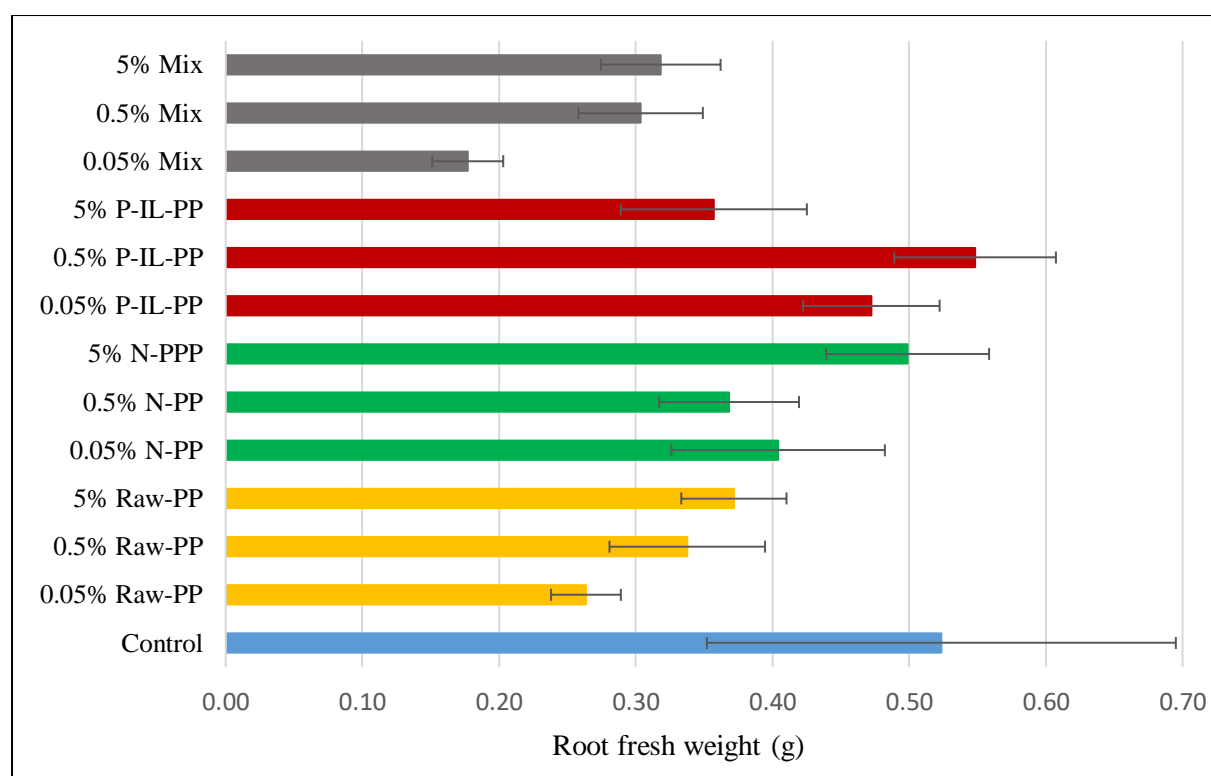


Figure 48. Root fresh weight of Brassica napus L. using tested treatments

Contrarily, the plant showed positive response in term of shoots fresh weight as most of treatments exceeding the control (5.55g) (Figure 49). The recorded shoots fresh weight can be ordered as follow: 5% Raw-PP (8.60 g) > 0.5% Mix (8.49 g) > 5% Mix (7.38 g) > 0.5% Raw-PP (7.02g) > 0.05% Mix (6.91g) > 0.5% P-IL-PP (6.62g) > 0.05% P-IL-PP (6.59g) > 0.05%

Raw-PP (6.54g) > 5% P-IL-PP (6.33g) > 5% N-PP (6.23g) > 0.5% N-PP (5.83g) > 0.05% N-PP (5.31g). This positive response can be explained by the high availability of nitrogen and phosphorus thus the produced shoots biomass increased which in turn explains the decrease in fresh shoot weight for 0.05% N-PP treatment. The dual effects of N-PP and P-IL-PP on roots and shoots fresh weights can be due to the slow release of nitrogen and phosphorus in soil and thus the plant needs more time to uptake these nutrients and use them for its nutritional and metabolic needs.

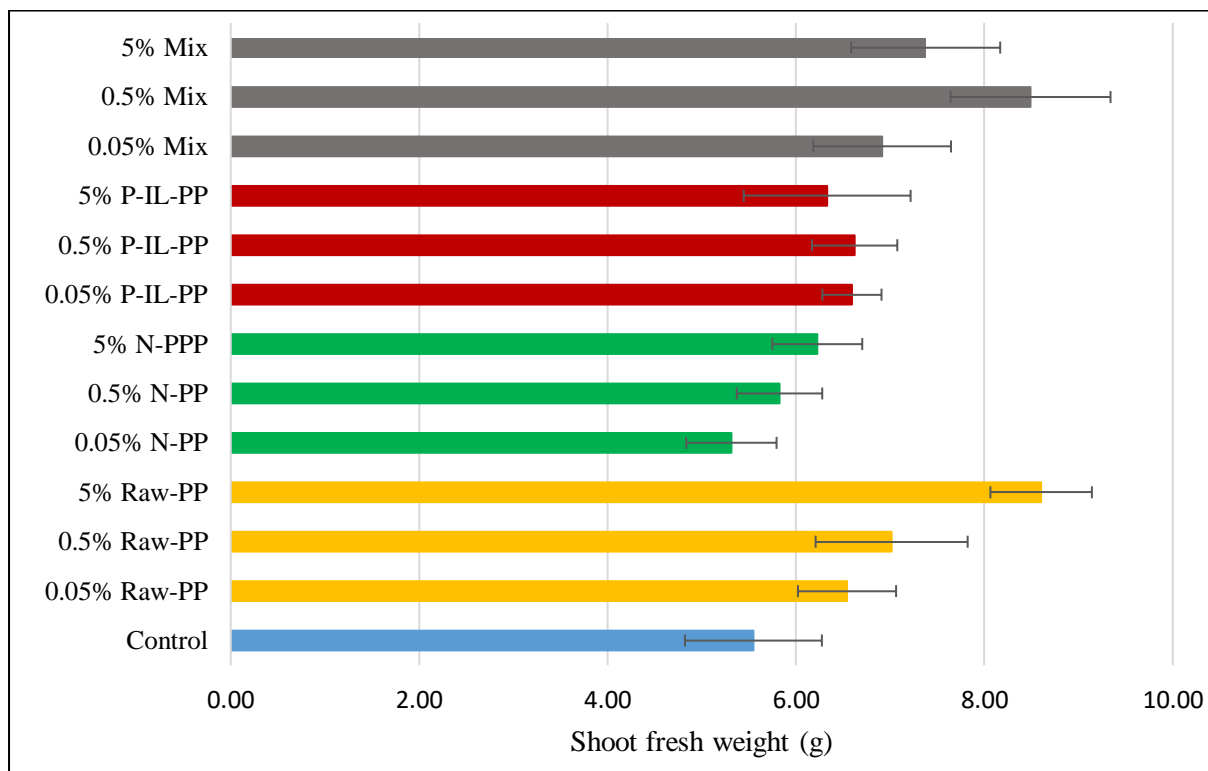


Figure 49. Shoots fresh weight of *Brassica napus* L. using tested treatments

The roots and shoots weights were also determined following oven drying at 70 °C for 3 days. Results of roots and shoots dry weights are shown in Figures 50 and 51. Similarly to results of roots and shoots fresh weight, the plants continue to show a negative response in terms of roots morphology as the dry weight was lower than control (0.08g) for most of treatments except 0.5% P-IL-PP (0.09g) and 0.05% N-PP (0.084) (Figure 50). However, most of treatments were favorable for shoots dry weight measurements in particular the ones with high content of nitrogen and phosphorus (Figure 51). Significantly higher shoots dry weight than control (0.48 g) were observed for 0.5% Raw-PP (0.57g), 5% PP (0.69g), 0.5% N-PP (0.52g), 5% N-PP (0.56g), 0.05% P-IL-PP (0.55g), 0.5% P-IL-PP (0.63g), 5% P-IL-PP (0.61g), 0.5% Mix (0.66g) and 5% Mix (0.54g). These results can be explained similarly to results of roots and

shoots fresh weight measurement assuming that the inhibitory effects of treatments appeared only in the roots while a beneficial effect is recorded in shoots.

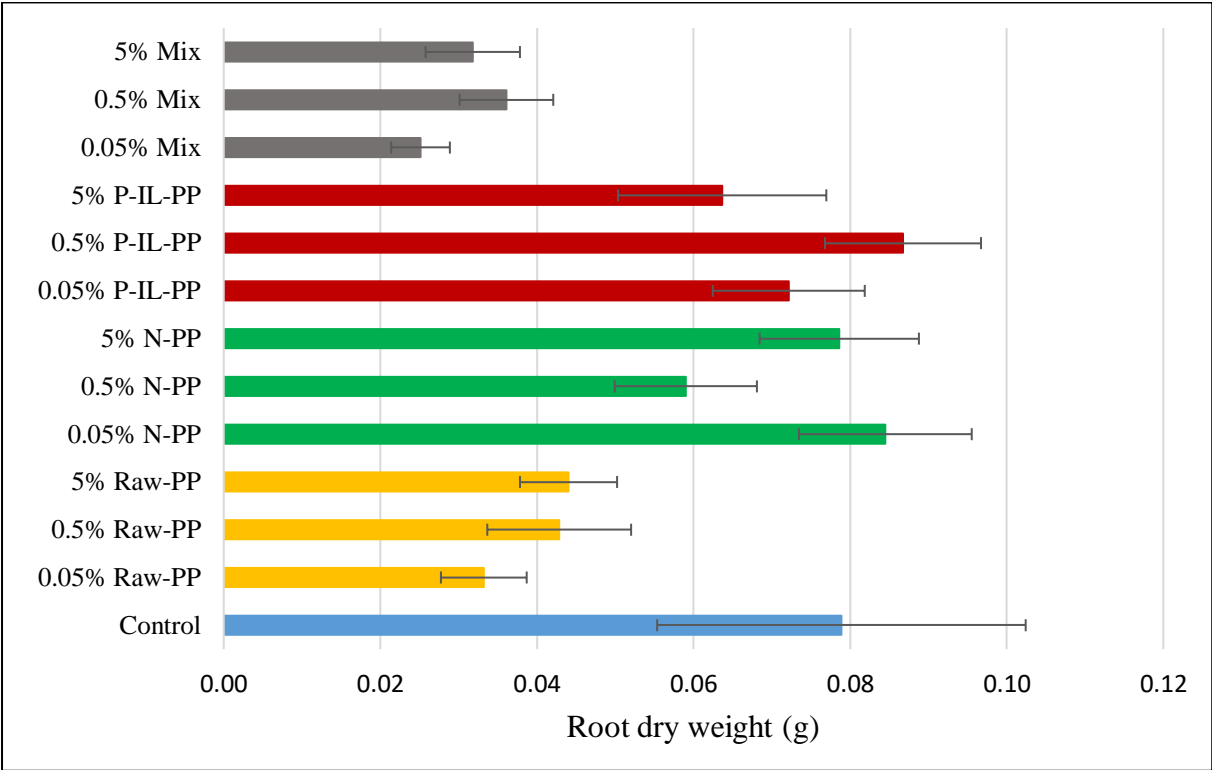


Figure 50. Roots dry weight of Brassica napus L. using tested treatments

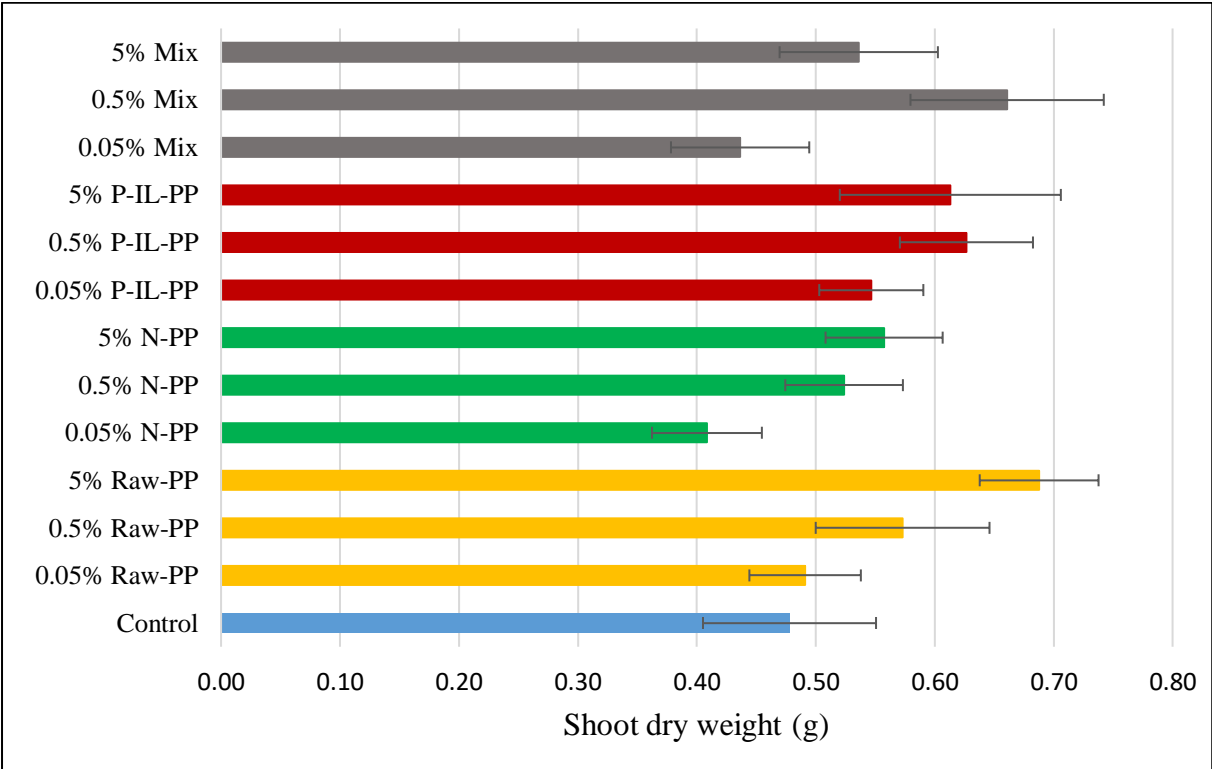


Figure 51. Shoots dry weight of Brassica napus L. using tested treatments

6 Conclusion

Biosorption and recovery of nutrients from AFW provide new solutions for several environmental concerns particularly water shortage and pollution, nutrient sources depletion and solid waste deposit. This Ph.D. dissertation systematically investigated the application of PP as an abundant AFW to remove and recover nutrients from aqueous solutions.

Characterization of PP showed that this biomaterial holds promising physicochemical characteristics such as highly negative zeta potential derived from the abundance of functional group namely $-\text{COOH}$ and $-\text{OH}$ which afford to PP not only the ability to successfully adsorb cations contaminants but also facilitate its activation with cationization method for anion adsorption purpose.

Batch adsorption study of NH_4^+ by PP showed that pH and adsorbent dose are parameters with the high effect on the process. NH_4^+ removal of 97% was achieved within 120 min using 400 mg PP at initial $\text{NH}_4\text{-N}$ concentration of $30 \text{ mg}\cdot\text{L}^{-1}$, pH 4 and 25°C temperature. The process was described by Langmuir isotherm model with a maximum $\text{NH}_4\text{-N}$ uptake of $6.18 \text{ mg}\cdot\text{g}^{-1}$ assuming that the adsorption occurs by monolayer coverage, and the active sites present on PP surface hold equal affinity to NH_4^+ under a chemisorption reaction according to the pseudo-second order kinetics model.

The performance of PP under real condition was proved by studying the adsorption of NH_4^+ from MPWW. The parameters pH and adsorbent dose continue to be the parameters with high effect on the process. Optimum NH_4^+ removal of 81.8% was achieved within 120 min using 1.5 g PP at pH 6 and 25°C . Maximum $\text{NH}_4\text{-N}$ uptake was $\sim 2.5 \text{ mg}\cdot\text{g}^{-1}$ as calculated by Langmuir model that was the best fitted isotherm model together with pseudo-second order kinetics model.

Modification of PP using iron-loading method have successfully enhanced PO_4^{3-} uptake due to the surface positive charges induced by Fe_3^+ . Batch adsorption study using factorial design method have showed that pH and adsorbent dose are the significant factors. Optimization results showed that 150 mg of IL-PP could achieve 90 % of PO_4^{3-} removal with a maximum of $49.12 \text{ mg}\cdot\text{g}^{-1}$ of $\text{PO}_4\text{-P}$ uptake within 60 min using initial $\text{PO}_4\text{-P}$ concentration of $40 \text{ mg}\cdot\text{L}^{-1}$ at pH 9 and 25°C temperature. Adsorption isotherm was found to follow both Langmuir and Freundlich models indicating the complexity of IL-PP's surface, and the process was found to be governed by chemisorption according to Elovich kinetics model.

Investigation on the use of N-PP and P-IL-PP as fertilizer have showed the non-toxicity of these materials through a positive response of *Brassica napus* L. during germination and

seedling phases. However further studies on other plant species have to be done in order to certify the suitability of N-PP and P-IL-PP for use in agricultural purposes, which will encourage the use of this approach particularly in regions that lack budgets for wastewater treatment facilities and suffer from the burden of AFW including PP.

7 Summary

In this Ph.D. dissertation, I have investigated the biosorption of ammonium (NH_4^+) and phosphate (PO_4^{3-}) from aqueous solutions using pomegranate peel (PP), followed by the recovery of these important nutrients elements by studying the possibility of using nutrient-loaded PP as fertilizer.

In the introduction part, I have given an overview of water shortage and pollution issues, including the problems related to the excess discharge of nutrients in water bodies. I have emphasized the major contribution of agriculture in these problems, which is inevitable due to the indispensable roles of water and nutrients in agricultural production. Therefore, there is a need for a sustainable and efficient technology that combines water purification and recycling with nutrient recovery, especially phosphorus that is facing a serious threat to depletion.

Among existing methods for nutrient removal and recovery, adsorption technology englobes all the required features and desired benefits. Furthermore, I have introduced the problem related to agricultural and food waste (AFW) disposal and the possibility of turning its burden into benefits by the use of these valueless bio-materials as bio-adsorbents for several valuable contaminant removal and recovery, especially nutrients. This approach works according to the 4R principle (Reduce, Reuse, Recover and Recycle): Reduce the overuse of water sources and wastes, Reuse AFW, Recover nutrients and Recycle nutrients and wastewater.

In the literature review section, I have discussed in detail the problem of nutrient release in water bodies by indicating their encountered forms, sources, and cycles. Afterward, I have presented the most relevant methods and technologies used for the removal and recovery of NH_4^+ and PO_4^{3-} from aqueous solutions. A focus was laid on the biosorption process that comes with several advantages such as simplicity, cost-effectivity, and various potential bio-adsorbents with the possibility of their reuse for soil fertilization. I have introduced the state of the art of this relatively new technology. I have presented methods for characterization and modification of AFW, process mechanisms, influencing parameters, in addition to the modeling of isotherm, kinetics, and thermodynamics. I have also presented the most relevant attempts at using nutrient-loaded bio-adsorbent as fertilizer. Among AFW tested as bio-adsorbent, PP, which is a valueless and widely produced fruit waste holds promising adsorptive characteristics in a raw and modified form or even as activated carbon/biochar.

In line with the main aim of this Ph.D. research, which is producing an efficient bio-adsorbent from AFW for NH_4^+ and PO_4^{3-} removal and recovery, I have started my experimental work with a screening experiment using seven AFW (pomegranate peel, banana peel, wheat husk,

compost, poplar bark, wheat bran, and sugar beet pulp) to test their efficiency to remove NH_4^+ from ammonium chloride (NH_4Cl) model solution. Among AFW tested, PP showed encouraging results, therefore it was selected for a detailed analytical study using the batch adsorption method.

During these studies I have explored PP in terms of its physicochemical characteristics by the determination of zeta potential, Fourier-transform infrared spectroscopy analysis (FT-IR), scanning electron microscopy (SEM), particle size distribution, and porosity. Then, I have investigated the effect of parameters such as pH, adsorbent dose, initial ammonium concentration, stirring speed, and contact time on the biosorption of NH_4^+ by PP using one factor at a time method (OFAT). I have found that the adsorbent dose and initial ammonium concentration were the parameters with the highest impact on the process, while the effect of other parameters such as pH and stirring rate was negligible. NH_4^+ removal of more than 97% was achieved within 120 min. For process modeling, adsorption isotherm was fitted to Langmuir and Freundlich models using the linear method. Results showed that the process is well described by the Langmuir model ($R^2 = 0.98$) with a maximum adsorption capacity of 6.18 mg $\text{NH}_4\text{-N/g}$. Investigations on the process kinetics showed that the system reached equilibrium within 120 min and can be adequately described by pseudo-second order model ($R^2 = 0.99$) assuming that the process is governed by chemisorption mechanism with sharing and exchange of electrons between PP and NH_4^+ .

Driven by the necessity to prove the efficiency of PP to remove NH_4^+ under real conditions, I have conducted a batch adsorption study using milking parlor wastewater (MPWW), which is characterized by a high content of NH_4^+ with other cations that are expected to effectively compete with NH_4^+ to be adsorbed on PP's surface. The effects of influencing parameters such as pH, adsorbent dose, stirring rate, temperature, and contact time were investigated using OFAT method to determine their optimum values for higher NH_4^+ removal. Results showed that using 1.5 g of PP achieved 81.84% of NH_4^+ removal at pH 6, temperature of 25 °C, and stirring rate of 300 rpm within 120 min. Investigation on the process isotherm was done using the linear method and showed that the process was well described by the Langmuir model ($R^2=0.99$) with a maximum adsorption capacity of ~2.5 mg $\text{NH}_4\text{-N /g}$. Kinetics were best fitted to the pseudo-second order model that describes a chemisorption mechanism. A brief comparison between the efficiency of PP to remove NH_4^+ from NH_4Cl model solution and MPWW was done. The obtained results of both studies introduce PP as a promising bio-adsorbent for NH_4^+ removal from aqueous solutions.

In the next study, I have investigated the application of PP for PO_4^{3-} removal from di-sodium hydrogen phosphate (Na_2HPO_4) model solution. For this purpose, PP was activated via saponification using sodium hydroxide (NaOH) followed by cationization using iron chloride (FeCl_3) to develop appropriate active sites able to attach PO_4^{3-} . Characterization of iron-loaded PP (IL-PP) was done using zeta potential measurement, SEM, and FT-IR analysis, which has confirmed the successful incorporation of Fe(III) on PP's surface. The equilibrium time and the effect of pH were determined using the batch adsorption method. For identification of the influencing parameters such as pH, adsorbent dose, temperature, and their interactions, the factorial design was applied using statistical software. Effective removal of phosphate up to 90% was achieved within 60 min, at pH 9 and 25 °C temperature using 150 mg dose of IL-PP. The experimental adsorption data were examined with conventional isotherm and kinetic models using the non-linear method. The results showed that the kinetics are best described by the Elovich model ($R^2=0.97$), which assumes the dominance of the chemisorption mechanism and a heterogeneous surface of IL-PP. The adsorption isotherm obeys both the Langmuir ($R^2 = 0.98$) and Freundlich ($R^2 = 0.94$) models with a maximum phosphate uptake of $49.12 \text{ mg}\cdot\text{g}^{-1}$. Investigation of thermodynamic parameters such as the standard Gibbs free energy change, standard enthalpy change, and standard entropy change showed that the process is spontaneous and endothermic in nature. These results introduce IL-PP as an efficient bio-adsorbent of phosphate.

The use of nutrient-loaded bio-adsorbent as fertilizer presents the cornerstone of the biosorption of nutrients by AFW, therefore, investigating the application of nitrogen-loaded PP and phosphorus-loaded IL-PP as fertilizer was the subject of the last study in this thesis to provide a preliminary assessment of their suitability for land application. Ecotoxicological bioassays like seeds germinations and pot experiments were used to evaluate the phytotoxicity effect of nitrogen-loaded PP and phosphorus-loaded IL-PP on the morphological and physiological responses of oilseed rape (*Brassica napus* L.) which is commonly used for this purpose. Phytotoxicity was assessed through the analysis of germination index (GI), relative seeds germination (RSG), relative root elongation (RRE), leaf counts, and plant habit in addition to plant fresh and dry weight. Germination results demonstrated no inhibitory effect on the recorded seeds and a beneficial effect has been observed with many seeds especially those using low percentages of nutrient-loaded bio-adsorbent. The results of pot experiments also supported the safety and efficiency of nitrogen-loaded PP and phosphorus-loaded PP as a fertilizer for agricultural crops.

The use of PP in large-scale technology for nutrients removal and recovery presents a win-win approach that combines water protection with nutrient sources preservation and AFW revalorization especially in developing countries known for the huge cultivation and processing of pomegranate fruit. While all objectives of this research thesis were answered, many points must be addressed for future research mainly:

- Further study to improve NH_4^+ adsorption capacity of PP is recommended.
- Further investigation based on Fixed-bed adsorption processes is required to scale up the process.
- Further improvement of PP modification in the directions of cost-saving, effectiveness, and environmental friendliness.
- Examining the potential of IL-PP for PO_4^{3-} removal and recovery from real wastewater to promote the large-scale application.
- Investigation of suitable methods for regeneration of nutrient-loaded PP and IL-PP.
- Further investigation for the production of high-quality nutrient fertilizers from nitrogen-loaded PP and phosphorus-loaded IL-PP.
- Investigation of the cost-efficiency of the whole process.

8 Összefoglalás

Disszertációmban gránátalma héj (pomegranate peel - PP) felhasználásával az ammónium (NH_4^+) és foszfát (PO_4^{3-}) ionok vizes oldatokból történő bioszorpcióját vizsgáltam, majd ezen fontos tápanyag-elemek visszanyerése céljából, tanulmányoztam az adszorbeátumok műtrágyaként történő felhasználásának lehetőségét is.

A bevezetésben áttekintettem a vízhiány és a vízszennyezés kérdéskörét, beleértve a tápanyagok túlzott kibocsátásával kapcsolatos problémákat. Hangsúlyoztam a mezőgazdaság jelentős, megkerülhetetlen szerepét ezekben a kérdésekben, hiszen a víz maga, és az abban oldott tápanyagok nélkülözhetetlenek a mezőgazdasági termelésben. Ezért, olyan fenntartható és hatékony technológiára van szükség, amely ötvözi a víztisztítást és a tápanyagok visszanyerését valamint azok újbóli felhasználását. Különösen fontos ebből a szempontból a foszfor, mert a foszfor bányák kimerülése komoly fenyegetést jelent napjainkban.

Az ismert, tápanyagok eltávolítására és visszanyerésére alkalmas módszerek közül az adszorpciós technológia rendelkezik minden szükséges előnyös tulajdonsággal.

Az adszorpció műveletére alapozva kifejlesztettem egy olyan eljárást, amely egyaránt megoldást kínál a mezőgazdasági- és élelmiszer-hulladékok (agricultural food waste - AFW) ártalmatlanítására, azok bioadszorbensként történő felhasználásával, valamint a szennyvizekből kivont értékes tápanyagok hasznosítására is.

Az irodalmi részben részletesen tárgyaltam a tápanyagokban gazdag vizek, szennyvizek problémáját, bemutatva azok fellelhető formáit, forrásait és ciklusait. Ezt követően bemutattam az NH_4^+ és PO_4^{3-} ionok vizes oldatokból történő eltávolítására és visszanyerésére használt legmegfelelőbb módszereket és technológiákat. A hangsúlyt a bioszorpciós folyamat kapta, hiszen ez számos előnnyel jár, mint például az egyszerűség, a költséghatékonyság és a különböző, potenciális bioadszorbeátum műtrágyaként történő újra felhasználásának lehetősége.

Ismerttettem ennek a viszonylag új technológiának a legújabb kutatási eredményeit. Bemutattam az AFW jellemzésére és módosítására alkalmas módszereket, az adszorpciós folyamat mechanizmusát, a meghatározó paramétereket, valamint az adszorpció izotermáinak, kinetikájának és a termodinamikájának leírását szolgáló modelleket. Bemutattam a legrelevánsabb tesztek is, melyek alkalmasak a tápanyaggal dúsított bioadszorbensek műtrágyaként történő alkalmazásának kimutatására.

A bioadszorbensként tesztelt AFW-k közül a gránátalma héj (PP), amely a mediterrán országokban széles körben fellelhető értéktelen gyümölcshulladék, ígéretes adszorpciós tulajdonságokkal rendelkezik eredeti és módosított formában csak úgy, mint aktív szénként alakítva.

A disszertációm fő célkitűzésének megfelelően – vagyis egy hatékony, mezőgazdasági vagy élelmiszeripari hulladék eredetű (AFW) bioadszorbens felkutatása, amely alkalmas NH_4^+ és PO_4^{3-} ion kinyerésére –, kísérleti munkámat hét különböző AFW szűrővizsgálatával indítottam: gránátalma héj, banán héj, búza pelyva, komposzt, nyárfa kéreg, búza korpa, cukorrépa szelet. Az ammonium-klorid modell oldatból történő NH_4^+ ion eltávolítási hatékonyság szempontjából a tesztelt hulladékok közül a gránátalma héj biztató eredményeket mutatott, ezért ezt részletes analitikai vizsgálatnak vettem alá különböző szakaszos rendszerű adszorpciós kísérletek segítségével. E vizsgálatok során feltártam a PP legfontosabb fizikai-kémiai jellemzőit zéta-potenciál meghatározásával, Fourier-transzformációs infravörös spektroszkópiai elemzéssel (FT-IR), pásztázó elektronmikroszkópos (SEM), részecskeméret-eloszlási és porozitási vizsgálatokkal.

Ezt követően OFAT (one factor at time) módszerrel (időben egy tényező választása) az NH_4^+ ionok PP-n történő adszorpciós művelete szempontjából fontos paraméterek hatásának vizsgálatát végeztem el, mint például a pH, az adszorbens dózisa, a kezdeti ammónium koncentráció, a keverési sebesség és az érintkezési idő. Azt tapasztaltam, hogy a legmeghatározóbb paraméterek az adszorbens dózis és a kezdeti ammónium koncentráció, míg például a pH és a keverési sebesség hatása elhanyagolható. Az NH_4^+ ionok 97% -ot meghaladó eltávolítási hatékonyságát 120 percen belül sikerült elérni.

A folyamat modellezéséhez a mérési adatokra a Langmuir és a Freundlich féle adszorpciós izoterma modellt illesztettem. Az eredmények alapján megállapítottam, hogy a folyamatot a Langmuir-modell ($R^2=0,98$) írja le kiválóan, itt a maximális adszorpciós kapacitás 6,18 mg $\text{NH}_4\text{-N/g}$. A folyamat kinetikai vizsgálatai azt mutatták, hogy a rendszer 120 percen belül elérte az egyensúlyt, és a folyamat megfelelően leírható pszeudo-másodrendű modellel ($R^2 = 0,99$), ebből adódóan feltételezhető, hogy a folyamatot kemisorpciós mechanizmus szabályozza az elektronoknak a PP és NH_4^+ közötti megosztásával és cseréjével.

A gránátalma héj ammónium-megkötő hatékonyságának bizonyítására nem csak modell oldatokkal, hanem valós oldatokkal is végeztem kísérleteket. Az NH_4^+ ionok valós körülmények között végzett eltávolítását szakaszos adszorpcióval, fejtőházi szennyvizet (milking parlol wastewater, MPWW) alkalmazva vizsgáltam. Ennek igen magas az

ammónium tartalma, és e mellett más kationokban is igen gazdag, melyek várhatóan hatékonyan versenyeznek a PP felületén található kation-kötőhelyekért. A pH, az adszorbens dózis, a keverési sebesség, a hőmérséklet és az érintkezési idő, befolyásoló szerepét OFAT módszerrel vizsgáltam, hogy meghatározzam a paraméterek optimális értékeit a minél nagyobb NH_4^+ eltávolítási hatékonyság elérése érdekében.

Az eredmények azt mutatták, hogy 1,5 g PP felhasználásával 81,84% -os NH_4^+ eltávolítást értem el pH= 6 értéknél, 25 ° C hőmérsékleten és 300 fordulat/perc keverési sebességgel, 120 percen belül. A folyamat izotermáját lineáris módszerrel elemeztem, és kimutattam, hogy a folyamatot a Langmuir-modell ($R^2 = 0,99$) írja le kielégítő módon, maximális adszorpciós kapacitás értéke ~ 2,5 mg $\text{NH}_4\text{-N}$ /g. A kinetika leginkább a pszeudo-másodrendű modellhez illeszkedett, tehát itt is kemiszorpciós mechanizmust feltételezhetünk.

A gránátalma héj (PP), mint NH_4^+ eltávolítására alkalmas bioadszorbens, hatékonyság vizsgálatát mind NH_4Cl modell oldatból mind pedig valós, fejtőházi szennyvízből elvégeztük. Mindkét vizsgálat a PP-t ígéretes bioadszorbensként igazolta az NH_4^+ vizes oldatokból történő eltávolítása céljából, akár valós szennyvizekből is.

A disszertációm második részében azt vizsgáltam meg, hogy a PP milyen módosítással tehető alkalmassá anionok, jelesül PO_4^{3-} eltávolításra, pl. dinátrium-hidrogén-foszfát (Na_2HPO_4) modell oldatból. Ezért a gránátalma héjat elszappanosítással aktiváltam (nátrium-hidroxid (NaOH) segítségével, majd vas-klorid (FeCl_3) alkalmazásával "kationoztam", vagyis megfelelő aktív helyeket alakítottam ki, amelyek képesek a PO_4^{3-} megkötésére.

A vassal-módosított gránátalma héj (iron-loaded pomegranate peel - IL-PP) jellemzését zéta potenciál méréssel, SEM és FT-IR elemzéssel végeztem, ami megerősítette a Fe^{3+} ion sikeres beépülését a PP felületére. Az egyensúlyi idő és a pH hatásának meghatározását szakaszos adszorpciós módszerrel határoztam meg. A befolyásoló paraméterek, mint például a pH, az adszorbens dózis, a hőmérséklet hatásának és kölcsönhatásainak megállapításához faktoriális tervet, statisztikai szoftvert alkalmaztam.

A foszfát ion, akár 90% -os hatékonyságú eltávolítását 60 percen belül, pH 9-nél és 25 ° C hőmérsékleten, 150 mg IL-PP dózis alkalmazásával értem el. A kísérleti adszorpciós adatokat hagyományos izotermákkal és kinetikus modellekkel vizsgáltam nem-lineáris módszerrel. Az eredmények azt mutatták, hogy a kinetikát legjobban az Elovich-modell írja le ($R^2 = 0,97$), amely feltételezi a kemiszorpciós mechanizmus dominanciáját és az adszorbens heterogén felületét. Az adszorpciós izotermia kielégíti mind a Langmuir ($R^2 = 0,98$), mind a Freundlich

($R^2 = 0,94$) modellt, 49,12 mg/g maximális foszfátfelvétel mellett. A termodinamikai paraméterek, például a standard Gibb's szabad energia változás, standard entalpia változás és standard entrópia változás vizsgálata azt mutatta, hogy a folyamat spontán és endoterm jellegű. Ezek az eredmények az IL-PP-t, a foszfát ionok hatékony bioadszorbenseként azonosíthatjuk.

A tápanyaggal telített bioadszorbensek műtrágyaként történő alkalmazási lehetősége a tápanyagok AFW általi bioszorpciójának sarokköve. Ezért a nitrogénnel vagy foszforral telített gránátalma héj műtrágyaként történő alkalmazásának vizsgálata volt disszertációm utolsó fejezete, hogy előzetes értékelést adhassak a bioadszorbeátumok műtrágyaként történő alkalmazhatóságáról.

Ökotoxikológiai vizsgálatokat, például csírázási- és növekedési-erély vizsgálati tesztek alkalmaztam a nitrogénnel- és foszforral telített gránátalma héj fitotoxicitási hatásának kimutatására. A teszthez, az erre a célra általánosan használt repce (*Brassica napus* L.) növényt választottam és mértem a morfológiai és fiziológiai válaszokat.

A fitotoxicitást a növény friss és száraz tömege mellett, a csírázási index (GI), a relatív csírázás (RSG), a relatív gyökérnyúlás (RRE), a levélszám és a növény habitusának elemzésével értékeltem.

A csírázási eredmények nem mutattak gátlóhatást, sőt sok esetben a csírázást segítő hatást is kimutatható, különösen azoknál a mintáknál, amelyeknél kis mennyiségben alkalmaztam a tápanyaggal telített bioadszorbenseket. A növekedési-erélyt vizsgáló kísérletek eredményei alátámasztották a nitrogénnel és foszforral telített PP műtrágyaként történő alkalmazásának biztonságosságát és hatékonyságát.

A gránátalma héj bioadszorbensként történő alkalmazása rendkívül előnyös megoldást jelenthet, mert ötvözi a vízvédelem, az élelmiszeripari hulladék mennyiségének csökkentésének és a talaj tápanyag utánpótlásának előnyét, ami nem csak hulladékgazdálkodás, és környezetvédelmi szempontból, de gazdaságossági szempontból is jelentős, különösen a gránátalma termesztéséről és feldolgozásáról ismert fejlődő országokban.

Bár a dolgozat minden célkitűzése megválaszolásra került, a jövőbeli kutatások során számos pontra kell összpontosítani, elsősorban:

- a gránátalma héj NH_4^+ adszorpció kapacitásának növelésének kérdésére,

- rögzített ágyas adszorpciós folyamat vizsgálatára a léptéknövelés érdekében,
- PP-módosítási lehetőségek fejlesztésére a költségtakarékosság, a hatékonyság és a környezetbarát technológiák irányába,
- a vassal telített gránátalma héj (IL-PP) vizsgálatára a PO_4^{3-} valódi szennyvízből történő eltávolításának és hasznosításának céljából,
- a tápanyaggal telített bioadszrobeátumok regenerálására alkalmas módszerek vizsgálatára,
- kiváló minőségű tápanyag-műtrágyák előállítási lehetőségeinek vizsgálatára nitrogénnel és foszforral telített gránátalma héjből,
- az egész folyamat költséghatékonyságának vizsgálatára.

9 New scientific results

1. Pomegranate peel (PP) is proven to be a bio-adsorbent for NH_4^+ removal from NH_4Cl model solution:

- ✚ 97% removal within 120 min using 400 mg PP and an initial $\text{NH}_4\text{-N}$ concentration of 30 $\text{mg}\cdot\text{L}^{-1}$ at pH 4 and a stirring rate of 100 rpm.
- ✚ Maximum adsorption capacity of 6.18 $\text{mg}\cdot\text{g}^{-1}$.
- ✚ Adsorption is controlled by chemisorption and the surface of PP is energetically homogenous.

2. PP can be considered as bio-adsorbent for NH_4^+ removal from real wastewater (MPWW):

- ✚ 81% removal within 120 min using 1.5 g PP, initial $\text{NH}_4\text{-N}$ concentration of 80 $\text{mg}\cdot\text{L}^{-1}$, and 300 rpm of stirring rate at pH 6 and 25 °C temperature.
- ✚ Maximum adsorption capacity of 2.49 $\text{mg}\cdot\text{g}^{-1}$ which is lower than the value obtained in NH_4Cl model solution due to the competition from other cations present in MPWW.
- ✚ Adsorption is controlled by chemisorption and the surface of PP is energetically homogenous.

3. Pomegranate peel was successfully modified by iron loading method for efficient phosphate (PO_4^{3-}) adsorption:

- ✚ 90% removal within 60 min using 150 mg IL-PP and 40 $\text{mg}\cdot\text{L}^{-1}$ of Initial $\text{PO}_4\text{-P}$ concentration at pH 6 and 25 °C temperature.
- ✚ Maximum adsorption capacity of 49.12 $\text{mg}\cdot\text{g}^{-1}$.
- ✚ The adsorption process is spontaneous, endothermic and controlled by the chemisorption mechanism in a heterogeneous surface of IL-PP.

4. Nitrogen-loaded PP (N-PP) and phosphorus-loaded IL-PP (P-IL-PP) can be safely and efficiently used as fertilizer since it is proven they have no toxicity effect and *Brassica napus* L. Showed a positive response to their use.

- ✚ GI of all used N-PP, IL-P-PP, and Mix treatments was above 50% indicating no inhibitory effect during the germination phase. Moreover, 0.05 and 0.5 % (N-PP, IL-P-PP, and Mix) showed a beneficial effect as their GI was higher than the control.
- ✚ Positive effect on the number of leaves produced was observed for all treatments except 0.5% P-IL-PP.
- ✚ A positive effect was observed on shoots dry and fresh weight for most of the treatments except 0.05% N-PP and 0.05% Mix.

10 Publications

Bellahsen N, Kertész S, Pásztor Z, Hodúr C (2018) Adsorption of nutrients using low-cost adsorbents from agricultural waste and by-products – Review. *Prog Agric Eng Sci* 14(1):1–30. <https://doi.org/10.1556/446.14.2018.1.1> (Q3)

Bellahsen N, Varga G, Halyag N, Kertész S, Tombácz E, Hodúr C (2020) Pomegranate peel as a new low-cost adsorbent for ammonium removal. *Int J Environ Sci Technol*. <https://doi.org/10.1007/s13762-020-02863-1> (Q2, IF: 2.860).

Hodúr C, Bellahsen N, Mikó E, Nagypál V, Šereš Z, Kertész S (2020) The adsorption of ammonium nitrogen from milking parlor wastewater using pomegranate peel powder for sustainable water, resources, and waste management. *Sustain* 12(12). <https://doi.org/10.3390/SU12124880> (Q2, IF: 3.251)

Bellahsen N, Kakuk B, Beszédes S, Bagi Z, Halyag N, Gyulvári T, Kertész S, El Amarti A, Tombácz E, Hodúr C (2021) Iron-loaded pomegranate peel powder as a new bio-adsorbent for phosphate removal. *Water* - under review (Q2, IF: 3.103).

11 Presentations in conferences

- Adsorption and recovery of phosphate ions from aqueous solution using Iron-loaded pomegranate peel powder: Miskolc IPW–IV. Sustainable Raw Materials International Project Week, Miskolc, Hungary, November 25-27, 2020.
- Adsorption and recovery of phosphate ions from aqueous solution using activated pomegranate peel powder: Student Conference on Conservation Science (SCCS Europe), Tihany, Hungary, August 25-29, 2020.
- Removal and recovery of ammonium from milking parlour wastewater using pomegranate peel: 1st International Conference on Advanced Production and Processing (ICAPP), Novi Sad, Serbia, October 10-11, 2019.
- Adsorption of ammonium from milking parlour wastewater by using pomegranate peel: PERMEA 2019 - Membrane Conference of Visegrád Countries, Budapest, Hungary, August 26-29, 2019.
- Removal of ammonium from milking parlour wastewater by using pomegranate peel: II. SUSTAINABLE RAW MATERIALS International Project Week and Scientific Conference, Szeged, Hungary, May 6-10, 2019.
- Adsorption of ammonium using pomegranate peel as low-cost adsorbent: International Conference on Science, Technology, Engineering and Economy (ICOSTEE), Szeged, Hungary, 25th October, 2018.
- Adsorption of ammonium by pomegranate peel: 4th International Congress Food Technology, Quality and Safety, Novi Sad, Serbia, October 23-25, 2018.
- Agricultural wastes as adsorbent (poster): Chemical Engineering Conference 2018, Veszprém, Hungary, April 24-26, 2018.

References

- [1] S. Bhattacharya, A.B. Gupta, A. Gupta, A. Pandey, *Water Remediation*, Springer, Singapore, 2018. https://doi.org/10.1007/978-981-10-7551-3_2.
- [2] D. Pooja, P. Kumar, P. Singh, S. Patil, *Sensors in Water Pollutants Monitoring: Role of Material.*, Springer, New York, 2019. <https://play.google.com/store/books/details?id=cPm4DwAAQBAJ>.
- [3] M.A. Hanjra, M.E. Qureshi, Global water crisis and future food security in an era of climate change, *Food Policy*. 35 (2010) 365–377. <https://doi.org/10.1016/j.foodpol.2010.05.006>.
- [4] J.F. Velasco-Muñoz, J.A. Aznar-Sánchez, L.J. Belmonte-Ureña, I.M. Román-Sánchez, Sustainable water use in agriculture: A review of worldwide research, *Sustain*. 10 (2018) 1–18. <https://doi.org/10.3390/su10041084>.
- [5] M.W. Rosegrant, C. Ringler, T. Zhu, *Water for Agriculture : Maintaining Food Security under Growing Scarcity*, *Annu. Rev. Environ. Resour.* 34 (2009) 22. <https://doi.org/10.1146/annurev.environ.030308.090351>.
- [6] A.Y. Hoekstra, The hidden water resource use behind meat and dairy, *Anim. Front.* 2 (2012) 3–8. <https://doi.org/10.2527/af.2012-0038>.
- [7] M.J. Tadros, N. AL-Mefleh, O. Mohawesh, Effect of irrigation water qualities on *Leucaena leucocephala* germination and early growth stage, *Int. J. Environ. Sci. Technol.* 9 (2012) 281–286. <https://doi.org/10.1007/s13762-012-0033-y>.
- [8] X. Cai, M.W. Rosegrant, C. Ringler, Physical and economic efficiency of water use in the river basin: Implications for efficient water management, *Water Resour. Res.* 39 (2003) 1013. <https://doi.org/10.1029/2001WR000748>.
- [9] H. Liu, Y. Dong, Y. Liu, H. Wang, Screening of novel low-cost adsorbents from agricultural residues to remove ammonia nitrogen from aqueous solution, *J. Hazard. Mater.* 178 (2010) 1132–1136. <https://doi.org/10.1016/j.jhazmat.2010.01.117>.
- [10] Z. Yuan, S. Jiang, H. Sheng, X. Liu, H. Hua, X. Liu, Y. Zhang, Human Perturbation of the Global Phosphorus Cycle: Changes and Consequences, *Environ. Sci. Technol.* 52 (2018) 2438–2450. <https://doi.org/10.1021/acs.est.7b03910>.
- [11] H. Bacelo, A.M.A. Pintor, S.C.R. Santos, R.A.R. Boaventura, C.M.S. Botelho, Performance and prospects of different adsorbents for phosphorus uptake and recovery from water, *Chem. Eng. J.* 381 (2019) 122566. <https://doi.org/10.1016/j.cej.2019.122566>.
- [12] K. Ravindra, K. Kaur, S. Mor, System analysis of municipal solid waste management in Chandigarh and minimization practices for cleaner emissions, *J. Clean. Prod.* 89 (2015) 251–256. <https://doi.org/10.1016/j.jclepro.2014.10.036>.
- [13] T. Wium-Andersen, A.H. Nielsen, T. Hvitved-Jacobsen, H. Brix, C.A. Arias, J. Vollertsen, Modeling the eutrophication of two mature planted stormwater ponds for runoff control, *Ecol. Eng.* 61 (2013) 601–613. <https://doi.org/10.1016/j.ecoleng.2013.07.032>.
- [14] B. He, T. Oki, S. Kanae, G. Mouri, K. Kodama, D. Komori, S. Seto, Integrated biogeochemical modelling of nitrogen load from anthropogenic and natural sources in Japan, 220 (2009) 2325–2334. <https://doi.org/10.1016/j.ecolmodel.2009.05.018>.
- [15] A.F. Bouwman, D.S. Lee, W.A.H. Asman, F.J. Dentener, K.W. Van Der Hoek, J.G.J. Olivier, A

- global high-resolution emission inventory for ammonia, *Global Biogeochem. Cycles*. 11 (1997) 561–587.
- [16] F. Albornoz, *Scientia Horticulturae* Crop responses to nitrogen overfertilization : A review, *Sci. Hortic. (Amsterdam)*. 205 (2016) 79–83. <https://doi.org/10.1016/j.scienta.2016.04.026>.
- [17] T.A.H. Nguyen, H.H. Ngo, W. Guo, T.V. Nguyen, Phosphorous removal from aqueous solutions by agricultural by-products: A critical review, *J. Water Sustain.* 2 (2012) 193–207. <https://doi.org/10.11912/jws.2.3.193-207>.
- [18] K.A. Macintosh, B.K. Mayer, R.W. McDowell, S.M. Powers, L.A. Baker, T.H. Boyer, B.E. Rittmann, Managing Diffuse Phosphorus at the Source versus at the Sink, *Environ. Sci. Technol.* 52 (2018) 11995–12009. <https://doi.org/10.1021/acs.est.8b01143>.
- [19] W.R. Moomaw, Energy , Industry and Nitrogen : Strategies for Decreasing Reactive Nitrogen Emissions, *J. Hum. Environ.* 31 (2002) 184–189. <https://doi.org/http://dx.doi.org/10.1579/0044-7447-31.2.184>.
- [20] J.W. Choi, S.Y. Lee, S.H. Lee, J.E. Kim, K.Y. Park, D.J. Kim, S.W. Hong, Comparison of surface-modified adsorbents for phosphate removal in water, *Water. Air. Soil Pollut.* 223 (2012) 2881–2890. <https://doi.org/10.1007/s11270-011-1072-6>.
- [21] A. Karachalios, M. Wazne, Phosphate removal from water by modified pine bark using ionic liquid analog, *Desalin. Water Treat.* 54 (2015) 1881–1892. <https://doi.org/10.1080/19443994.2014.893209>.
- [22] International Fertilizer Association (IFA), THE CRUCIAL ROLE OF PLANT NUTRITION IN THE 2030 SUSTAINABLE DEVELOPMENT AGENDA, (n.d.) 1–9.
- [23] J. Cooper, R. Lombardi, D. Boardman, C. Carliell-Marquet, The future distribution and production of global phosphate rock reserves, *Resour. Conserv. Recycl.* 57 (2011) 78–86. <https://doi.org/10.1016/j.resconrec.2011.09.009>.
- [24] O. Eljamal, J. Okawauchi, K. Hiramatsu, M. Harada, Phosphorus sorption from aqueous solution using natural materials, *Environ. Earth Sci.* 68 (2013) 859–863. <https://doi.org/10.1007/s12665-012-1789-6>.
- [25] D. Cordell, A. Rosemarin, J.J. Schröder, A.L. Smit, Towards global phosphorus security: A systems framework for phosphorus recovery and reuse options, *Chemosphere.* 84 (2011) 747–758. <https://doi.org/10.1016/j.chemosphere.2011.02.032>.
- [26] J. Woods, A. Williams, J.K. Hughes, M. Black, R. Murphy, Energy and the food system, (2010) 2991–3006. <https://doi.org/10.1098/rstb.2010.0172>.
- [27] A. Bhatnagar, M. Sillanpää, A. Witek-krowiak, Agricultural waste peels as versatile biomass for water purification – A review, *Chem. Eng. J.* 270 (2015) 244–271. <https://doi.org/10.1016/j.cej.2015.01.135>.
- [28] H. Huang, J. Liu, L. Ding, Recovery of phosphate and ammonia nitrogen from the anaerobic digestion supernatant of activated sludge by chemical precipitation, *J. Clean. Prod.* 102 (2015) 437–446. <https://doi.org/10.1016/j.jclepro.2015.04.117>.
- [29] S. Sengupta, T. Nawaz, J. Beaudry, Nitrogen and Phosphorus Recovery from Wastewater, *Curr. Pollut. Reports.* 1 (2015) 155–166. <https://doi.org/10.1007/s40726-015-0013-1>.

- [30] B.K. Mayer, L.A. Baker, T.H. Boyer, P. Drechsel, M. Gifford, M.A. Hanjra, P. Parameswaran, J. Stoltzfus, P. Westerhoff, B.E. Rittmann, Total Value of Phosphorus Recovery, *Environ. Sci. Technol.* 50 (2016) 6606–6620. <https://doi.org/10.1021/acs.est.6b01239>.
- [31] C. Hodúr, N. Bellahsen, E. Mikó, V. Nagypál, Z. Šereš, S. Kertész, The adsorption of ammonium nitrogen from milking parlor wastewater using pomegranate peel powder for sustainable water, resources, and waste management, *Sustain.* 12 (2020) 4880. <https://doi.org/10.3390/SU12124880>.
- [32] E. Papargyropoulou, R. Lozano, J. K. Steinberger, N. Wright, Z. Bin Ujang, The food waste hierarchy as a framework for the management of food surplus and food waste, *J. Clean. Prod.* 76 (2014) 106–115. <https://doi.org/10.1016/j.jclepro.2014.04.020>.
- [33] R. Ravindran, A.K. Jaiswal, Exploitation of Food Industry Waste for High-Value Products, *Trends Biotechnol.* 34 (2015) 58–69. <https://doi.org/10.1016/j.tibtech.2015.10.008>.
- [34] C.M. Galanakis, Recovery of high components from food wastes : Conventional , emerging technologies and commercialized applications, *Trends Food Sci. Technol.* 26 (2012) 68–87. <https://doi.org/10.1016/j.tifs.2012.03.003>.
- [35] A. Arevalo-gallegos, Z. Ahmad, M. Asgher, R. Parra-saldivar, H.M.N. Iqbal, sustainable material to produce value-added products with a zero waste approach — A review, *Int. J. Biol. Macromol.* 99 (2017) 308–318. <https://doi.org/10.1016/j.ijbiomac.2017.02.097>.
- [36] M. Sulyman, J. Namiesnik, A. Gierak, Low-cost adsorbents derived from agricultural by-products/wastes for enhancing contaminant uptakes from wastewater: A review, *Polish J. Environ. Stud.* 26 (2017) 479–510. <https://doi.org/10.15244/pjoes/66769>.
- [37] S. De Gisi, G. Lofrano, M. Grassi, M. Notarnicola, Characteristics and adsorption capacities of low-cost sorbents for wastewater treatment : A review, *Sustain. Mater. Technol.* 9 (2016) 10–40. <https://doi.org/10.1016/j.susmat.2016.06.002>.
- [38] V.. Gupta, H. Sadegh, M. Yari, R.S. Ghoshekandi, B. Maazinejad, M. Chahardori, Removal of ammonium ions from wastewater A short review in development of efficient methods, 1 (2015) 149–158. <https://doi.org/10.7508/gjesm.2015.02.007>.
- [39] E.A. Deliyanni, E.N. Peleka, N.K. Lazaridis, Comparative study of phosphates removal from aqueous solutions by nanocrystalline akagan ´ eite and hybrid surfactant-akagan ´ eite, 52 (2007) 478–486. <https://doi.org/10.1016/j.seppur.2006.05.028>.
- [40] K. Karageorgiou, M. Paschalis, G.N. Anastassakis, Removal of phosphate species from solution by adsorption onto calcite used as natural adsorbent, 139 (2007) 447–452. <https://doi.org/10.1016/j.jhazmat.2006.02.038>.
- [41] K. Gunes, Point and nonpoint sources of nutrients to lakes - ecotechnological measures and mitigation methodologies - case study, *Ecol. Eng.* 34 (2008) 116–126. <https://doi.org/10.1016/j.ecoleng.2008.07.004>.
- [42] M. Selman, S. GREENHALGH, Eutrophication: Sources and Drivers of Nutrient Pollution, WRI POLICY NOTE WATER Qual. EUTROPHICATION HYPOXIA. (2009).
- [43] C.H. Wong, G.W. Barton, J.P. Barfor, The nitrogen cycle and its application in wastewater treatment, Elsevier, 2003. <https://doi.org/10.1016/B978-012470100-7/50026-1>.
- [44] J.W. Erisman, J.N. Galloway, S. Seitzinger, A. Bleeker, N.B. Dise, A.M.R. Petrescu, A.M. Leach,

- W. De Vries, Consequences of human the global nitrogen cycle, *Philos. Trans. R. Soc. B; Biol. Sci.* 368 (2013) 1–9.
- [45] E. Go, G. Leo, A. Bo, Ammonium removal from aqueous solutions by reverse osmosis using cellulose acetate membranes, 184 (2005) 149–155. <https://doi.org/10.1016/j.desal.2005.03.062>.
- [46] N. Romano, C. Zeng, Reviews in Fisheries Science Toxic Effects of Ammonia , Nitrite , and Nitrate to their Toxicity , Physiological Consequences , and Coping Mechanisms Toxic Effects of Ammonia , Nitrite , and Nitrate to Decapod Crustaceans : A Review on Factors Influencing, (2013) 37–41. <https://doi.org/10.1080/10641262.2012.753404>.
- [47] B. Kartal, J.G. Kuenen, M.C.M. van Loosdrecht, Sewage Treatment with Anammox, *Science* (80-.). 328 (2010) 702–704. <https://doi.org/10.1126/science.1185941>.
- [48] J. Huang, C. Shang, Air Stripping, in: and N.K.S. L. K. Wang, Y.-T. Hung (Ed.), *Handb. Environ. Eng., The Humana, Totowa, NJ, 2006*.
- [49] T.A. Pressley, D.F. Bishop, S.G. Roan, Ammonia-Nitrogen Removal by Breakpoint Chlorination Thomas, *Environ. Sci. Technol.* 6 (1972) 622–628.
- [50] H. Liu, Y. Dong, H. Wang, Y. Liu, Adsorption behavior of ammonium by a bioadsorbent – Boston ivy leaf powder, *J. Environ. Sci.* 22 (2010) 1513–1518. [https://doi.org/10.1016/S1001-0742\(09\)60282-5](https://doi.org/10.1016/S1001-0742(09)60282-5).
- [51] N. Widiastuti, H. Wu, H. Ming, D. Zhang, Removal of ammonium from greywater using natural zeolite, *DES.* 277 (2011) 15–23. <https://doi.org/10.1016/j.desal.2011.03.030>.
- [52] H. Sadegh, R. Shahryari-ghoshekandi, M. Kazemi, Study in synthesis and characterization of carbon nanotubes decorated by magnetic iron oxide nanoparticles, (2014) 129–135. <https://doi.org/10.1007/s40089-014-0128-1>.
- [53] M.L. Gerardo, M.P. Zacharof, R.W. Lovitt, Strategies for the recovery of nutrients and metals from anaerobically digested dairy farm sludge using cross-flow microfiltration, *Water Res.* 47 (2013) 4833–4842. <https://doi.org/10.1016/j.watres.2013.04.019>.
- [54] M.D. Mullen, Phosphorus in Soils—Biological Interactions, *Earth Syst. Environ. Sci.* (2019) 1–8. <https://doi.org/10.1016/b978-0-12-409548-9.11992-x>.
- [55] J.T. Bunce, E. Ndam, I.D. Ofiteru, A. Moore, D.W. Graham, D.W. Graham, A Review of Phosphorus Removal Technologies and Their Applicability to Small-Scale Domestic Wastewater Treatment Systems, *Front. Environ. Sci.* 6 (2018) 1–15. <https://doi.org/10.3389/fenvs.2018.00008>.
- [56] L.A. Wendling, P. Blomberg, T. Sarlin, O. Priha, M. Arnold, Phosphorus sorption and recovery using mineral-based materials : sorption mechanisms and potential phytoavailability, *Appl. GEOCHEMISTRY.* (2013). <https://doi.org/10.1016/j.apgeochem.2013.07.016>.
- [57] L.E. De-Bashan, Y. Bashan, Recent advances in removing phosphorus from wastewater and its future use as fertilizer (1997–2003), *Water Res.* 38 (2004) 4222–4246. <https://doi.org/10.1016/j.watres.2004.07.014>.
- [58] D.A. Vaccari, P.F. Strom, J.E. Alleman, *Environmental Biology for Engineers and Scientists.*, New York, 2006.

- [59] C. Wu, Y. Peng, C. Wan, S. Wang, Performance and microbial population variation in a plug-flow A₂O process treating domestic wastewater with low C / N ratio, (2011) 461–467. <https://doi.org/10.1002/jctb.2539>.
- [60] I. Michalak, K. Chojnacka, A. Witek-krowiak, State of the Art for the Biosorption Process — a Review, (2013) 1389–1416. <https://doi.org/10.1007/s12010-013-0269-0>.
- [61] J. Huang, N.R. Kankanamge, C. Chow, D.T. Welsh, T. Li, P.R. Teasdale, Removing ammonium from water and wastewater using cost-effective adsorbents: A review, *J. Environ. Sci.* (2017). <https://doi.org/10.1016/j.jes.2017.09.009>.
- [62] D.C. Johnston, I. Azreen, Y. Lija, A.Y. Zahrim, Fruit waste adsorbent for ammonia nitrogen removal from synthetic solution : Isotherms and kinetics Fruit waste adsorbent for ammonia nitrogen removal from synthetic solution : Isotherms and kinetics, (2016). <https://doi.org/10.1088/1755-1315/36/1/012028>.
- [63] T.A.H. Nguyen, H.H. Ngo, W.S. Guo, J. Zhang, S. Liang, D.J. Lee, P.D. Nguyen, X.T. Bui, Modification of agricultural waste/by-products for enhanced phosphate removal and recovery: Potential and obstacles, *Bioresour. Technol.* 169 (2014) 750–762. <https://doi.org/10.1016/j.biortech.2014.07.047>.
- [64] L.S. Oliveira, A.S. Franca, LOW-COST ADSORBENTS FROM AGRI-FOOD WASTES, in: L.V.G. and M.N. Bruno (Ed.), *Food Sci. Technol. New Res.*, 2008: pp. 1–39.
- [65] S. Yin, X. Ma, D.E. Ellis, Initial stages of H₂O adsorption and hydroxylation of Fe-terminated, *Surf. Sci.* 601 (2007) 2426–2437. <https://doi.org/10.1016/j.susc.2007.04.059>.
- [66] A. Abdul, F. Aberuagba, Comparative Study of the Adsorption of Phosphate by Activated Charcoal from Corncoobs , Groundnut Shells and Rice-Husks, *J Technol.* 9 (2005) 59–63.
- [67] C. Namasivayam, A. Sakoda, M. Suzuki, Removal of phosphate by adsorption onto oyster shell powder — kinetic studies, *J. Chem. Technol. Biotechnol.* 80 (2005) 356–358. <https://doi.org/10.1002/jctb.1175>.
- [68] E. Worch, *Adsorption Technology in Water Treatment. Fundamentals, Processes, and Modeling.*, Berlin/Boston, 2012.
- [69] J. Zhang, D. Ph, W. Shan, J. Ge, Z. Shen, D. Ph, Y. Lei, D. Ph, W. Wang, Kinetic and Equilibrium Studies of Liquid-Phase Adsorption of Phosphate on Modified Sugarcane Bagasse, *J. Environ. Eng.* (2012) 252–258. [https://doi.org/10.1061/\(ASCE\)EE.1943-7870.0000408](https://doi.org/10.1061/(ASCE)EE.1943-7870.0000408).
- [70] T.L. Eberhardt, S. Min, Biosorbents prepared from wood particles treated with anionic polymer and iron salt : Effect of particle size on phosphate adsorption, *Bioresour. Technol.* 99 (2008) 626–630. <https://doi.org/10.1016/j.biortech.2006.12.037>.
- [71] Z. Liu, Y. Xue, F. Gao, X. Cheng, K. Yang, Removal of ammonium from aqueous solutions using alkali-modified biochars, *Chem. Speciat. Bioavailab.* ISSN. 28 (2016) 26–32. <https://doi.org/10.1080/09542299.2016.1142833>.
- [72] Z. Wang, H. Guo, F. Shen, G. Yang, Y. Zhang, Y. Zeng, L. Wang, H. Xiao, S. Deng, Biochar produced from oak sawdust by Lanthanum (La)-involved pyrolysis for adsorption of ammonium (NH₄⁺), nitrate (NO₃⁻), and phosphate (PO₄³⁻), *Chemosphere.* 119 (2015) 646–653. <https://doi.org/10.1016/j.chemosphere.2014.07.084>.
- [73] J. Hou, L. Huang, Z. Yang, Y. Zhao, C. Deng, Adsorption of ammonium on biochar prepared

- from giant reed, *Environ. Sci. Pollut. Res.* (2016) 19107–19115.
<https://doi.org/10.1007/s11356-016-7084-4>.
- [74] M.A. Wahab, S. Jellali, N. Jedidi, *Bioresource Technology* Effect of temperature and pH on the biosorption of ammonium onto *Posidonia oceanica* fibers : Equilibrium , and kinetic modeling studies, *Bioresour. Technol.* 101 (2010) 8606–8615.
<https://doi.org/10.1016/j.biortech.2010.06.099>.
- [75] R. Boopathy, S. Karthikeyan, Adsorption of ammonium ion by coconut shell-activated carbon from aqueous solution : kinetic , isotherm , and thermodynamic studies, *Env. Sci Pollut Res.* 20 (2013) 533–542. <https://doi.org/10.1007/s11356-012-0911-3>.
- [76] S. Benyoucef, M. Amrani, Adsorption of phosphate ions onto low cost Aleppo pine adsorbent, *Desalination.* 275 (2011) 231–236. <https://doi.org/10.1016/j.desal.2011.03.004>.
- [77] B.K. Biswas, K. Inoue, K.N. Ghimire, H. Harada, K. Ohto, H. Kawakita, Removal and recovery of phosphorus from water by means of adsorption onto orange waste gel loaded with zirconium, *Bioresour. Technol.* 99 (2008) 8685–8690. <https://doi.org/10.1016/j.biortech.2008.04.015>.
- [78] A.C.A. de Lima, R.F. Nascimento, F.F. de Sousa, J.M. Filho, A.C. Oliveira, Modified coconut shell fibers: A green and economical sorbent for the removal of anions from aqueous solutions, *Chem. Eng. J.* 185–186 (2012) 274–284. <https://doi.org/10.1016/j.cej.2012.01.037>.
- [79] Z.Z. Ismail, Kinetic study for phosphate removal from water by recycled date-palm wastes as agricultural by-products Kinetic study for phosphate removal from water by recycled date-palm wastes as agricultural, *Int. J. Environ. Stud.* 69 (2012) 135–149.
<https://doi.org/10.1080/00207233.2012.656975>.
- [80] X. Xu, Y. Gao, B. Gao, X. Tan, Y. Zhao, Q. Yue, Y. Wang, Characteristics of diethylenetriamine-crosslinked cotton stalk / wheat stalk and their biosorption capacities for phosphate, *J. Hazard. Mater.* 192 (2011) 1690–1696. <https://doi.org/10.1016/j.jhazmat.2011.07.009>.
- [81] Q.-Y. Yue, W.-Y. Wang, B.-Y. Gao, X. Xu, J. Zhang, Q. Li, Phosphate Removal from Aqueous Solution by Adsorption on Modified Giant Reed, *Water Environ. Res.* 82 (2010) 374–381.
<https://doi.org/10.2175/106143009x12529484815719>.
- [82] L. Martínez, S. Ben, D. Alami, G. Hodaifa, C. Faur, S. Rodríguez, J.A. Giménez, J. Ochando, Adsorption of iron on crude olive stones, *Ind. Crop. Prod. J.* 32 (2010) 467–471.
<https://doi.org/10.1016/j.indcrop.2010.06.017>.
- [83] G. Hodaifa, S. Ben, D. Alami, J.M. Ochando-pulido, M.D. Víctor-ortega, Iron removal from liquid effluents by olive stones on adsorption column : breakthrough curves, *Ecol. Eng.* 73 (2014) 270–275. <https://doi.org/10.1016/j.ecoleng.2014.09.049>.
- [84] C. Chen, S. Chen, Adsorption Properties of a Chelating Resin Containing Hydroxy Group and Iminodiacetic Acid for Copper Ions, *J. Appl. Polym. Sci.* 94 (2004) 2123–2130.
<https://doi.org/10.1002/app.21079>.
- [85] G. Hodaifa, C.A. Garcia, S. Rodriguez-perez, Revalorization of Agro-Food Residues as Bioadsorbents for Wastewater Treatment, in: J.K. Verma, S. Nishith (Eds.), *Aqueous Phase Adsorpt. Theory, Simulations Exp.*, Taylor & F, London, New York, 2019.
- [86] Z.Z. Ismail, B.B. Hameed, Recycling of raw corn cob residues as an agricultural waste material for ammonium removal : kinetics , isotherms , and mechanisms, *Int. J. Environ. Waste Manag.* 13 (2014) 217–230.

- [87] P. Kumar, S. Sudha, S. Chand, V.C. Srivastava, Phosphate Removal from Aqueous Solution Using Coir- Pith Activated Carbon Phosphate Removal from Aqueous Solution Using Coir-Pith Activated Carbon, *Sep. Sci. Technol.* (2010) 37–41. <https://doi.org/10.1080/01496395.2010.485604>.
- [88] B.K. Suyamboo, R.S. Perumal, Equilibrium , Thermodynamic and Kinetic Studies on Adsorption of a Basic Dye by Citrullus Lanatus Rind, *Iran. J. Energy Environ.* 3 (2012) 23–34. <https://doi.org/10.5829/idosi.ijee.2012.03.01.0130>.
- [89] M. Aliabadi, I. Khazaei, H. Fakhraee, M.T.H. Mousavian, Hexavalent chromium removal from aqueous solutions by using low-cost biological wastes : equilibrium and kinetic studies, *Int. J. Environ. Sci. Technol.* 9 (2012) 319–326. <https://doi.org/10.1007/s13762-012-0045-7>.
- [90] M. Divya Jyothi, Phosphate pollution control in waste waters using new bio-sorbents, *Int. J. Water Resour. Environ. Eng.* 4 (2012) 73–85. <https://doi.org/10.5897/ijwree11.132>.
- [91] C. Namasivayam, D. Sangeetha, Equilibrium and kinetic studies of adsorption of phosphate onto ZnCl₂ activated coir pith carbon, *J. Colloid Interface Sci.* 280. 280 (2004) 359–365. <https://doi.org/10.1016/j.jcis.2004.08.015>.
- [92] L. Shang, H. Xu, S. Huang, Adsorption of Ammonium in Aqueous Solutions by the Modified Biochar and its Application as an Effective, *Water. Air. Soil Pollut.* 320 (2018). <https://doi.org/doi.org/10.1007/s11270-018-3956-1> Adsorption.
- [93] H.I. Yang, K. Lou, A.U. Rajapaksha, Y.S. Ok, Adsorption of ammonium in aqueous solutions by pine sawdust and wheat straw biochars, *Env. Sci Pollut Res.* (2017). <https://doi.org/10.1007/s11356-017-8551-2>.
- [94] W. Lee, S. Yoon, J. Kwon, M. Lee, Y. Choi, Anionic surfactant modification of activated carbon for enhancing adsorption of ammonium ion from aqueous solution, *Sci. Total Environ.* 639 (2018) 1432–1439. <https://doi.org/10.1016/j.scitotenv.2018.05.250>.
- [95] D. Myers, *Surfaces, interfaces, and colloids: Principles and Applications*, John Wiley, New York, 1999.
- [96] Z. Xu, J. Cai, B. Pan, Mathematically modeling fixed-bed adsorption in aqueous systems, *J. Zhejiang Univ. A (Applied Phys. Eng.* 14 (2013) 155–176. <https://doi.org/10.1631/jzus.A1300029>.
- [97] A. Ramesh, D.J. Lee, J.W.C. Wong, Thermodynamic parameters for adsorption equilibrium of heavy metals and dyes from wastewater with low-cost adsorbents, *J. Colloid Interface Sci.* 291. 291 (2005) 588–592. <https://doi.org/10.1016/j.jcis.2005.04.084>.
- [98] S.K. Milonjić, A consideration of the correct calculation of thermodynamic parameters of adsorption, *J. Serbian Chem. Soc.* 72 (2007) 1363–1367. <https://doi.org/10.2298/JSC0712363M>.
- [99] Y. Liu, Y. Liu, Biosorption isotherms , kinetics and thermodynamics, *Sep. Purif. Technol.* 61 (2008) 229–242. <https://doi.org/10.1016/j.seppur.2007.10.002>.
- [100] S.D. Johanningsmeier, G. Harris, Pomegranate as a Functional Food and Nutraceutical Source, *Annu. Rev. Food Sci. Technol.* 2 (2010) 181–201. <https://doi.org/10.1146/annurev-food-030810-153709>.
- [101] I. Kahramanoglu, Trends in Pomegranate Sector: Production, Postharvest Handling and

- Marketing, *Int. J. Agric. , For. Life Sci.* 3 (2019) 239–246.
- [102] L.U. Opara, M.R. Al-ani, Y.S. Al-Shuaibi, Physico-chemical Properties , Vitamin C Content , and Antimicrobial Properties of Pomegranate Fruit (*Punica granatum L.*), *Food Bioprocess Technol.* (2009) 315–321. <https://doi.org/10.1007/s11947-008-0095-5>.
- [103] S. Talekar, A.F. Patti, R. Vijayaraghavan, A. Arora, Complete Utilization of Waste Pomegranate Peels to Produce a Hydrocolloid, Punicalagin Rich Phenolics, and a Hard Carbon Electrode, *ACS Sustain. Chem. Eng.* 6 (2018) 16363–16374. <https://doi.org/10.1021/acssuschemeng.8b03452>.
- [104] E. Demiray, S.E. Karatay, D. Gönül, Evaluation of Pomegranate Peel in Ethanol Production by *Saccharomyces cerevisiae* and *Pichia stipitis* Ekin, *Energy.* (2018). <https://doi.org/10.1016/j.energy.2018.06.200>.
- [105] H. Jalal, M.A. Pal, S.R. Ahmad, M. Rather, M. Andrabi, S. Hamdani, Physico-chemical and functional properties of pomegranate peel and seed powder, *Pharma Innov. Journal Innovation J.* 7 (2018) 1127–1131.
- [106] C. Zhu, X. Zhai, L. Li, X. Wu, B. Li, Response surface optimization of ultrasound-assisted polysaccharides extraction from pomegranate peel, *Food Chem.* 177 (2015) 139–146. <https://doi.org/10.1016/j.foodchem.2015.01.022>.
- [107] J. Banerjee, R. Singh, R. Vijayaraghavan, D. Macfarlane, A.F. Patti, A. Arora, Bioactives from fruit processing wastes : Green approaches to valuable chemicals, *Food Chem.* 225 (2017) 10–22. <https://doi.org/10.1016/j.foodchem.2016.12.093>.
- [108] E. Jami, A. Shabtay, M. Nikbachat, E. Yosef, J. Miron, I. Mizrahi, Effects of adding a concentrated pomegranate-residue extract to the ration of lactating cows on in vivo digestibility and profile of rumen bacterial population, *J. Dairy Sci.* 95 (2012) 5996–6005. <https://doi.org/10.3168/jds.2012-5537>.
- [109] A. Shabtay, M. Nikbachat, A. Zenou, E. Yosef, O. Arkin, O. Sneer, A. Shwimmer, Effects of adding a concentrated pomegranate extract to the ration of lactating cows on performance and udder health parameters, *Anim. Feed Sci. Technol.* 175 (2012) 24–32. <https://doi.org/10.1016/j.anifeedsci.2012.04.004>.
- [110] M.T.H. Siddiqui, Characterization and Process Optimization of Biochar Produced Using Novel Biomass , Waste Pomegranate Peel : A Response Surface Methodology Approach, *Waste and Biomass Valorization.* (2017). <https://doi.org/10.1007/s12649-017-0091-y>.
- [111] M.M. Abou, E. Nour, M.J.M. Wadi, A. Shams, M.J.M. Wadi, Suppressive effect of compost / pomegranate peel tea combination against *Fusarium oxysporum f. sp. lupini* , and *Rhizoctonia solani* as an alternative synthetic fungicide, *Egypt. J. Exp. Biol.* 16 (2020) 13–25. <https://doi.org/10.5455/egyjebb.20191208124236>.
- [112] F. Hadrich, S. Cherif, Y.T. Gargouri, S. Adel, Antioxidant and Lipase Inhibitory Activities and Essential Oil Composition of Pomegranate Peel Extracts, *J. Oleo Sci.* 63 (2014) 515–525. <https://doi.org/10.5650/jos.ess13163>.
- [113] K. Mahdavi, A. Farhad, Application of response surface methodology for the optimization of supercritical fluid extraction of essential oil from pomegranate (*Punica granatum L.*) peel, *J. Food Sci. Technol.* (2016). <https://doi.org/10.1007/s13197-016-2284-y>.
- [114] D. Gu, X. Zhu, T. Vongsay, M. Huang, Phosphorus and Nitrogen Removal Using Novel Porous

- Bricks Incorporated with Wastes and Minerals, *Pol. J. Environ. Stud.* 22 (2013) 1349–1356.
- [115] J. Ventura, F. Alarcón-aguilar, R. Roman-ramos, E. Campos-sepulveda, M.L. Reyes-vega, V.D. Boone-villa, E.I. Jasso-villagómez, C.N. Aguilar, Quality and antioxidant properties of a reduced-sugar pomegranate juice jelly with an aqueous extract of pomegranate peels, *Food Chem.* 136 (2013) 109–115. <https://doi.org/10.1016/j.foodchem.2012.07.039>.
- [116] M. Grabeža, R. Škrbičb, M.P. Miloš P. Stojiljković, Vesna Rudić-Grujića, A. Aleksandra, P. Snježana, V. Vučić, K.Š. Bosa Mirjanić-Azariće, T.J. Nebojša Menković, N. Vasiljević, Beneficial effects of pomegranate peel extract on plasma lipid profile , fatty acids levels and blood pressure in patients with diabetes mellitus type-2 : A randomized , double-blind , placebo-controlled study, *J. Funct. Foods.* (2019). <https://doi.org/10.1016/j.jff.2019.103692>.
- [117] M. Moghadam, M. Salami, M. Mohammadian, M. Khodadadi, Food Hydrocolloids Development of antioxidant edible films based on mung bean protein enriched with pomegranate peel, *Food Hydrocoll.* 104 (2020) 105735. <https://doi.org/10.1016/j.foodhyd.2020.105735>.
- [118] E. Demiray, S.E. Karatay, G. Dönmez, Efficient bioethanol production from pomegranate peels by newly isolated *Kluyveromyces marxianus*, *Energy Sources, Part A Recover. Util. Environ. Eff.* (2019) 1–10. <https://doi.org/10.1080/15567036.2019.1600621>.
- [119] K. Jain, P. Suryawanshi, A. Chaudhari, Recovery of acerbic anaerobic digester for biogas production from pomegranate shells using organic loading approach, *Indian J. Biochem. Biophys.* 57 (2020) 86–94.
- [120] R.D. Kirtane, P.C. Suryawanshi, M.R. Patil, A.B. Chaudhari, R.M. Kothari, Optimization of organic loading rate for different fruit wastes during biomethanization, *J. Sci. Ind. Res.* 68 (2009) 252–255.
- [121] A. El Barnossi, F. Moussaid, A.I. Housseini, Tangerine, banana and pomegranate peels valorization for sustainable environment: A review, *Biotechnol. Reports.* (2020) e00574. <https://doi.org/10.1016/j.btre.2020.e00574>.
- [122] M. Afsharnia, M. Saeidi, A. Zarei, M.R. Narooie, H. Biglari, Phenol Removal from Aqueous Environment by Adsorption onto Pomegranate Peel Carbon Mojtaba, *Electron. Physician.* 8 (2016) 3248–3256. <https://doi.org/10.19082/3248>.
- [123] S. Ben-Ali, I. Jaouali, S. Souissi-Najar, A. Ouederni, Characterization and adsorption capacity of raw pomegranate peel biosorbent for copper removal, *J. Clean. Prod.* 142 (2016) 3809–3821. <https://doi.org/10.1016/j.jclepro.2016.10.081>.
- [124] R.A.K. Rao, F. Rehman, Adsorption of Heavy Metal Ions on Pomegranate (*Punica granatum*) Peel : Removal and Recovery of Cr (VI) Ions from a Multi-metal Ion System, *Adsorpt. Sci. Technol.* Vol. 28 (2010) 195–211.
- [125] Z.N. Abdulrazak, Pomegranate peel as sorbent in the removal of Pb (II) from wastewater, *J. Eng. Sustain. Dev.* 20 (2016) 25–35.
- [126] M. Eid, M. Ali, H. Abdelsalam, N.S. Ammar, H.S. Ibrahim, Response surface methodology for optimization of the adsorption capability of ball-milled pomegranate peel for different pollutants, *J. Mol. Liq.* 250 (2018) 433–445. <https://doi.org/10.1016/j.molliq.2017.12.025>.
- [127] A. Bhatnagar, A.K. Minocha, Adsorptive removal of 2 , 4-dichlorophenol from water utilizing *Punica granatum* peel waste and stabilization with cement, *J. Hazard. Mater.* 168 (2009)

- 1111–1117. <https://doi.org/10.1016/j.jhazmat.2009.02.151>.
- [128] F. Gündüz, B. Bayrak, Biosorption of malachite green from an aqueous solution using pomegranate peel: Equilibrium modelling, kinetic and thermodynamic studies Figen, *J. Mol. Liq.* (2017). <https://doi.org/10.1016/j.molliq.2017.08.095>.
- [129] T.H. Ibrahim, A.S. Gulistan, M.I. Khamis, H. Ahmed, A. Aidan, Produced water treatment using naturally abundant pomegranate peel, *Desalin. Water Treat.* (2015) 1–9. <https://doi.org/10.1080/19443994.2015.1010235>.
- [130] M.H. Salmani, M. Abedi, S.A. Mozaffari, H.A. Sadeghian, Modification of pomegranate waste with iron ions a green composite for removal of Pb from aqueous solution : equilibrium , thermodynamic and kinetic studies, *AMB Express.* 7 (2017) 225. <https://doi.org/10.1186/s13568-017-0520-0>.
- [131] C. Ecjhaio, T.S. Najim, S.A. Yassin, Removal of Cr (VI) from Aqueous Solution Using Modified Pomegranate Peel : Equilibrium and Kinetic Studies, *E-Journal Chem.* 6 (2009) 129–142.
- [132] M. Akram, X. Xu, B. Gao, Q. Yue, S. Yanan, R. Khan, M.A. Inam, Adsorptive removal of phosphate by the bimetallic hydroxide nanocomposites embedded in pomegranate peel, *J. Environ. Sci. (China).* 91 (2020) 189–198. <https://doi.org/10.1016/j.jes.2020.02.005>.
- [133] M.A.M.H. Salmani, S.A. Mozaffari, Adsorption of Cd ions from aqueous solutions by iron modified pomegranate peel carbons : kinetic and thermodynamic studies, *Int. J. Environ. Sci. Technol.* (2016). <https://doi.org/10.1007/s13762-016-1002-7>.
- [134] M.R. Moghadam, N. Nasirizadeh, Z. Dashti, E. Babanezhad, Removal of Fe (II) from aqueous solution using pomegranate peel carbon : equilibrium and kinetic studies, *Int. J. Ind. Chem.* 4 (2013).
- [135] S.N. Turkmen, A.S. Kipcak, N. Tugrul, E.M. Derun, S. Piskin, The Adsorption of Zinc Metal in Waste Water Using ZnCl₂ Activated Pomegranate Peel, *Int. J. Mater. Metall. Eng.* 9 (2015) 477–480.
- [136] N.K. Amin, Removal of direct blue-106 dye from aqueous solution using new activated carbons developed from pomegranate peel : Adsorption equilibrium and kinetics, *J. Hazard. Mater.* 165 (2009) 52–62. <https://doi.org/10.1016/j.jhazmat.2008.09.067>.
- [137] M.A. Ahmad, N.A. Ahmad Puad, O.S. Bello, Kinetic, equilibrium and thermodynamic studies of synthetic dye removal using pomegranate peel activated carbon prepared by microwave-induced KOH activation, *Water Resour. Ind.* 6 (2014) 18–35. <https://doi.org/10.1016/j.wri.2014.06.002>.
- [138] M. Khawaja, M. Shafaq, A.A. Kazi, A. Zia-ur-rehman, MuhammadHamid, Adsorption studies of pomegranate peel activated charcoal for nickel (II) ion, *J. Chil. Chem. Soc.* 60 (2015) 2642–2645.
- [139] A. Bhatnagar, A.K. Minocha, Biosorption optimization of nickel removal from water using *Punica granatum* peel waste, *Colloids Surfaces B Biointerfaces.* 76 (2010) 544–548. <https://doi.org/10.1016/j.colsurfb.2009.12.016>.
- [140] E.S.Z. El-Ashtoukhy, N.K. Amin, O. Abdelwahab, Removal of lead (II) and copper (II) from aqueous solution using pomegranate peel as a new adsorbent, *Desalination.* 223 (2008) 162–173. <https://doi.org/10.1016/j.desal.2007.01.206>.

- [141] J. Chen, S. Lü, Z. Zhang, X. Zhao, X. Li, P. Ning, M. Liu, Environmentally friendly fertilizers: A review of materials used and their effects on the environment, *Sci. Total Environ.* 613–614 (2018) 829–839. <https://doi.org/10.1016/j.scitotenv.2017.09.186>.
- [142] D. Harikishore Kumar Reddy, K. Vijayaraghavan, J.A. Kim, Y.S. Yun, Valorisation of post-sorption materials: Opportunities, strategies, and challenges, *Adv. Colloid Interface Sci.* 242 (2017) 35–58. <https://doi.org/10.1016/j.cis.2016.12.002>.
- [143] A. Robalds, L. Dreijalte, O. Bikovens, M. Klavins, A novel peat-based biosorbent for the removal of phosphate from synthetic and real wastewater and possible utilization of spent sorbent in land application, *Desalin. Water Treat.* (n.d.). <https://doi.org/10.1080/19443994.2015.1061450>.
- [144] X. Wang, S. Lü, C. Gao, C. Feng, X. Xu, X. Bai, N. Gao, J. Yang, M. Liu, L. Wu, Recovery of Ammonium and Phosphate from Wastewater by Wheat Straw-based Amphoteric Adsorbent and Reusing as a Multifunctional Slow-Release Compound Fertilizer, *ACS Sustain. Chem. Eng.* (2016). <https://doi.org/10.1021/acssuschemeng.5b01494>.
- [145] L. Xie, S. Lü, M. Liu, C. Gao, X. Wang, L. Wu, Recovery of ammonium onto wheat straw to be reused as a slow-release fertilizer, *J. Agric. Food Chem.* 61 (2013) 3382–3388. <https://doi.org/10.1021/jf4004016>.
- [146] Z. Ma, Q. Li, Q. Yue, B. Gao, W. Li, X. Xu, Q. Zhong, Adsorption removal of ammonium and phosphate from water by fertilizer controlled release agent prepared from wheat straw, *Chem. Eng. J.* 171 (2011) 1209–1217. <https://doi.org/10.1016/j.cej.2011.05.027>.
- [147] Ł. Tuhy, M. Samoraj, Z. Witkowska, P. Rusek, K. Chojnacka, Conversion of spent mushroom substrate into micronutrient fertilizer via biosorption in a pilot plant, *Ecol. Eng.* 84 (2015) 370–374. <https://doi.org/10.1016/j.ecoleng.2015.09.032>.
- [148] L. Shang, H. Xu, S. Huang, Y. Zhang, Adsorption of Ammonium in Aqueous Solutions by the Modified Biochar and its Application as an Effective N-Fertilizer, *Water. Air. Soil Pollut.* 229 (2018). <https://doi.org/10.1007/s11270-018-3956-1>.
- [149] Y. Zhang, Z. Li, I.B. Mahmood, Recovery of NH₄⁺ by corn cob produced biochars and its potential application as soil conditioner, *Front. Environ. Sci. Eng.* 8 (2014) 825–834. <https://doi.org/10.1007/s11783-014-0682-9>.
- [150] Y. Yao, B. Gao, J. Chen, M. Zhang, M. Inyang, Y. Li, A. Alva, L. Yang, Engineered carbon (biochar) prepared by direct pyrolysis of Mg-accumulated tomato tissues: Characterization and phosphate removal potential, *Bioresour. Technol.* 138 (2013) 8–13. <https://doi.org/10.1016/j.biortech.2013.03.057>.
- [151] T.A.H. Nguyen, H.H. Ngo, W.S. Guo, J. Zhang, S. Liang, K.L. Tung, Feasibility of iron loaded “okara” for biosorption of phosphorous in aqueous solutions, *Bioresour. Technol.* 150 (2013) 42–49. <https://doi.org/10.1016/j.biortech.2013.09.133>.
- [152] H.N. Tran, S.J. You, A. Hosseini-Bandegharaei, H.P. Chao, Mistakes and inconsistencies regarding adsorption of contaminants from aqueous solutions: A critical review, *Water Res.* 120 (2017) 88–116. <https://doi.org/10.1016/j.watres.2017.04.014>.
- [153] H.N. Tran, Y.F. Wang, S.J. You, H.P. Chao, Insights into the mechanism of cationic dye adsorption on activated charcoal: The importance of π - π interactions, *Process Saf. Environ. Prot.* 107 (2017) 168–180. <https://doi.org/10.1016/j.psep.2017.02.010>.

- [154] J. Ding, F. Zhao, Y. Cao, L. Xing, W. Liu, S. Mei, S. Li, Cultivation of Microalgae in Dairy Farm Wastewater Without Sterilization Cultivation of Microalgae in Dairy Farm Wastewater Without Sterilization, *Int. J. Phytoremediation*. (2015) 37–41. <https://doi.org/10.1080/15226514.2013.876970>.
- [155] C. Palma, E. Contreras, J. Urra, M.J. Martínez, Eco-friendly technologies based on banana peel use for the decolourization of the dyeing process wastewater, *Waste and Biomass Valorization*. 2 (2011) 77–86. <https://doi.org/10.1007/s12649-010-9052-4>.
- [156] T.A. Sial, M.N. Khan, Z. Lan, F. Kumbhar, Z. Ying, J. Zhang, D. Sun, X. Li, Contrasting effects of banana peels waste and its biochar on greenhouse gas emissions and soil biochemical properties, *Process Saf. Environ. Prot.* 122 (2019) 366–377. <https://doi.org/10.1016/j.psep.2018.10.030>.
- [157] C. Zhong, Y. Zu, X. Zhao, Y. Li, Y. Ge, W. Wu, Y. Zhang, Effect of superfine grinding on physicochemical and antioxidant properties of pomegranate peel, *212 Int. J. Food Sci. Technol.* 2016,. 51 (2016) 212–221. <https://doi.org/10.1111/ijfs.12982>.
- [158] F. Pagnanelli, S. Mainelli, F. Veglià, L. Toro, Heavy metal removal by olive pomace : biosorbent characterisation and equilibrium modelling, *Chem. Eng. Sci.* 58 (2003) 4709–4717. <https://doi.org/10.1016/j.ces.2003.08.001>.
- [159] K. V Savaji, O. Niitsoo, A. Couzis, Influence of particle / solid surface zeta potential on particle adsorption kinetics, *J. Colloid Interface Sci.* 431 (2014) 165–175. <https://doi.org/10.1016/j.jcis.2014.05.030>.
- [160] X. Cui, H. Hao, C. Zhang, Z. He, X. Yang, Science of the Total Environment Capacity and mechanisms of ammonium and cadmium sorption on different wetland-plant derived biochars, *Sci. Total Environ.* 539 (2016) 566–575. <https://doi.org/10.1016/j.scitotenv.2015.09.022>.
- [161] Y. He, H. Lin, Y. Dong, L. Wang, Preferable adsorption of phosphate using lanthanum-incorporated porous zeolite: Characteristics and mechanism, *Appl. Surf. Sci.* 426 (2017) 995–1004. <https://doi.org/10.1016/j.apsusc.2017.07.272>.
- [162] G. Nechifor, D.E. Pascu, M. Pascu, G.A. Traistaru, A.A. Bunaciu, H.Y. Aboul-Enein, Study of adsorption kinetics and zeta potential of phosphate and nitrate ions on a cellulosic membrane, *Rev. Roum. Chim.* 58 (2013) 591–597.
- [163] F. Güzel, Ö. Aksoy, G. Akkaya, Application of Pomegranate (*Punica granatum*) Pulp as a New Biosorbent for the Removal of a Model Basic Dye (Methylene Blue), *World Appl. Sci. J.* 20 (2012) 965–975. <https://doi.org/10.5829/idosi.wasj.2012.20.07.1609>.
- [164] P.D. Pathak, S.A. Mandavgane, B.D. Kulkarni, Characterizing fruit and vegetable peels as bioadsorbents, *Curr. Sci.* 110 (2016) 2114–2115.
- [165] D.D. Waal, A.M. Heyns, Infrared spectra of the ammonium ion in ammonium hexavanadate, *Spectrochim. Acta.* 46 (1990).
- [166] W.S. Carvalho, D.F. Martins, F.R. Gomes, I.R. Leite, L. Gustavo da Silva, R. Ruggiero, E.M. Richter, Phosphate adsorption on chemically modified sugarcane bagasse fibres, *Biomass and Bioenergy*. 35 (2011) 3913–3919. <https://doi.org/10.1016/j.biombioe.2011.06.014>.
- [167] A. Kotoulas, A. Agathou, I.E. Triantaphyllidou, T.I. Tatoulis, C.S. Akrotos, A.G. Tekerlekopoulou, D. V. Vayenas, Zeolite as a Potential Medium for Ammonium Recovery and Second Cheese

- Whey Treatment, Water (Switzerland). (2019). <https://doi.org/10.3390/w11010136>.
- [168] R.A.K. Rao, F. Rehman, Adsorption of Heavy Metal Ions on Pomegranate (*Punica granatum*) Peel : Removal and Recovery of Cr (VI) Ions from a Multi-metal Ion System, *Adsorpt. Sci. Technol.* 28 (2010) 195–211.
- [169] S. Fauzia, F. Furqani, R. Zein, E. Munaf, Adsorption and reaction kinetics of tatrazine by using *Annona muricata* L seeds, *J. Chem. Pharm. Res.* 7 (2015) 573–582.
- [170] N. Morin-crini, P. Badot, Adsorption isotherm models for dye removal by cationized starch-based material in a single component system : Error analysis, *J. Hazard. Mater.* 157 (2008) 34–46. <https://doi.org/10.1016/j.jhazmat.2007.12.072>.
- [171] F. Anthony, K. Godfrey, Simultaneous adsorption of Ni (II) and Mn (II) ions from aqueous solution onto a Nigerian kaolinite clay, *Integr. Med. Res.* 3 (2014) 129–141. <https://doi.org/10.1016/j.jmrt.2014.03.002>.
- [172] K.Y. Foo, B.H. Hameed, Insights into the modeling of adsorption isotherm systems, *Chem. Eng. J.* 156 (2010) 2–10. <https://doi.org/10.1016/j.cej.2009.09.013>.
- [173] S. Jellali, M. Ali, M. Anane, K. Riahi, N. Jedidi, Biosorption characteristics of ammonium from aqueous solutions onto *Posidonia oceanica* (L .) fi bers, *Desalination.* 270 (2011) 40–49. <https://doi.org/10.1016/j.desal.2010.11.018>.
- [174] L. Gu, J. Xu, L. Lv, B. Liu, H. Zhang, X. Yu, Z. Luo, Dissolved organic nitrogen (DON) adsorption by using Al-pillared bentonite, *Desalination.* 269 (2011) 206–213. <https://doi.org/10.1016/j.desal.2010.10.063>.
- [175] R. Liu, L. Chi, X. Wang, Y. Sui, Y. Wang, H. Arandiyani, Review of metal (hydr)oxide and other adsorptive materials for phosphate removal from water, *J. Environ. Chem. Eng.* (2018). <https://doi.org/10.1016/j.jece.2018.08.008>.
- [176] A.F. de Sousa, T.P. Braga, E.C.C. Gomes, A. Valentini, E. Longhinotti, Adsorption of phosphate using mesoporous spheres containing iron and aluminum oxide, *Chem. Eng. J.* 210 (2012) 143–149. <https://doi.org/10.1016/j.cej.2012.08.080>.
- [177] B. Zhang, N. Chen, C. Feng, Z. Zhang, Adsorption for phosphate by crosslinked/non-crosslinked-chitosan-Fe(III) complex sorbents: Characteristic and mechanism, *Chem. Eng. J.* 353 (2018) 361–372. <https://doi.org/10.1016/j.cej.2018.07.092>.
- [178] N. Özbay, A.F.J. Yarg, R.Z.F. Yarbay-, E. Önal, Full Factorial Experimental Design Analysis of Reactive Dye Removal by Carbon Adsorption, *J. Chem.* (2013). <https://doi.org/10.1155/2013/234904>.
- [179] F. Geyikçi, H. Büyükgüngör, Factorial experimental design for adsorption silver ions from water onto montmorillonite, *Acta Geodyn. Geomater.* 10 (2013) 363–370. <https://doi.org/10.13168/AGG.2013.0035>.
- [180] D.T. Mekonnen, E. Alemayehu, B. Lennartz, Removal of phosphate ions from aqueous solutions by adsorption onto leftover coal, *Water (Switzerland).* 12 (2020) 1–15. <https://doi.org/10.3390/W12051381>.
- [181] A.K. Hegazy, N.T. Abdel-Ghani, G.A. El-Chaghaby, Adsorption of phenol onto activated carbon from *Rhazya stricta* : determination of the optimal experimental parameters using factorial design, *Appl. Water Sci.* (2013). <https://doi.org/10.1007/s13201-013-0143-9>.

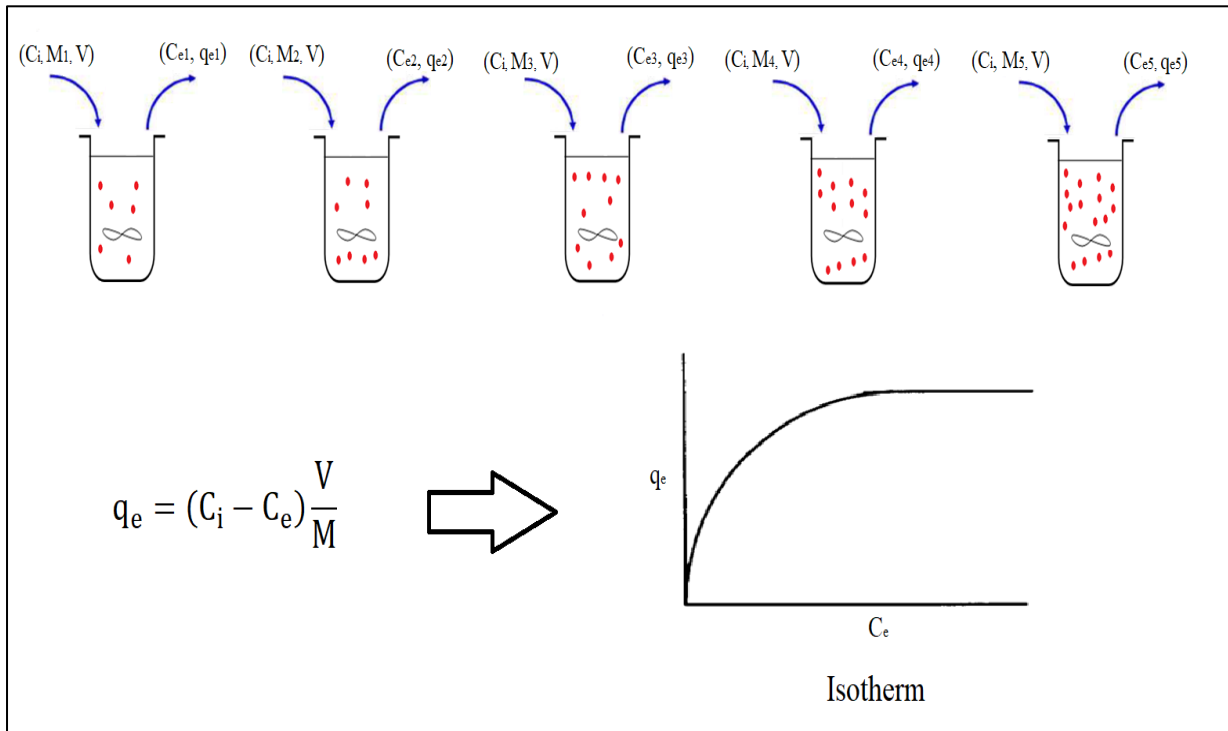
- [182] S. Mtaallah, I. Marzouk, B. Hamrouni, Factorial experimental design applied to adsorption of cadmium on activated alumina Salma Mtaallah , Ikhlass Marzouk and Béchir Hamrouni, *Jounal Water Reuse Desalin.* 08 (2018) 76–85. <https://doi.org/10.2166/wrd.2017.112>.
- [183] A. Regti, A. El Kassimi, M.R. Laamari, M. El Haddad, Competitive adsorption and optimization of binary mixture of textile dyes: A factorial design analysis, *J. Assoc. Arab Univ. Basic Appl. Sci.* 24 (2017) 1–9. <https://doi.org/10.1016/j.jaubas.2016.07.005>.
- [184] K.L. Tan, B.H. Hameed, Insight into the adsorption kinetics models for the removal of contaminants from aqueous solutions, *J. Taiwan Inst. Chem. Eng.* 74 (2017) 25–48. <https://doi.org/10.1016/j.jtice.2017.01.024>.
- [185] L. Zeng, X. Li, J. Liu, Adsorptive removal of phosphate from aqueous solutions using iron oxide tailings, *Water Res.* 38 (2004) 1318–1326. <https://doi.org/10.1016/j.watres.2003.12.009>.
- [186] H. Ye, F. Chen, Y. Sheng, G. Sheng, J. Fu, Adsorption of phosphate from aqueous solution onto modified palygorskites, *Sep. Purif. Technol.* 50 (2006) 283–290. <https://doi.org/10.1016/j.seppur.2005.12.004>.
- [187] N.Y. Mezenner, A. Bensmaili, Kinetics and thermodynamic study of phosphate adsorption on iron hydroxide-eggshell waste, *Chem. Eng. J.* 147 (2009) 87–96. <https://doi.org/10.1016/j.cej.2008.06.024>.
- [188] A. Bonilla-Petriciolet, D.I. Mendoza-castillo, H.E. Reynel-ávila, *Adsorption Processes for Water Treatment and Purification*, Springer, 2017.
- [189] F. Peng, P.W. He, Y. Luo, X. Lu, Y. Liang, J. Fu, Adsorption of Phosphate by Biomass Char Deriving from Fast Pyrolysis of Biomass Waste, *Clean - Soil, Air, Water.* 40 (2012) 493–498. <https://doi.org/10.1002/clen.201100469>.
- [190] S. Benyoucef, M. Amrani, Removal of phosphorus from aqueous solutions using chemically modified sawdust of Aleppo pine (*Pinus halepensis* Miller): kinetics and isotherm studies, *Environmentalist.* 31 (2011) 200–207. <https://doi.org/10.1007/s10669-011-9313-1>.
- [191] T.S. Anirudhan, P. Senan, Adsorption of phosphate ions from water using a novel cellulose-based adsorbent, *Chem. Ecol.* 27 (2011) 147–164. <https://doi.org/10.1080/02757540.2010.547487>.
- [192] W.M. Cho, B. Ravindran, J.K. Kim, K.H. Jeong, D.J. Lee, D.Y. Choi, Nutrient status and phytotoxicity analysis of goat manure discharged from farms in South Korea, *Environ. Technol. (United Kingdom).* 38 (2017) 1191–1199. <https://doi.org/10.1080/09593330.2016.1239657>.
- [193] B. Ravindran, S.K.S. Kumari, T.A. Stenstrom, F. Bux, Evaluation of phytotoxicity effect on selected crops using treated and untreated wastewater from different configurative domestic wastewater plants, *Environ. Technol. (United Kingdom).* 37 (2016) 1782–1789. <https://doi.org/10.1080/09593330.2015.1132776>.
- [194] S. Mercy, M.B. S, I. Jenifer, Application Of Different Fruit Peels Formulations As A Natural Fertilizer For Plant Growth, *Int. J. Sci. Technol. Res.* 3 (2014) 300–307.
- [195] S.G.A.R.M. Dayarathna, B. Karunarathna, Effect of different fruit peel powders as natural fertilizers on growth of Okra (*Abelmoschus esculentus* L.), *J. Agric. Sci. - Sri Lanka.* 16 (2021) 67–79. <https://doi.org/10.4038/jas.v16i1.9184>.
- [196] K. Xu, F. Lin, X. Dou, M. Zheng, W. Tan, C. Wang, Recovery of ammonium and phosphate from

urine as value-added fertilizer using wood waste biochar loaded with magnesium oxides, *J. Clean. Prod.* 187 (2018) 205–214. <https://doi.org/10.1016/j.jclepro.2018.03.206>.

- [197] O. Sioud, A. Beltifa, N. Ayeb, M. Hb, Characterization of Industrial Dairy Wastewater and Contribution to Reuse in Cereals Culture : Study of Phytotoxic Effect, *Austin J. Environ. Toxicol.* 2 (2016).
- [198] G. Feigl, D. Kumar, N. Lehotai, N. Tugyi, Á. Molnár, A. Ördög, Á. Szepesi, K. Gémes, G. Laskay, L. Erdei, Z. Kolbert, Physiological and morphological responses of the root system of Indian mustard (*Brassica juncea* L. Czern.) and rapeseed (*Brassica napus* L.) to copper stress, *Ecotoxicol. Environ. Saf.* 94 (2013) 179–189. <https://doi.org/10.1016/j.ecoenv.2013.04.029>.

Appendices

Appendix 1: Isotherm determination



Appendix 2: Batch adsorption method

